

BACHELOR THESIS

Some hydrographical changes in the Sognefjord and its tributaries, the Sogndalsfjord and the Barsnesfjord (Western Norway), the last century

by
126 Theresa Reß

Bachelor Work in Geology

Subject Code: GE-491

Date of Submission: 10.06.2015



Agreement regarding the electronical deposit of scientific publications in HiSF Brage – Institutional archive of Sogn og Fjordane University College

The author(s) hereby give(s) Sogn og Fjordane University College the right to make this thesis available in HiSF Brage provided that the thesis is awarded *grade B* or better.

I guarantee that I - together with possible co-authors - have the right of authorship to the material thus have legal rights to allow HiSF to publish the material in Brage.

I guarantee that I have no knowledge or suspicion indicating that this material is illegal according to Norwegian law.

Please fill in your candidate number and name below and tick off the appropriate answer:

Candidate number and name

YES ___ NO___

Candidate number and name

YES ___ NO___

Candidate Number and name

YES ___ NO___

Eingereicht am: _____

Angenommen am: _____

Von: _____

Bingen, den _____

Betreuer (FH): Prof. Dr. Elke Hietel

Betreuer (extern): Prof. Torbjørn Dale

Associated Prof. Dr. Matthias Paetzel

Declaration of Academic Honesty:

Hereby I affirm that the submitted work

“Some hydrographical changes in the Sognefjord and its tributaries the Sogndalsfjord and the Barsnesfjord (Western Norway), the last century”

has been completed by me autonomously and without outside help. I thereby neither used other than the stated reference sources or materials, nor perpetrated I any other form of plagiarism. Furthermore I declare that the work has not been published in an equal or similar way before and has not been submitted for any other purposes before.

Eidesstattliche Erklärung:

Hiermit erkläre ich an Eides statt, dass ich die vorliegende Bachelorarbeit

“Hydrographische Veränderungen im Sognefjord und seinen Seitenarmen, dem Sogndalsfjord und dem Barsnesfjord (West Norwegen), im letzten Jahrhundert”

Selbstständig und ohne fremde Hilfe angefertigt habe. Ich habe dabei nur die in der Arbeit angegebenen Quellen und Hilfsmittel benutzt. Die Arbeit wurde in gleicher oder ähnlicher Form noch keiner anderen Prüfung vorgelegt und auch noch nicht veröffentlicht.

(Place, Date)

(Signature)

Table of Contents

Abstract.....	VI
Acknowledgement	VII
1. Introduction.....	1
1.1 General background.....	1
1.2 Objectives.....	1
1.2.1 Explanation Objective 1.....	2
1.2.2 Explanation Objective 2.....	3
1.2.3 Explanation Objective 3.....	3
1.2.4 Explanation Objective 4.....	3
1.2.5 Explanation Objective 5.....	4
1.3 Setting.....	4
1.3.1 Fjords.....	4
1.3.2 Geography.....	9
1.3.3 Historical setting.....	16
1.3.4 Climate setting.....	22
2. Materials and Methods	26
2.1 The Barsnesfjord and Sogndalsfjord	28
2.2 The Sognefjord and Sognesjøen.....	29
2.3 The Nordic Sea and Station Mike.....	30
2.4 Characteristics of the various data and some assumptions.....	30
3. Results	32
3.1 Climate	32
3.1.1 Precipitation.....	32
3.1.2 Temperature	36
3.2 Hydrography Outer Barsnesfjord.....	40
3.2.1 Salinity	40
3.2.2 Temperature	44
3.3 Sognalsfjord.....	49
3.3.1 Salinity	49
3.3.2 Temperature	53
3.3 Sognesjøen	58
3.3.1 Salinity	58
3.3.2 Temperature	64

3.4 Station Mike	70
3.4.1 Salinity	70
3.4.2 Temperature	76
4. Discussion	82
4.1 Discussion Objective 1.....	82
4.1.1 Discussion	82
4.1.2 Conclusion.....	83
4.2 Discussion Objective 2.....	83
4.2.1 Discussion	83
4.2.2 Conclusion	84
4.3 Discussion Objective 3.....	85
4.3.1 Outer Barsnesfjord	85
4.3.2 Sogndalsfjord	87
4.3.3 Sognesjøen	88
4.3.4 Conclusion.....	89
4.4 Discussion Objective 4.....	90
4.4.1 Outer Barsnesfjord	90
4.4.2 Sogndalsfjord	93
4.4.3 Sognesjøen	95
4.4.4 Nordic Sea	98
4.4.5 Conclusion.....	102
4.5 Discussion Objective 5	102
4.5.1 Discussion.....	102
4.5.2 Conclusion.....	109
4.5.3 Possible biological consequences of hydrographic changes	113
5. Conclusion	114
6. References	117
7. Figure References	121
8. Appendix (on CD-Rom)	122
8.1 Appendix I – Rawdata Climate	122
8.2 Appendix II – Rawdata Barsnesfjord	122
8.3 Appendix III – Rawdata Sogndalsfjord	122
8.4 Appendix IV – Rawdata Sognesjøen	122
8.5 Appendix V – Rawdata Station Mike	122

8.6 Appendix VI – Seasonal Graphs and Tables of all data	122
8.7 Appendix VII – Bachelor thesis.....	122

Abstract

The thesis investigates the changes in hydrography, especially in salinity and temperature at the Sognefjord and its tributaries Sogndalsfjord and Barsnesfjord during the last century. Thereby in particular a potential correlation with the building of the water power plants since the 1960s and the climatic changes is examined. Thus several data sets regarding the different water bodies' salinities and temperatures are analyzed, especially focusing on the upper water layers and the seasonal features. Overall there is a general drop in salinity observed by comparing the period before the building of the water power plants around 1960 and the period after finishing the largest plants in 1989.

Thus it accounts for 0.77‰ decrease at the Sognesjøen and 5.27‰ at the Sogndalsfjord during winter time at 0 m depth. Regarding the summer period a slightly smaller drop of 0.15‰ is visible at the Sognesjøen.

Against that the winter and summer temperatures also show significant changes, in particular a magnifying trend of the changes with going deeper into the fjord. Thus the winter values rise at 0.32°C at the Sognesjøen while they drop around 0.68°C at the Sogndalsfjord in 0 m depth. Regarding the summer period an increase of around 1.12°C is visible at the Sognesjøen.

The salinity changes, in particular in winter time, originated by a changed inflow of dammed water through the water power plants but partly also by general increase in the average amount of precipitation.

Regarding the temperature changes, these are related to both, simultaneous increases in air temperature but also effects due to inflow of different temperate water masses through the water power plants. The increasing effect with going deeper into the fjord is owing to the "Land-Ocean"-Effect, the difference in heat penetration in the single regions and the darkening of the coastal water.

Acknowledgement

I would like to especially thank my supervisor Torbjørn Dale for his great guidance and support during the entire process of writing this bachelor thesis. Beside that I in particular want to say thank you to Matthias Paetzel for his part as second supervisor and personal point of contact, also regarding all aspects of being an exchange student in Sogndal. Beside that I would like to thank the other bachelor thesis writers, Anders Tysnes, Aleksander Johannes Rongved, Marius Røthe Bøen, Sigrid Klakken and Anna Marina Elenor Eriksson who honestly included me regarding the writing process as well as the social student life in Sogndal. Special thanks also to the entire "From Mountain to Fjord"-group 2014 which not only provided me with the basic data for my work, but also enabled an awesome time in Sogndal during the autumn semester of 2014. Additionally many thanks go to Sabrina Kaufmann, who also strongly contributed data and information, finally becoming base for this work. However, also regarding the planning of the entire stay abroad, she was a big help, that I really appreciated. Besides that I would like to especially thank Prof. Dr. Elke Hietel for being my supervisor at my University in Bingen. Thanks also to the International Office and Administration in Bingen for support and help regarding the entire stay. Furthermore thank you to Erasmus for sponsoring both semesters in Sogndal.

1. Introduction

1.1 General background

Norway is one of the leading countries, regarding the production of hydroelectric energy by using water power plants. Thus, also in the region around the Sognefjord several plants have been built since 1960, contributing to this renewable energy source. The Sogneregion thereby produces approximately 12-13% of all hydroelectric power made in Norway (Anonymous, 2014). However, some water power plants might have the ability to cause significant changes in the fjord hydrography as they create differences in freshwater inflow. Beside that the general change in local and global climate can also create noticeable variations due to higher temperatures and differences in the average amount of precipitation.

This bachelor thesis focuses on the question whether there are noticeable changes in the fjord hydrography the last century and especially what will be the most likely sources. Thus an investigation of the surface water masses of the fjords water bodies will be performed by using salinity and temperature data of the Sognesjøen, the Sogndalsfjord and the Barsnesfjord. However, especially climatic influences can also be transported into the fjord through the connection with the Nordic Seas. Regarding that, additionally a comparison of hydrographical fjord and Ocean data will be done, enabling discovering overall global effects from the Nordic Sea. In view of these possible sources causing hydrographical changes, the single water bodies of the fjords and the Nordic Seas are examined. This bachelor thesis shall thereby contribute to figure out the most probable reasons for hydrographical changes in the Sognefjord, thus studying the possible influencing factors from all directions. As thereby caused changes in the hydrography are mainly seen in the surface water layers, the main focus will be placed on the upper water masses. Reason for that is the lower density of freshwater compared to salt water and of warmer water compared to colder water.

1.2 Objectives

The research in this bachelor thesis overall has two main tasks, finally leading to several objectives. Thus its main issue is the potential correlation of hydrographical changes in the Sognefjord with the building of the water power plants. Additionally the effects due to

climate changes have to be investigated, finally allowing a weighing of the most likely source of the changes.

This approach is important to consider all possible influences on global and local scale. According to these main tasks several objectives arise, allowing a gradual investigation of the different issues.

The thereby emerging objectives are:

1. Are data available to examine possible changes in temperature and salinity in the Nordic Sea, as well as the Sognefjord and especially the tributaries Sogndalsfjord and Barsnesfjord?
2. Are water power plants, climatic variations or both capable of causing significant changes in the fjords hydrography?
3. Does the hydrographical data show any yearly changes at the Sognesjøen, as well as in the Sogndalsfjord and Barsnesfjord during the last 50 to 100 years?
4. Is it possible to determine seasonal timing and thus direction of the changes in salinity and temperature?
5. Can the origin of these changes in the fjord hydrography be ascertained and be classified to effects caused by climate, water power plants or both?

1.2.1 Explanation Objective 1

Are data available to examine potential changes in temperature and salinity in the Nordic Sea, as well as the Sognefjord and especially the tributaries Sogndalsfjord and Barsnesfjord?

To be able to investigate the fjords hydrography and potential changes it is relevant to have sufficient data for the different water bodies. Therefore the continuity and quality of the data are significant, enabling an analysis and comparison. If sufficient data are available a further examination is possible, enabling to form graphs and tables. Based on these a subsequent analyses and interpretation of the particularities are possible, finally allowing making statements about the development and possible causes of salinity and temperature variations in the different water bodies.

1.2.2 Explanation Objective 2

Are water power plants or climatic variations capable of causing significant changes in the fjords hydrography?

Due to the building of water power plants with dams for hydroelectric power production, the question arises whether these plants can have significant influences on the fjord environments and especially the hydrographical parameters salinity and temperature. Therefore an analysis is necessary, to figure out if the power plants can have effects on salinity and temperature values. The same analysis is necessary regarding climate variations. As the climate is changing, differences in the average temperature and precipitation might also lead to changes in the fjord hydrography. Hence climate has to be investigated, whether and to what extend the different factors can cause hydrographical changes. To determine the main reason for potential changes in hydrography of the fjords it is necessary to take all factors into account.

1.2.3 Explanation Objective 3

Does the hydrographical data show any yearly changes at the Sognesjøen, as well as in the Sogndalsfjord and Barsnesfjord during the last 50 to 100 years?

In case of sufficient data available, it has to be examined whether there are noticeable changes in the salinity and temperature conditions of the different water bodies over the last 50 to 100 years. Thus a precise study of the available data has to be done to figure out whether there are visible changes in the salinity and temperature values.

1.2.4 Explanation Objective 4

Is it possible to determine seasonal timing and thus direction of the changes in salinity and temperature?

In case of noticeable changes in temperature and salinity, it is of main interest to figure out the timing of these changes during the year. As water power plants are supposed to cause changes, that are mainly observed in specific seasons, a further fragmentation of the given data is used, to get closer to the occurrence of the different variations. This enables to restrict the potential reasons and thus to get closer to the final source, being most likely to have caused the changes.

1.2.5 Explanation Objective 5

Can the origin of these changes in the fjord hydrography be ascertained and be classified to effects caused by climate, water power plants or both?

If significant changes are apparent in the water bodies, it is of main interest, to figure out the major influencing factor causing these changes. Thus it is essential, to try to examine the main source for the changes in the hydrographical factors salinity and temperature. Thereby a close look on the previously examined timing is used, to figure out the main direction of the influences and finally the major origin which can be due to effects from the climate, from the water power plants or of both.

1.3 Setting

1.3.1 Fjords

1.3.1.1 Geological Structure

In scientific context, a fjord is often described as “(...) a deep, high-latitude estuary which has been (or is presently being) excavated or modified by land-based ice” (Syvitski et al. 1987, S.3). Thereby estuary means that the circulation of the surface water strongly correlates with the waters stratification, caused by the inflow of fresh water. Reason for this fresh water inflow is the common feature of most fjords, having rivers in the one end and the ocean in the other end. Due to different salinities and thus densities of the water masses, they form layers, influencing the circulation. In general the term “fjord” is associated with semi-enclosed waterbodies which are located along coastal regions, penetrating land-inwards. Overall, there are several definitions describing the term “fjord” including or barring different kinds of estuaries (Syvitski et al., 1987).

The fjords are made by glacial movement, which leads to excavation of the weakest ground. The general process can be seen in Figure 1. Overall the reason for their origin is thereby glacio-fluvial movement along fault lines within the mountainous regions. During the last glacial maximum around 17,000 years before present, the glaciers started to move along the weakest part of the land, digging out the ground. Thus fjords originated in glacial movement during the postglacial times, which occurred about 40 times during the last two to three million years (Nesje and Whillans, 1994). The thereby emerging deepening is mostly long and narrow, typically with a larger length than width (Syvitski et al, 1987).

Afterwards it gets filled with sea water, finally resulting in a new fjord. As glaciers have been occurring especially in higher latitudes, fjords are also mainly found in these high latitudes. According to this and as they are narrow inlets of ocean water, they often feature steep sidewalls, due to their location at mountainous regions. Another characteristic is the existence of one or more deep basins, as well as of a shallow sill at the mouth of the fjord (Haakstad et al., 1994). This has a strong effect on the circulation as well as on the water exchange within the fjords.

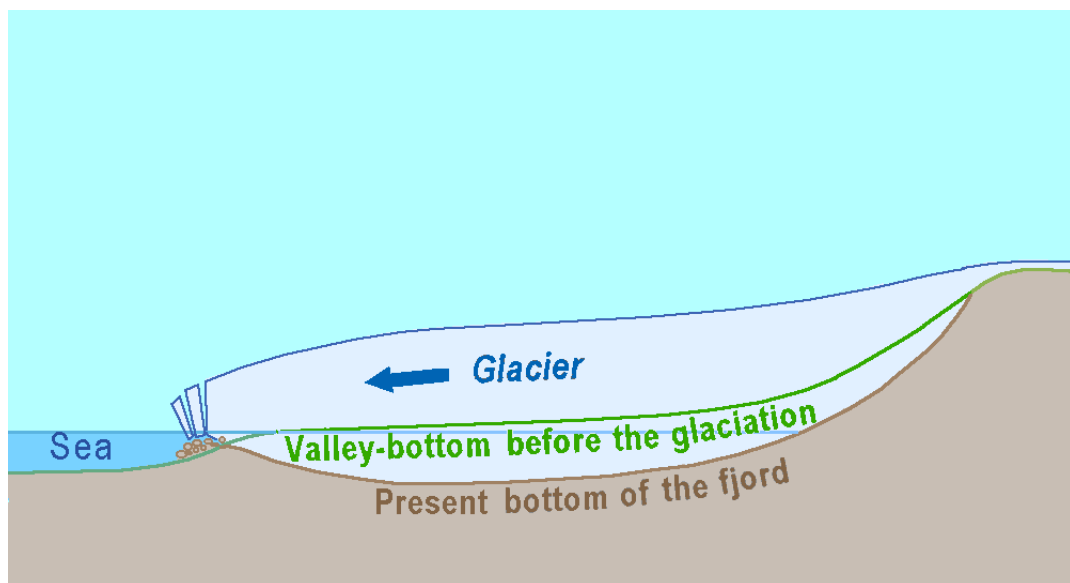


Figure 1: Formation process of a fjord: excavation of bottom material through excavation by a glacier (wikimedia.org, 2015)

As fjords are very immature estuaries and changing within relatively short periods compared to other environments, they have a net sediment accumulation. Hence they are highly interesting for researches regarding the sedimentology. Furthermore, due to their location at the boundary between ocean and land, fjords are mixing regions of salty ocean water and freshwater from rivers and land runoff. This makes them also interesting study areas, regarding the hydrography as well as the geomorphology. Besides that, fjords also contribute to the freshwater inflow into the coastal waters, being also a popular research topic. Regarding the overall circulations and water exchange manners, big differences between different fjords can occur. This is related to the hydrography being highly influenced from the bottom bathymetry (Syvitski et al., 1987).

1.3.1.2 Hydrographical Structure

The general hydrographic structure within a fjord usually consists of three layers, having the lowest density at the surface and the highest in the bottom water. Thus fjords mainly feature a typical stratification, usually consisting of three layers. This structure with three layers can also be seen at Figure 2. The uppermost layer thereby is the brackish water layer. It is caused through the land runoff of freshwater due to rivers and precipitation. This layer can have a depth of a few meters and is featuring the lowest density due to the inflow of freshwater (Stigebrandt, 2001). The uppermost layer is then flowing outwards in direction of the open ocean.

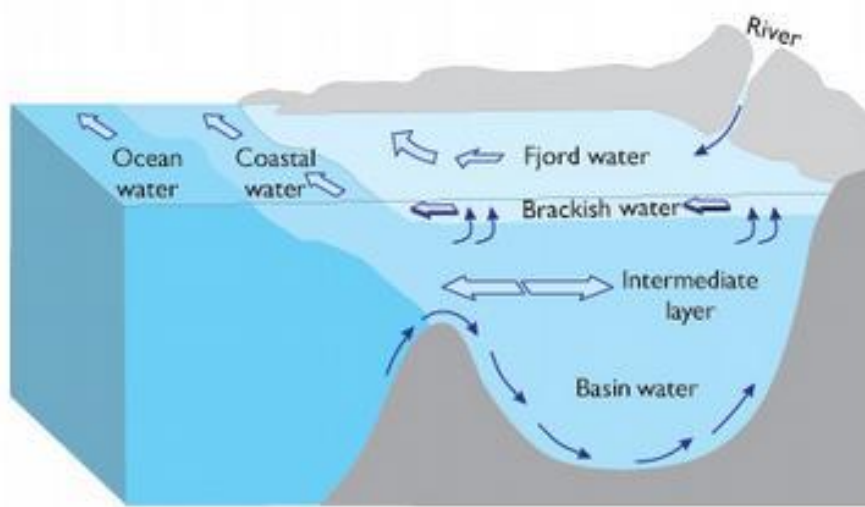


Figure 2: Main water structure within a fjord. The different water masses are shown by different colors. The brackish water mass is floating on top of the intermediate water mass, while the basin water is located in the bottom, behind the sill (imr.no, 2015).

Right underneath this surface water mass a compensation current occurs due to entrainment. This current makes up for the loss of salt water, floating inwards and forming the top part of the second layer within a fjord, the intermediate water mass (Dale, pers. com.). This water mass is located between the brackish water and the upper end of the sill, being much saltier and heavier than the surface water. Regarding this location, its thickness is strongly dependent on the depth of the sill (Stigebrandt, 2001).

The third and lowermost layer is called the basin water, due to its occurrence from the sill downwards to the bottom of the fjord. This water mass has the highest density and is trapped behind the sill. Exactly this high density is also the reason for the water mass to be mainly stagnant and thus staying at the bottom of the fjord for relatively long periods. As it

is located behind the sill, it does not have a direct connection with the ocean water, requiring more effort to become exchanged (Stigebrandt, 2001).

1.3.1.3 Circulation and Water Exchange

As fjords are transition zones with the open ocean, they are mixing places of salty ocean water and fresh water. This also causes the most common circulation patterns within fjords. Overall, there are three kinds of circulations within a fjord, causing the different water masses to mix. The first and most significant one regarding the surface water layer is the estuarine circulation. Due to the inflow of fresh water caused by river runoff and precipitation, two water masses with different salinities and thus densities are available. The low salinity fresh water and fjord water with higher salinity are then mixed by winds and tides causing turbulences, but also by turbulent mixing in the border zone between the brackish and the intermediate water mass. This entrainment is finally also the driving force for the compensation current. Through the mixture of water masses having different salinities the brackish surface water is formed (Stigebrandt, 1981). This current generated and causing the mixing is called estuarine circulation. It mainly occurs in the upper layers until around 50m (Hurdle, 1986). However, this depth is usually shallower in fjords. Due to this constant addition of freshwater to the fjords the brackish water is forced outwards and mixed into the coastal current along the coast. Thus, depending on the emerging amounts of brackish water the strength and thickness of the compensation current varies (Syvitski et al., 1987). The added coastal water in this current makes up for the loss of surface water inside the fjord, as the compensation current replaces the salt water mixed into the outgoing brackish water at the surface. Thereby the compensation current has an opposite direction and is going inwards into the fjord (Dale, pers. com.). The general circulation pattern in a fjord can also be seen in Figure 3.

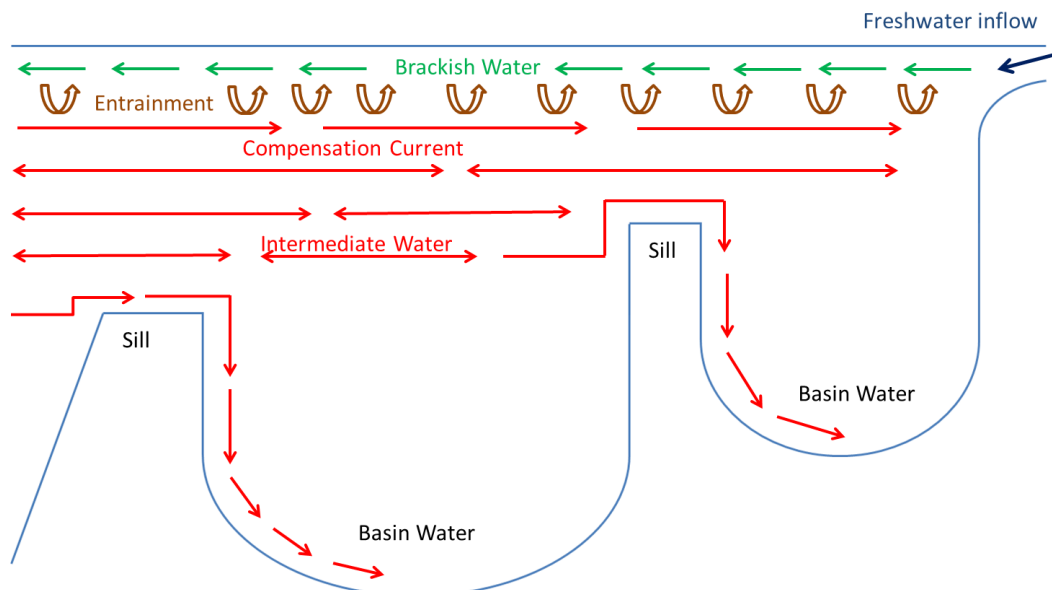


Figure 3: Water circulation within a fjord, showing the brackish water layer on top, entraining with the compensation current as uppermost part of the intermediate layer and the basin water in the bottom.

The second circulation is the intermediate circulation. Due to its location, the main influencing factor on its flow is the change in wind direction along the coast. Thereby the wind causes an increase or decrease of the depth of the coastal wedge depending on the direction of the wind. These variations are forcing the intermediate water to move in or out of the fjord (Dale, pers. com.). Thus intermediate currents cause a water exchange with the coastal region as well as turbulences within the layer. Besides that eddies are the main control of the density in this layer, as they are causing vertical exchange (Hurdle, 1986). As surface water and intermediate water are having a direct connection with the open ocean, this also affects their water exchange rates between inside and outside a fjord. Due to the direct linking of the coastal water and these fjord layers, the surface and intermediate water have faster rates of exchange than the third layer, the bottom or basin water (Hurdle, 1986).

The third water circulation, the deep water circulation, is then occurring within the bottom water, causing its exchange. The exchange thereby depends on the density of the coastal water above sill depth. A renewal of basin water occurs when the density of this coastal water is higher than the density of the basin water. In that case the denser coastal water can pass the sill, enter the fjord and finally sink down into the basin. There it is replacing the old bottom water by lifting it above sill level and thus causing the old bottom water to flow out of the fjord (Stigebrandt, 2001). This water exchange mainly depends on the sill depth as well as on the density of the coastal water above sill level (Syvitski et al., 1987). However,

due to the natural fluctuations within the density of the coastal water, the basin water exchange might intermit for a while, causing the fjords bottom water to stay stagnant. A shallow sill can contribute to those disruptions of basin water exchange (Syvitski et al., 1987). Thus, the basin water has the slowest exchange rate of the fjords water masses, depending on several factors like seasonal density fluctuations in the coastal water and depth of the sill (Stigebrandt, 1981). Stagnant bottom water can lead to a lack of oxygen within the basin water during long periods without water renewal.

However, the entire fjord circulation is a variable system, also depending on several other factors. Besides climate, freshwater runoff, tides as well as water exchange with the open ocean or geomorphology also the size of a fjord is relevant (Haakstad et al., 1994). According to the length and width of the fjord, different influencing factors are feasible. A distraction through the Coriolis force, centrifugal forces in curvy fjords, but also bottom thresholds causing slower flowing speeds (Sætre, 2007). Also changes in wind or less inflow of freshwater can cause variations in pressure gradients, surface mixing, as well as internal waves that change the stratifications. A main factor is also the salinity of the water masses that can cause changes in circulation patterns and stratifications. Thus an exact prediction of circulation patterns within a specific fjord is difficult, as the hydrography can vary from fjord to fjord (Syvitski et al., 1987). Such variation can be seen in the Sogndalsfjord and the Barsnesfjord. Thus, while the basin water of the Sogndalsfjord is exchanged in summer time, the Barsnesfjord changes its bottom water in winter time (Dale, pers. com.).

1.3.2 Geography

The aim of this bachelor thesis is to analyse potential hydrographical changes in the Sognefjord and especially in its tributaries, the Sogndalsfjord and Barsnesfjord during the last century. Main focus thereby is the examination of possible sources of these changes, with major attention on influences through the hydroelectric power plants and the overall change in climate. Thus, as these factors will cause the strongest changes mainly in the innermost parts of the fjords, comparisons and analyses will also start at the innermost Barsnesfjord.

1.3.2.1 The Barsnesfjord

As a part of the Sognefjord in western Norway, the Barsnesfjord is connected with the Sogndalsfjord, one of the Sognefjords main tributaries. It has a north-east direction and is located northwards in the council of Sogndal (Paetzel and Schrader, 1991). The fjord starts with crossing the Loftesnes-Bridge at the end of the Sogndalsfjord, flowing in northern direction with a total length of around 4.5 km. Besides that the Barsnesfjord has a maximum width of around 1.4 km, a surface area of 4.5 km² and a total volume of approximately 0.165 km³ (Dale and Hovgaard, 1993).

Overall the Barsnesfjord is divided into two basins, each time separated by a shallow sill. The Outer Barsnesfjord starts at the end of the Sogndalsfjord at Loftesnes-Bridge, having a 7.5 m shallow sill. It then stretches around 2 km towards the isles between Barsnes and Kvam, where the second sill of around 29 m marks the start of the Inner Barsnesfjord. The Inner part stretches around 2.5 km eastwards until it reaches the innermost part of the fjord, where the Årøy-River is entering (Paetzel and Schrader, 1991). Both basins can also be seen on Figure 4. While the Outer Barsnesfjord reaches a maximum depth of around 80 m, the Inner Barsnesfjord is less deep, only accounting for approximately 60 m. Both fjords feature relatively steep side walls with a flat bottom (Dale and Hovgaard, 1993).



Figure 4: Barsnesfjord at the innermost end of the Sogndalsfjord, separated by the Loftesnes-Bridge. It is divided into Outer and Inner Barsnesfjord with the border between Kvam and Barsnes. The Årøy-River with the Water Power Plant is found in the inner end.

As the Sogndalsfjord is connected to the Sognefjord through a 25 m deep sill and the Sogndalsfjord and Barsnesfjord are separated by an only 7.5 m deep sill, there is just a restricted water circulation between the main fjord and its tributaries. As a consequence the two basins of the Barsnesfjord both show more or less anoxic conditions. While the Inner part is more or less permanently anoxic, the Outer Barsnesfjord features longer oxic

periods. Hence there is in general less oxygen available in the Inner basin compared to the Outer one. As a consequence there is an accumulation of undisturbed sedimentary records in these lowermost depths (Paetzel and Schrader, 1991). Beside that the Barsnesfjord receives its main fresh water inflow through the Årøy-River at its inner end (Dale and Hovgaard, 1993). The river itself starts right underneath the glacier Jostedalbreen and is connected with the Veitastrond-Lake and the lake Hafslovatnet. Due to the origin close to the glacier, the Årøy-River usually carries along the largest water volume in the spring and summer months, caused by snowmelt. Hence, the annual water discharge accounts for around $35 \text{ m}^3/\text{s}$, varying between $2\text{-}4 \text{ m}^3/\text{s}$ in winter and $50\text{-}60 \text{ m}^3/\text{s}$ in summer (Dale, pers. com.). Regarding the timing, the runoff overall is relatively low until around April with afterwards increasing trend, until it reaches its peak around July. Thus, overall the Barsnesfjord and Sogndalsfjord gain the most freshwater in spring and summer time. However, since May 1983 a water power plant is working between the lake Hafslovatnet and the Barsnesfjord. This hydroelectric power plant partly imitates the natural water runoff, thus showing similar values like in the time before the regulation. However, in some periods there are differences in water runoff compared to the natural behavior (Urdal and Sægrov, 2008). Reason for that is the slight damming capacity of the Veitastrond lake and lake Hafslovatnet, as the water level in the lakes may fluctuate with about 3 m at the Veitastrond lake and 1 m at lake Hafslovatnet (Dale, pers. com.).

1.3.2.2 The Sogndalsfjord

The Sogndalsfjord is one of the main tributaries of the Sognefjord, located in the Sogn og Fjordane county in the western part of Norway. It stretches in a southwestern direction, starting between Nornes and Fimreite and ending up near Sogndalsfjøra, where it finally enters the Barsnesfjord. This can also be seen at Figure 5. At the outermost point at Nornes Strait a 25 m deep sill separates the Sogndalsfjord from the Sognefjord, which soon reaches a depth of more than 900 m (Paetzel and Dale, 2010). From this outer border the Sogndalsfjord stretches with a length of around 15 km and a maxima width of 1.6 km inwards, reaching a maximum depth of 263 m. The overall surface area accounts for around 17.5 km^2 with a total volume of approximately 1.934 km^3 (Dale and Hovgaard, 1993). At its inner end, located at the municipal Sogndal, the Sogndalsfjord is separated from the Outer Barsnesfjord by a 7.5 m shallow sill. The Loftesnes-Bridge is thereby apparently marking the border.



Figure 5: Sogndalsfjord, a tributary of the main Sognefjord, separated from the Barsnesfjord by the Loftesnes-Bridge. The border to the Sognefjord is marked between Nornes and Fimreite.

Overall the Sogndalsfjord, like the Barsnesfjord, features fairly steep side walls and a flat bottom. Due to the shallow sills at the outlet into the Sognefjord and especially at the entrance into the Barsnesfjord, the entire fjord circulation is restricted as already mentioned in chapter “1.3.2.1 The Barsnesfjord”. Beside the main inflow from the Barsnesfjord, the Sogndalsfjord receives its main amount of fresh water from the Sogndalsriver (Dale and Hovgaard, 1993). Thus, while the Årøy-River supplies around $1.0 \text{ km}^3/\text{year}$, the Sogndalsriver accounts for approximately $0.3 \text{ km}^3/\text{year}$. Regarding the oxygen occurrence, the bottom water of the fjord usually features more than the critical value of 2 ml/l O_2 , overall still showing oxic conditions (Paetzel and Dale, 2010).

1.3.2.3 The Sognefjord and Sognesjøen

The Sognefjord is the longest and deepest fjord in Norway, as well as the second longest fjord in the world. It is 205 km in length and has a maximum depth of 1308 m. The water volume is roughly 525 km^3 with a surface area of about 950 km^2 (Hermansen, 1974). The Sognefjord originated during recent ice ages, caused by the glacial melting (Manzetti and Stenersen, 2010). It is located in the county Sogn og Fjordane at the eastern part of Skjolden, going outwards to the west coast of Norway. This can also be seen at Figure 6. At the seaward entrance the fjord is separated from the coast by a 155 m deep sill. Right behind the sill the Sognefjord features a depth of more than 200 m and around 3 km width. This width decreases with getting further inland, from around 4 – 5 km in the western part

to 2 – 3 km in the east (Nesje and Whillians, 1994). It is surrounded by mountains in the north, south and east, as well as from the Nordic Sea in western direction.

Due to this location, it is divided into three sections, the coastal, middle and inner part, as this causes big changes in topography and climate. While the coastal region is relatively flat, surrounded by mountains up to around 500 m only, the region is getting steeper inwards, showing mountains up to 2400 m in direction of Jotunheimen. Additionally the fjord has a further subdivision into more small and narrow tributaries (Lødøen, 1998). Overall, the inner part features six main branches, the Fjærlandsfjord, Sogndalsfjord, Lustrafjord, Årdalsfjord, Lærdalsfjord and Aurlandsfjord including the Nærøyfjord (Nesje and Whillians, 1994). Latter is a Unesco World Heritage Site and thus an important part of the western Norwegian fjord landscape (Anonymous, 2004). There are also other side arms, however becoming smaller with getting closer to the coast, where there are only few at all (Nesje and Whillians, 1994).



Figure 6: The Sognefjord, the second largest fjord in the world, located in Sogn og Fjordane in western Norway. Additionally the fixed hydrographic measuring station, located at the Sognesjøen.

Overall the Sognefjord features a low salinity surface, caused by fresh water inflow through precipitation and river runoff. Most rivers thereby enter the fjord at its innermost parts or within the tributaries, bringing in water that is often influenced by glaciers. Even in case of the Sognefjord this leads to the largest inflow of fresh water in spring and summer time due to snow and glacial melting (Mikalsen and Sejrup, 2000).

Besides that the fjord also features around 200 m of deglaciation sediment at its deepest part (Aarseth et al., 2008). Due to this and its location at the transition zone of ocean and land, the Sognefjord is a popular basis for scientific researches in geological, hydrographical and biological direction. The main hydrographical data are thereby delivered by the IMR,

the Institute of Marine Research in Norway. It collects continuous data from all Norwegian Seas, including the Sognefjord. The measuring station thereby is located at the Sognesjøen around 20 km inside of the fjords mouth, delivering salinity and temperature data. As it is located quite close to the Nordic Sea and thus at the transition zone, it is influenced by outflowing fjord water in the surface layers, inflowing coastal water in the deeper layers, and even Atlantic water in the deepest parts. The general water depth at the Sognesjøen is around 400 m, with the Atlantic water starting at approximately 150 m depth. More detailed information about the Sognesjøen and the data sampling can be found in Chapter “2.2 The Sognefjord and Sognesjøen”.

1.3.2.4 The Nordic Sea and Station Mike

The Nordic Sea describes the ocean that is located between the eastern coast of Greenland and the line, going from the western coast of Norway along the south of Spitzbergen. In the north it is zoned by the Fram Strait, while the southern border is formed by the Greenland-Scotland Ridge (Walczowski, 2014). Thereby it includes the Greenland Sea, the Iceland Sea, as well as the Norwegian Sea also causing the name GIN Sea. The Nordic Sea has a significant location, as it is connected to the Arctic Ocean by the Fram Strait, as well as to the North Atlantic by the submarine Ridge between Greenland and Scotland (Skjoldal et al., 2004). Thus it is the mixing place of several different water masses flowing in from all directions. This can also be seen in Figure 7. Due to this location, the Nordic Sea plays an important role for the world’s climate as well as for the formation of most of the world’s deep ocean water masses (Walczowski, 2014). The latter is caused by on the one hand the inflow of warm, high salinity Atlantic Gulf Water from the south. These water mass has a strong effect on the local climate and causes the highest salinity values to occur in the surface layers of the Nordic Sea. On the other hand very cold, low salinity Arctic Water is flowing in from the north. The two water masses then mix, causing a sinking of the cool, high density water and thus forming most of the world’s deep ocean water (Walczowski, 2014).

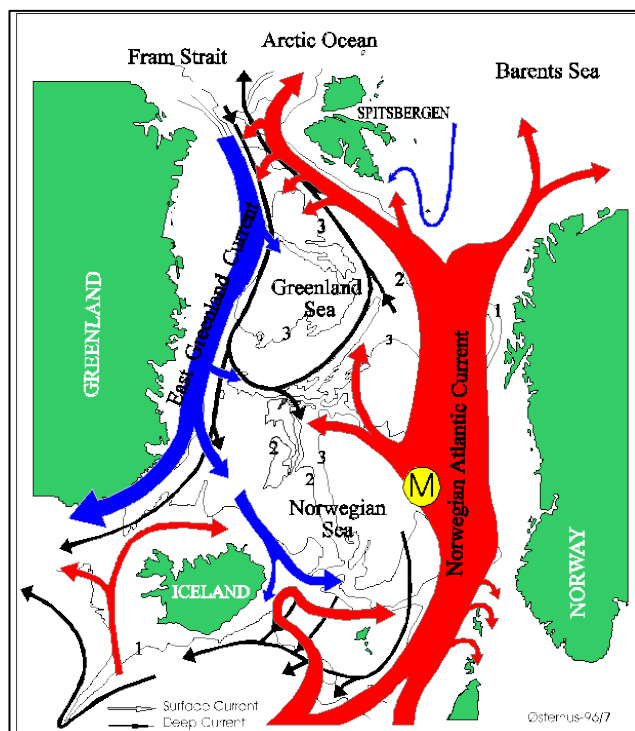


Figure 7: The Nordic Sea, consisting of the Greenland, Iceland and Norwegian Sea. Its location is between the Norwegian west coast and Greenland's east coast. The yellow "M" marks Ocean Weather Station Mike, a fixed oceanographic measuring station (gstatic.com, 2015).

The division into the different seas, the Greenland, Iceland and Norwegian Sea was made due to the Nordic Seas topography. The main feature thereby is the Mid-Ocean Ridge, which is a continuation of the Mid-Atlantic Ridge. It consists of three major parts, the Kolbeinsey Ridge, the Mohn Ridge and the Knipovich Ridge. The Kolbeinsey Ridge is stretching from the North Icelandic Shelf to Jan Mayen, where it is interrupted by the Jan Mayen Fracture Zone. At this zone the Mohn Ridge starts towards the north-east. At the end of this Mohn Ridge, the Knipovich Ridge then stretches northward into the Fram Strait. Beside these main Ridges, the Nordic Sea also contains four major basins. At the western end of the Mohn and Knipovich Ridges, the two basins of the Greenland Sea are located, the Greenland Basin and the Boreas Basin. Furthermore, there are two more basins in the Norwegian Sea, the Lofoten Basin and the Norwegian Basin. The Lofoten Basin is thereby located north of the Greenland basin. In addition the Norwegian Basin is in place between the Greenland-Scotland Ridge and the Iceland Plateau, which is the area between Iceland and Jan Mayen, east of the Kolbeinsey Ridge. The Norwegian Basin additionally is the deepest and largest basin within the entire Nordic Sea (Skjoldal et al., 2004).

Data about the hydrographical situation within the Nordic Sea are supplied by the European Ocean Observatory Network (EuroSITES), which is operating the Ocean Weather Ship

Station (OWS) Mike. More detailed information about Ocean Weather Ship Station Mike and the observed data can be found in chapter “2.3 The Nordic Sea and Station Mike”. The exact location of the measuring station in front of the Norwegian west coast can also be seen in Figure 7.

1.3.3 Historical setting

1.3.3.1 *Hydroelectric Power Production in Norway*

With around 4,000 rivers as well as many glaciers, fjords and lakes Norway has a large potential of hydroelectric power production. This production is typically characterized by a water reservoir in an elevated region, often at higher located mountain ranges. Additionally this water source is often connected with a second reservoir, like glaciers, located in even higher elevations. Thus there are good conditions available for energy production with water power plants (Gonzalez et al., 2011). Due to this large potential in water power, Norway was on the 7th place in the international ranking 2011 of countries producing the most hydroelectric power. Overall the entire water management in Norway is governed by the Norwegian Water Resources and Energy Directorate (NVE) (nve.no, 2015). According to the regional plan for water management at the Sogn og Fjordane region (Anonymous, 2014), hydroelectric power production is the most important energy source in Norway, accounting for 94.8% of the entire energy production. Approximately 12-13% therefrom is produced in the Sogn og Fjordane region, causing an average energy production of approximately 14,710 GWh/yr. The Inner Sognefjord is thereby main producer with an energy production of 9,854 GWh/yr (Anonymous, 2014). Especially due to the increasing need in reducing the greenhouse gases, this CO₂-free resource of energy is increasingly important. The following numbers are all taken from papers released by NVE with stand 2013. Thus, regarding the Sogn og Fjordane region, the largest water power plants are located in Aurland and Tyin, with an average annual production of 2,508 GWh and 1,450 GWh. A map showing all water power plants in the region of the Inner Sognefjord can be seen in Figure 8. The energy production was increasing since the building of the big power plant in Aurland due to simultaneously rise in energy consumption in the capital Oslo. Hence the average winter production of Aurland is rising since 1970, accounting for around 100 m³/s at full workload in winter (Manzetti and Stenersen, 2010).



Figure 8: Overview over all existing water power plants in the region of the inner Sognefjord. Power plants producing more than 1 MW are marked with large quarters, the circles depict pumping power stations (Solbakken et al., 2012).

Nevertheless, the building of water power plants for the purpose of hydroelectric power production in Norway has caused a strong intervention into the ambient environment of rivers, lakes and fjords. By damming the water for the production of electricity the natural flow regime of many rivers has been changed. Thus, some have a different pathway since the damming, due to less water volume or they even dried out almost entirely. In some parts, for example at the Ikjefjorden, all water is transported to another fjord, the Masfjorden, which is located south of the Sognefjord. Thereby almost all rivers suffered a change in their regular amount of water, which is usually less in winter due to snow accumulation and only little rain, as well as larger in summer, owing to snow melt and higher precipitation. Beside that this damming has even further impacts, also affecting the final recipients of the water masses. Thus also the fjords are influenced by the potential changes in water inflow.

The advantage of water power is the adjustable adaption to the specific amounts of energy required during the different times throughout the year. Thus in case of high energy demands more water can be released to finally produce enough energy to satisfy these needs. Hence, in winter time more energy can be produced, satisfying the additional energy demand caused by more heating and indoor activities. Beside that less water needs to be released in summer, as there is less heating and overall energy consumption. However, this specific adaption of water release has wide-ranging effects on the surrounding environment, as it alters the natural amount of water carried within the rivers. The difference between the natural water runoff compared with the situation after building of the water power plants has also already been investigated in the frame of other papers, like from Opdal et al. (2013). Thus the hydroelectric power plants alter the flow of water within the rivers, what can also be seen on Figure 9. Overall there is a larger release of water apparent during the winter months, especially from January to March, and on the other side a much weaker water release in summer time, mainly from Mai to July. This again also affects the fjords, which experience a change in water inflow during the year. Due to this potential change several fjord properties are influenced, like the usual input of nutrients, the currents and the entire fjord and coastal hydrography and biology.

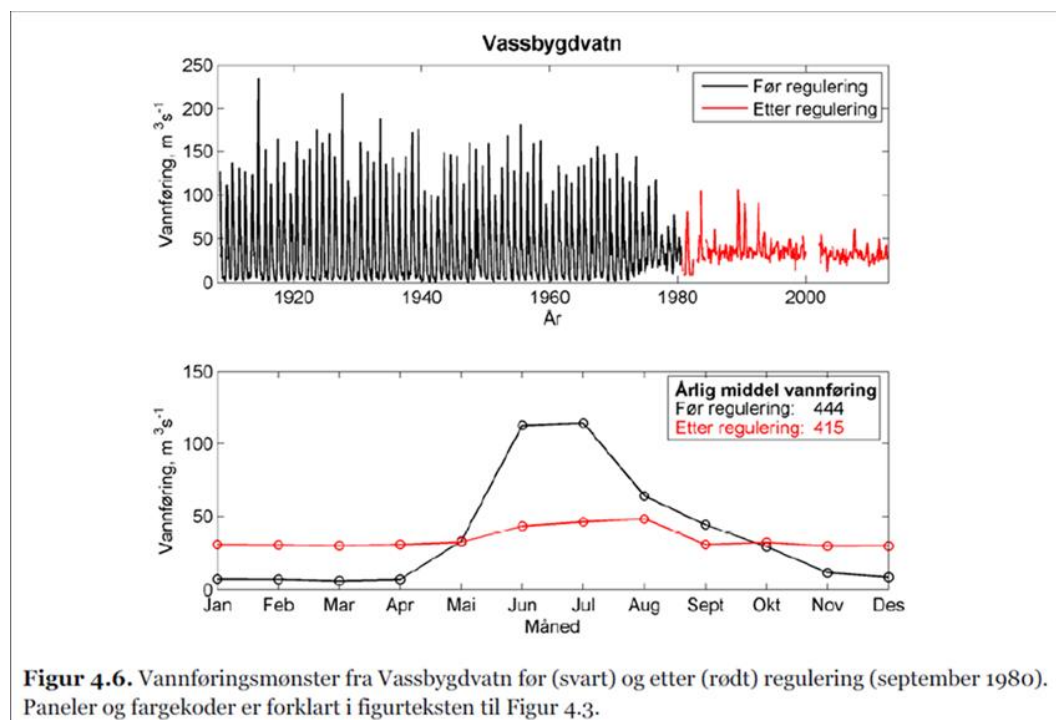


Figure 9: The graphs show the water draining to the Aurlandsfjord. Thereby it shows the flow pattern before (black) and after (red) the water regulation. The x-axis shows the months from January to December, while the y-axis shows the water flow in m^3/s (Opdal et al., 2013).

However, overall there are two kinds of water power plants that are built in Norway. The first kind is using a dam, impounding the water masses to finally generate hydroelectric power. Thereby the natural water regime is changed, as large water masses can be released throughout the entire year, producing energy in response to the current demands. Thus this kind of water power plants can lead to changes in the seasonal cycles of water discharge. Besides that there are also water power plants without dams. These are more or less following the natural seasonal inflow rates and hence do not change the timing and amount of the water masses, finally entering the fjords. Regarding the fjord hydrography, these water power plant versions thus are less likely to cause significant changes (Urdal and Sægrov, 2008).

1.3.3.2 Considerations of specific features

As the main factor observed in the frame of this work is the potential influence of water power plants, the climate or both on the fjords hydrography, a further subdivision is used to show correlations at the best. Accordingly the specific features of the possible influences are taken into account, to enable an optimal examination of the data. Thereby the major research area is the Sognefjord and its tributaries Sogndalsfjord and Barnesfjord. Additionally the Nordic Sea is examined to show global effects as well as possible influences from outside the fjord.

In the Sogn region the general building of the largest water power plants started in the 1960s. Beside that the largest plants have been built and finished by 1989. Thus these years are marking significant times, showing the period before, while and after the building of the water power plants in the Sognefjord region. Overall this enables to divide the time in these three periods, the pre-impact period, the transitional period and the full-impact period, as also seen in Figure 10. This is relevant to reveal potential differences and changes between these times, which might indicate influences of the hydroelectric power production. Hence, by examining the available data a consideration of these three periods is useful for determining the sources of the changes. The periods are thus especially observed and analyzed by tables showing the average salinity and temperature values during these periods. The time until 1960 thereby marks the period before the building of the large water power plants, the pre-impact period, with fairly natural water flow conditions. From 1961 until 1989 represents the time period while most of the large plants have been build and thus the transition period. The last and third period, the full-impact period, lasting from

1990 until today is then showing the time after completing the largest water power plants, potentially showing signs following the change in water inflow into the fjord. Thus by regarding the average values within these periods, possibly occurring changes will become visible.

1. Period	2. Period	3. Period
Pre-Impact Period	Transitional Period	Full-Impact Period
before - 1960	1961 - 1989	1990 - today

Figure 10: Table depicting the division into the three periods, before, while and after building of the large water power plants in the Sogne region.

As variations in freshwater inflow and climate will have the largest influence on the surface values of salinity and temperature within the fjord, these are the factors which are observed in this work. Both, climatic variations as well as changes in the water inflow are mostly pronounced in the upper surface layers of the fjords as these are directly at the mercy of outside influences. Moreover freshwater has a lower density than seawater and consequently signals of changes in freshwater load will be mainly visible in the surface water. Likewise it might occur that an increase in temperature reduces the density of the heated water mass (Dale, pers. com.). Thus, the main focus of this work is laying on these upper water masses, which are most likely to reveal changes in the hydrography. Thus the 0 m to 25 m layers are mainly examined, as they are directly showing the most pronounced changes.

Besides examining the periods of the building of the water power plants and the most important water layers, seasonal variations also have to be taken into account. Like mentioned before, water power plants might change the amount of water flowing into the fjords, especially regarding the natural seasonal averages. If the amount of water added has been changed through the building of the water power plants, this potentially becomes visible by observing the single periods only. Thus beside annual salinity and temperature values, a further division into summer and winter periods are used. The winter season is thereby defined by the months from January to March. Reason for this definition is the highest snow accumulation occurring during that period, as well as cold temperatures and little precipitation. Thus, naturally there would only be a small water inflow into the fjords due to snow and ice formation, as well as less precipitation (Figure 9). The summer season is defined by the months from May to July. Reason for that is again the natural water volume carried in the rivers through that period and the potential change owing to the water power plants. During these months there are the highest snow melt, large amounts

of precipitation as well as high temperatures occurring. Thus there is usually a large water inflow into the rivers. Due to the water dammed by the water power plants this inflow might become less, showing significant changes within the surface water salinity and temperature. These definitions for the seasons are also used for the climate data, showing local air temperature and precipitation, to allow a subsequent comparison with the hydrographical data.

1.3.3.3 Main working hypothesis

Due to the natural seasonal water inflow into the fjord, also the main working hypothesis is given. As the highest water inflow in an undisturbed fjord is in summer, the salinity values are supposed to be lower in that period. However, as many water power plants use dams impounding the water masses, they cause changes in the natural flowing regime of the fjords. Thus they cause less fresh water inflow during summer time compared to the natural flow regime. This could finally cause an increased surface salinity in the water bodies during the summer period. On the other hand, due to the high snow accumulation and less precipitation in winter the water inflow is naturally smaller, causing significantly higher salinity values compared to summer. However, again caused by the water damming, this inflow can now be higher than it usually would be. Thus, as the dams release more water than in normal winter flow regimes, they can cause a decrease in surface salinity values during the winter periods. Overall the building of the water power plants might have changed this naturally occurring seasonal water inflow, thus causing variations in the fjords hydrography, especially in the salinity and temperature values.

Beside that there is also the possibility of the salinity staying the same, while the change in water inflow mainly causes a thinner or thicker brackish water layer. As a consequence the compensation current possibly becomes lifted up or sinks down around 1 m or 2 m. This could cause more solar heat to be added to the compensation current and thus being transported into the fjords, overall causing an increase in water temperature.

However, there are also several other factors affecting the temperatures of the rivers. Thus it has to be kept in mind that the damming also changes the depth from which the water is finally taken. Thus in an unregulated environment the water entering the fjords is coming from the surface of the water source, for example from the lake surface. Against that, in regulated rivers the water streaming down is usually tapped from the deeper and colder part, featuring temperatures of around 4°C. As a result the regulated water will in summer

time thus be colder than unregulated water, while it is warmer in winter time. However, it has to be kept in mind that the Årøy-Power-Plant is an exception, still getting its water from the lake surface. Besides that, global warming might lead to warmer river water in general, thus finally also affecting the fjords. Additionally there can also be influences due to the origin of many rivers, being in the catchment area of glaciers. In case of an overall warmer summertime more ice from the glaciers might melt, finally increasing flow and volume of the rivers. This would also cause the river water to become colder, again having the ability to influence the fjords surface water in summer time (Dale, pers. com.). Overall this shows many factors which have to be kept in mind by considering potential causes for changes in temperature and salinity in the fjords. All the effects are strongest close to the fresh water outlets and are getting weaker with increasing distance. Thus the strongest signals are expected to be seen in the Inner part of the Sognefjord, while they are weakest at the outer end at the Sognesjøen and the output into the Nordic Sea.

1.3.4 Climate setting

1.3.4.1 Effects of Climate Change on Fjords

The climate is closely connected with the world's water masses, the rivers, fjords, lakes and oceans and hence strongly influencing the fjord water masses. Thus, around 22% of the average annual amount of winter precipitation directly enters the fjords. Regarding the Sogndalsfjord the average freshwater inflow accounts for 1,800 million m³ per year (Skoftealand, 1970). Overall, especially variations in the factors air temperature and the amount and distribution of precipitation can cause significant changes in the water bodies' hydrography. Thereby the global, but also local climate changes can cause effects in the different water properties. Thus in the frame of this bachelor thesis the local air temperature and precipitation values are observed, too. This enables to compare potential changes in the water hydrography with the climatic conditions during the same time, revealing possible correlations. Within the fjords, changes caused by climatic variations are strongest visible in the upper water layers, as these are directly influenced by temperature variations as well as changes in precipitation. Thus, a rise in precipitation, air temperature or water inflow into the fjord can reduce the density of the surface water mass, thereby maintaining the strongest signals in the surface. Signals indicating climatic changes are mainly seen in the salinity and water temperature values of the fjords. Thus, salinity and water temperature are important hydrographic properties, indicating climatic variations.

1.3.4.2 Climate Data

The climate data have been supplied by the Norwegian Meteorological Institute, which collects weather and climate data from historical to real time observations. Thereby the inherent internet page (dnmi.no, 2015) enables free access to all data available, comprising information about present and past climate. The Meteorological Institute thereby uses own weather stations, as well as from other institutions.

Already in the frame of “From Mountain to Fjord” 2014 the relevant data have been downloaded and used by Herman Blom. Thereby specifically the stations at Hafslø, Ytre Solund, Lavik, Fana Stend, Fjærland and Flesland were of interest. While Hafslø, Ytre Solund, Lavik and Fjærland are located in the county of Sogn og Fjordane in Western Norway, Fana Stend and Flesland are situated in the county of Hordaland, south of Sogn og Fjordane and thus close to Bergen. The locations can also be seen in Figure 11. All stations thereby specifically supplied climate data including temperature and precipitation values of the various regions. In the context of the study-program these data have then been analysed and used to answer the question of the science project 2014. The thereby downloaded data and originated graphs have then also been used for this thesis, forming the basis of the climate research.



Figure 11: Map showing the climate stations for precipitation measurements at Fana Stend, Ytre Solund, Lavik and Hafslø, as well as the stations at Flesland and Fjærland for temperature measurements.

1.3.4.3 The Barsnesfjord and Sogndalsfjord

Both, the Barsnesfjord and the Sogndalsfjord are located in the inner part of the Sognefjord. As a result their climate is less influenced by coastal conditions but mainly by inland effects. Regarding the different weather stations, the average temperature measured at Fjærland is most representative for the climate surrounding of the two fjords. Against that Hafslø mainly depicts the precipitation values, as it is the climate station closest to the Barsnesfjord and the Sogndalsfjord.

1.3.4.4 The Sognefjord and Sognesjøen

The Sognefjord data are delivered by the hydrographic station at the Sognesjøen, which is located around 20 km inwards from the entrance of the Sognefjord. Thus the climate is already strongly influenced by maritime effects. Regarding the average temperature, the climate station at Flesland is major representative. Thereby the average temperatures are higher than at Fjærland due to the influence of the warm Atlantic water along the coast. The precipitation conditions of the Sognesjøen and thus of the Sognefjord are mostly represented by the climate station at Ytre Solund.

1.3.4.5 The Nordic Sea and Station Mike

The climate over the Nordic Sea and thus at Station Mike is then featuring coastal and ocean influences only. Regarding the collected climate data of the different weather stations, the information from Ytre Solund is also mainly representative for Station Mike. Overall the climate at the Nordic Sea is strongly influenced by the North Atlantic Oscillation (NAO) as well as the inflow of Atlantic water. The NAO index describes the pressure difference occurring between the high air pressure system over the Azores and the low air pressure system over Iceland. Dependent on the strength and persistence of these pressure systems, there is a different appearance of large-scale westerly winds across the North Atlantic into the Nordic Seas (Anonymous, 2000). Thus a positive NAO index is correlated with strong westerly winds causing mild and wet climate over the Nordic Seas and consequently over the entire Sognefjord. On the other hand a negative NAO index causes the mild and wet climate to be carried towards southern Europe, resulting in cold and dry climate at Station Mike and the Sognefjord.

Overall the North Atlantic Oscillation is a winter phenomenon, mainly visible from December to March due to the strongest atmospheric circulation there (Skjoldal et al., 2004). Beside that the NAO also influences the water transport and distribution as well as vertical mixing and surface heat fluxes at the Nordic Sea. Additionally to the NAO the Nordic Seas climate is also influenced by high level cloud cover and relatively large amounts of precipitation. In average this region has between 340 mm/year and 500 mm/year precipitation, being especially strong along the Norwegian coast and thus close to the region of Station Mike. There about 1000 mm/year precipitation is typical due to wind-induced uplift of moist air against the steep mountain ranges of Norway. In general there is approximately a balance between precipitation and evaporation at Station Mike (Anonymous, 2000).

Another factor influencing the weather of the Nordic Sea is the Atlantic Multi-decadal Oscillation (AMO). It is describing a naturally occurring variability in the sea surface temperature of the North Atlantic Ocean. Thereby the AMO has a regularity of around 60 to 80 years with cold and warm phases lasting for periods between 20 and 40 years. The Atlantic Multidecadal Oscillation is already occurring since the last 1,000 years, as has been observed with proxy records. In general the effects of the AMO comprise temperature and precipitation changes over most of the northern hemisphere, causing droughts and Atlantic hurricanes. Thus a positive AMO is correlated with less precipitation, while a negative AMO features high precipitation amounts, respectively. Since around 1990 the AMO is featuring a warm phase (noaa.gov, 2015)

The entire region features a relatively mild climate, with temperatures that are around 10°C higher compared to other regions at the same latitudes. Reason for that is the common south-westerly wind, causing a warming of the ocean currents. This heat is then also trapped during the winter period, influencing the regions climate. According to this and because of the large amount of heat carried up with the Atlantic Current, the entire region is very sensitive for climate changes (Walczowski, 2014). This is significant as there are strong yearly, multidecadal and decadal changes in the strength of the westerly's caused by the NAO. Thus there was a shift from weak ones around 1960 to strong winds in the 1990s (Furevik et al., 2006).

2. Materials and Methods

All hydrographical and meteorological data have already been used in the frame of the “From Mountain to Fjord”-program 2014 at the University College of Sogn og Fjordane in Sogndal. Thereby they have been examined by the participating students with regards to a science project, covering the question “Water power plants: The impact of river water regulation on the Sognefjord environment”. The final results were presented on a public seminar on 17th of December 2014 at the Hogskulen i Sogn og Fjordane. Thus the participants of the course either downloaded or collected the data by taking samples at different locations within or near the Sognefjord. Afterwards they dealt with the data in order to give an answer on the science project, creating graphs and excel sheets. These are finally also the basic data used for further examinations in the frame of this bachelor thesis. Figure 12 shows the locations of the different measuring stations which are also explained more detailed in the subsequent Chapters.

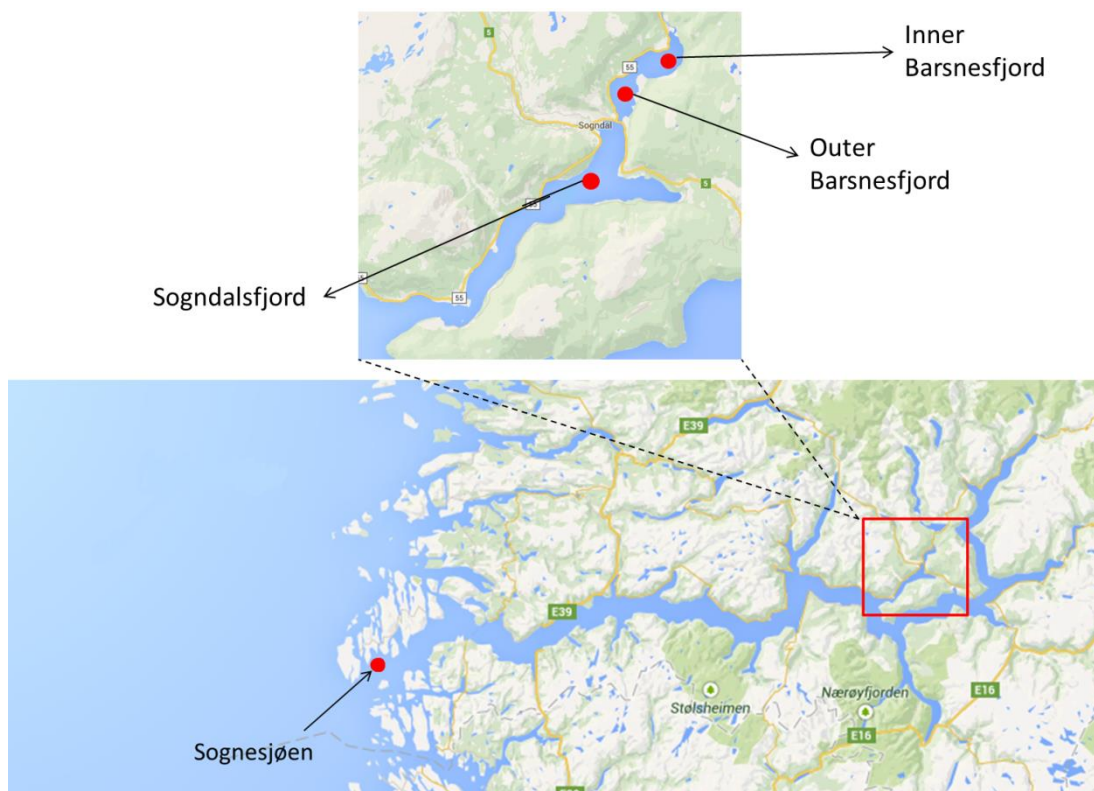


Figure 12: Map showing the different hydrographic measuring Stations. The Sognesjøen representing the water masses of the Sognefjord, the Sogndalsfjord and the Outer and Inner Barsnesfjord. Station Mike is located too far outside, as can be seen on Figure 7.

The two main devices that have been used for the data sampling are a CTD sensor and a Nansen Water Bottle. CTD thereby stands for conductivity, temperature and depth (Crescentini et al., 2012). The device measures the conductivity and the temperature values

of the water masses at certain depths, while density and salinity can be calculated from these measurements. Regarding large measurements like at the Nordic Sea, the measured information is in real-time directly sent back to the ship due to a cable connecting the CTD instrument with a computer aboard. In case of smaller works like for the measurements at the Barsnesfjord, also devices can be used that do not directly transfer the data. These can afterwards be downloaded on specific platforms. The CTD itself consists of several small probes fitted into a frame, as also visible in Figure 13. Due to a remotely controlled device the single bottles can be closed individually, allowing taking samples at different depths (Lawson and Larson, 2001).

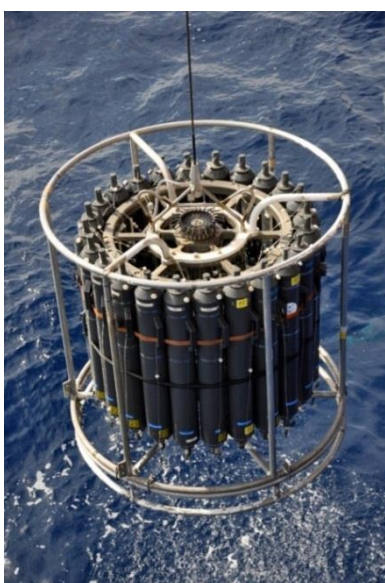


Figure 13: CTD sensor used for deep sea hydrographical measurements. (schmidtocean.org, 2015)

The Nansen reversing water bottle is an apparatus used previously for taking sea-water samples from different water depths. The peculiarity is the preservation of the water temperature without the appearance of changes higher than one-hundredth of a degree celsius when bringing the bottle to the surface. It consists of a cylindrical body containing a central tube which is surrounded by several concentric chambers of non-conducting material. These are simultaneously filled with water, serving the purpose of insulation. The cylindrical form prevents the apparatus from heating by compression. The general function of a Nansen Water Bottle can be seen in Figure 14. While the water bottle is let down into the water, its base is open, enabling the water masses to freely pass the devise. At the requested depth, when lifting the apparatus up again, a weight hanging from the sides of the lid cause it to drop and thus encloses the three single parts, locking the water mass inside. The temperature is then determined by using a thermometer that is also sheltered against pressure (Mill, 1900).



Figure 14: Nansen water bottle before, during and after reversing. (oceanworld.tamu.edu, 2015)

2.1 The Barsnesfjord and Sogndalsfjord

The hydrographical data of the Barsnesfjord and the Sogndalsfjord have been supplied through the “100 year record of hydrographical data in the Inner and Outer Barsnesfjord and the Sogndalsfjord” (Kaufmann, 2014). This document thereby includes temperature and salinity data from the Inner and Outer Barsnesfjord as well as from the Sogndalsfjord. Additionally temperature and salinity data from the surface layers of the Barsnesfjord are used, ranging from 1982 to 1985. All these data have been provided by the “Norwegian Water Resources and Energy Directorate” (NVE) (nve.no, 2015).

Furthermore data sampled in the frame of the “From Mountain to Fjord”-program of the Sogn og Fjordane University have been added. As this course is taking place during the winter semester, these data are covering the winter values of the fjords. The data have been collected during diverse excursions, realized by taking samples from a boat. Overall the used equipment for all measurements was a CTD sensor after 2001 and a Nansen water bottle before 1980. Beside that a salinometer was used from 1981 until 1983.

As already mentioned above, all data used for this thesis have already been processed in the frame of the “From mountain to Fjord”-program 2014. Thus the students Ina Kleitz and Dirk Oosterholt examined the data of the Barsnesfjord and the Sogndalsfjord in respect of the Science project 2014. By using the different data sets, finally enough information have been available to form useful graphs and excel sheets. Thereby they used the depths 1 m, 5

m, 10 m, 20 m, 30 m, 40 m, 50 m, 60 m, 75 m, as well as partly 50 m, 100 m, 150 m and 200 m for producing documents and files. These have also been used in the course of this bachelor thesis, as the fundamental data about the fjords. However it has to be mentioned, that the results of the Inner Barsnesfjords are only shown in Appendix VI, as they do not reveal further information regarding the overall question of this work. The data regarding the Inner and Outer Barsnesfjord have also already been used before (Kaufmann, 2014).

2.2 The Sognefjord and Sognesjøen

Also in the course of the “From Mountain to Fjord”-program 2014 the data regarding the Sognesjøen region have been downloaded from the homepage of Havforskningsinstituttet (imr.no, 2015b), the Institute of Marine Research (IMR) in Norway. The IMR has its headquarter in Bergen, however, with several branches dislodged. The main work done by the IMR is the supply of the public with information about the marine environment and aquaculture of the Nordic Sea as well as the Norwegian Coastal Region. Thus the IMR collects continuous data by using instruments like vessels, observations buoys and manual measurements. Therefore they, among others established eight fixed hydrographical stations in the time between 1935 and 1947 which are located along the Norwegian coast from Lista up to the Nordkapp. These are measuring the coastal and the oceanic climate. As mentioned in Chapter “1.3.4.4 The Sognefjord and Sognesjøen”, regarding the Sognefjord the measuring station is located at the Sognesjøen, supplying hydrographical temperature and salinity data with a regularity of two measurements per months. Thus it is delivering continuous long-time measurements that can be used for scientific researches. While the station measures the depths of 1 m, 10 m, 50 m, 75 m and 100 m since 1935, 20 m and 30 m are first measured since 1971 and 5 m since 1994 (imr.no, 2015a). All depths have then been used for the science project as well as for this thesis. Thereby two students of the “From Mountain to Fjord”-program, Maike Dierks and Elizabeth van Kapel worked up the data with regard to that project. Thus they produced graphs and excel sheets to utilize the data from the Sognesjøen station. The results have then been used for further examinations within the scope of this work.

2.3 The Nordic Sea and Station Mike

The data giving information about the Nordic Sea have been measured at the Ocean Weather Ship Station (OWS) Mike, which is located at 66°N and 2°E in the Norwegian Sea. It delivers the longest continuous time series of hydrographic measurements at the Nordic Sea. EuroSITES thereby is an integrated European network, measuring water properties in water masses with more than 1000 m depth. In total they are running nine deep-ocean observatory sites. At Station Mike they therefore use a CTD-sensor, measuring at depths between 0m and 2000m (Figure 13). While the data on water temperature, density and salinity are measured since 1948, the oxygen concentration values are measured since 1950 (eurosites.info, 2015a). However, the oxygen concentration values have not been used in the frame of this thesis. At Station Mike all four factors are measured in a daily routine as well as additionally every week at depths down to 2000 m and down to depths around 1000 m three to four times a week. Hence “Station Mike” is delivering a huge data set for all investigated factors.

Under the program of “From Mountain to Fjord” all required hydrographical data have been downloaded from the EuroSITES homepage (eurosites.info, 2015b), covering salinity-, temperature-, oxygen- and density values of the Nordic Sea. However, only the upper water masses of the ocean are entering the fjords. Thus just the upper 0 m to 500 m have been downloaded and finally used, as only these are closely connected with the fjord systems and hence signaling global changes. The data have then been examined in respect to the science projects topic. Thereby a group of two persons, Nicolai Heinnickel and me, Theresa Reß, has worked on the data creating graphs and excel files which could be used for subsequent interpretations. Both, the excel files containing the entire data sets as well as the graphs have then been placed at the disposal for the purpose of this bachelor thesis.

2.4 Characteristics of the various data and some assumptions

Additionally to the above mentioned sources of the different data, there are some particularities within the values that have to be mentioned.

Thus, there have been slight changes used, regarding the seasons in case of the Sogndalsfjord and the Outer Barsnesfjord. In both cases there are only few data available for the pre-defined winter and summer periods. Hence, in case of these two fjords, the winter season is defined two months longer, finally lasting from November until March. Through the addition of November and December enough data are available to make useful

and meaningful graphs. Even though the period is now two months longer than at Station Mike and the Sognesjøen, it still represents the time of the highest snow accumulation, cold temperatures and less precipitation. Thus it still indicates the time of the main winter period. The summer season at the Sogndalsfjord and Outer Barsnesfjord is defined by the months from May to August and thereby also lasts one month longer than at the Nordic Sea and the Sognesjøen. Reason is again the low amount of data during the months from May to July. Thus to enable useful graphs, the month August is added. In this case, too, the addition does not change the overall indication of the period. Even though the season lasts one month longer, it still represents the time with the highest temperatures, the highest snow melt as well as a lot of precipitation. Thus it still indicates the defined summer period.

Furthermore, considering the summer temperature data from the Sogndalsfjord and from the Outer and Inner Barsnesfjord, the values representing the last period from around 2000 until the end of the measurements are sampled mainly during August. Thus it has to be taken into account, that the sampling took place during a period with warmer air temperatures than in case of the other data. Hence, a potential temperature increase within that time can maybe be related to this late time of sampling. This has to be considered while analyzing and describing the graphs.

The same is valid in case of the salinity values of the three fjords, the Sogndalsfjord as well as the Outer and Inner Barsnesfjord. The summer data representing the last measured period from around 1999 until the end are also mainly sampled during August. Thus, unlike the rest of the data these values are sampled during a period with higher overall air temperatures. Besides that the winter salinity values representing the period from 2005 until 2014 have been sampled mainly at the aqua-culture-station. While the rest of the data has been gained more in the middle part of the Fjord, these values are sampled close to the shore, being possibly stronger influenced by the Sogndalsriver, which however is usually small in winter time. Thus the data might depict stronger fluctuations then during the previous periods. Hence, by observing the data, this has to be considered.

3. Results

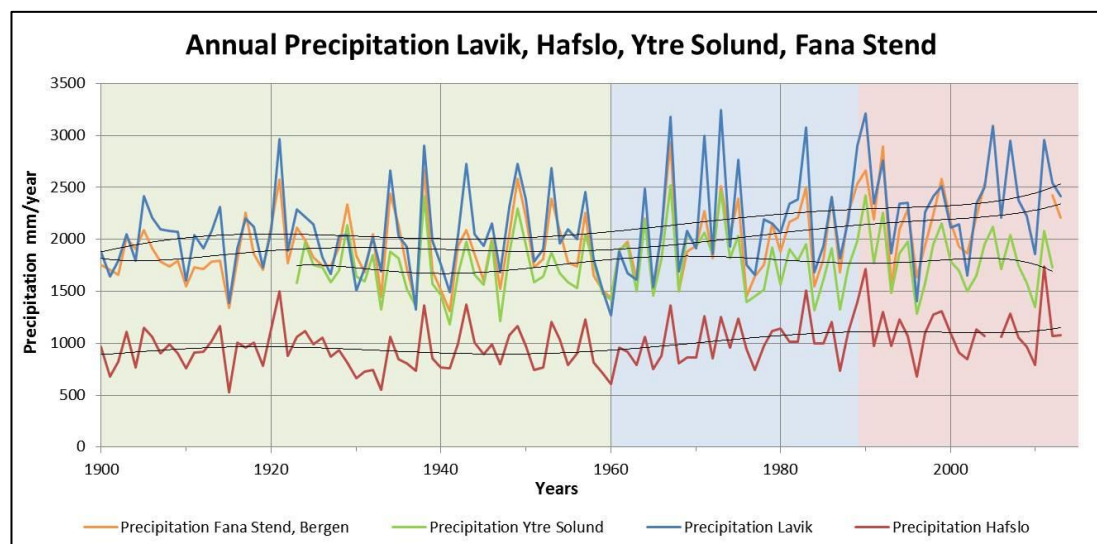
3.1 Climate

3.1.1 Precipitation

The subsequent precipitation Graphs 1 to 3 show the average amount of precipitation in mm/year for annual, winter and summer situation. It was measured at the four climate stations in Lavik, Hafslo, Ytre Solund and Fana Stend, Bergen. The measuring period is from 1900 until 2013, what can be seen on the x-axes, ranging from 1900 until 2015. However, while Lavik, Hafslo and Fana Stend, Bergen have been measured since 1900, Ytre Solund was first added in 1923. Against that the y-axes depict the precipitation in mm/year. The different background colors depict the three periods, before, while and after building of the water power plants.

The Tables 1 to 3 represent the average precipitation during the three periods (Figure 10) before, during and after building of the water power plants, what is also marked by the three background colors. Additionally the tables show the difference between period one and three in mm/year and %.

3.1.1.1 Annual



Graph 1: Average annual precipitation in mm/year measured at the four climate stations at Fana Stend, Ytre Solund, Lavik and Hafslo from 1900 until 2013. The y-axis represents the precipitation in mm/year, while the x-axis shows the measured years. The three colors depict the different periods: green = pre-impact period, blue = transitional period, red = full-impact period. Additionally trend lines have been included.

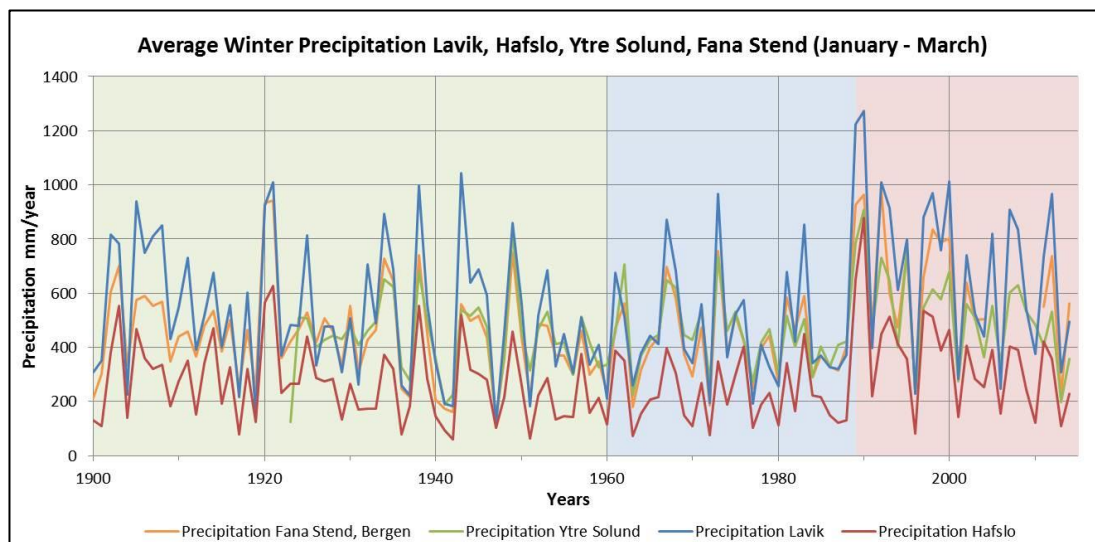
Precipitation [mm/year]: Annual					
	1. Period 1900-1960	2. Period 1961-1989	3. Period 1990-2013	Change 1. to 3.	Change in %
Fana Stend, Bergen	1872,37	2018,56	2211,26	338,89	18,10%
Ytre Solund	1708,18	1807,82	1813,60	105,41	6,17%
Lavik	2017,36	2189,79	2368,99	351,64	17,43%
Hafslo	930,26	1023,23	1119,78	189,52	20,37%

Table 1: Average annual precipitation in mm/year for Fana Stend, Ytre Solund, Lavik and Hafslo, calculated for the three pre-defined periods, as well as the difference between period 1 and 3 in mm/year and %. The three colors depict the different periods: green = pre-impact period, blue = transitional period, red = full-impact period.

Graph 1 shows the average annual precipitation values, with fluctuations between 1500 mm/year and 300 mm/year at Fana Stend, Ytre Solund and Lavik, while the fluctuations at Hafslø are leveling between 500 mm/year and 1500 mm/year. Beside that it is striking that the yearly variations at all stations are following the same patterns. Additionally at all measuring stations fluctuations from around 1000 mm/year are visible through the entire period (Graph 1). However at Lavik the general fluctuations seem to be higher, accounting for variations of more than 1500 mm/year during some periods. This trend of higher fluctuations is occurring in a similar way at Fana Stend, Bergen, which in general shows values close to those measured at Lavik.

Furthermore it is clearly visible that the average amount of precipitation is lowest at Hafslo, followed by Ytre Solund, Fana Stend and Lavik being relatively similar. Regarding the single graphs, the precipitation at Lavik and Fana Stend seems to increase after 1960, causing a rise to 338.89 mm/year more rain at Fana Stend and 351.64 mm/year more at Lavik (Table 1). Beside larger average precipitation at both stations, at Lavik this also causes higher fluctuations between maxima and minima values. The amount of rain at Hafslo and Ytre Solund also seems to show a slight increase by comparing the first and the last period. Thus the precipitation increases at 189.52 mm/year at Hafslo, and 105.41 mm/year at Ytre Solund, indicating more precipitation especially after around 1980. Thus, overall there is a significant increase in precipitation at all stations.

3.1.1.2 Seasonal



Graph 2: Average winter precipitation in mm/year measured at the four climate stations at Fana Stend, Ytre Solund, Lavik and Hafslø from 1900 until 2013. The y-axis represents the precipitation in mm/year, while the x-axis shows the measured years. The three colors depict the different periods: green = pre-impact period, blue = transitional period, red = full-impact period.

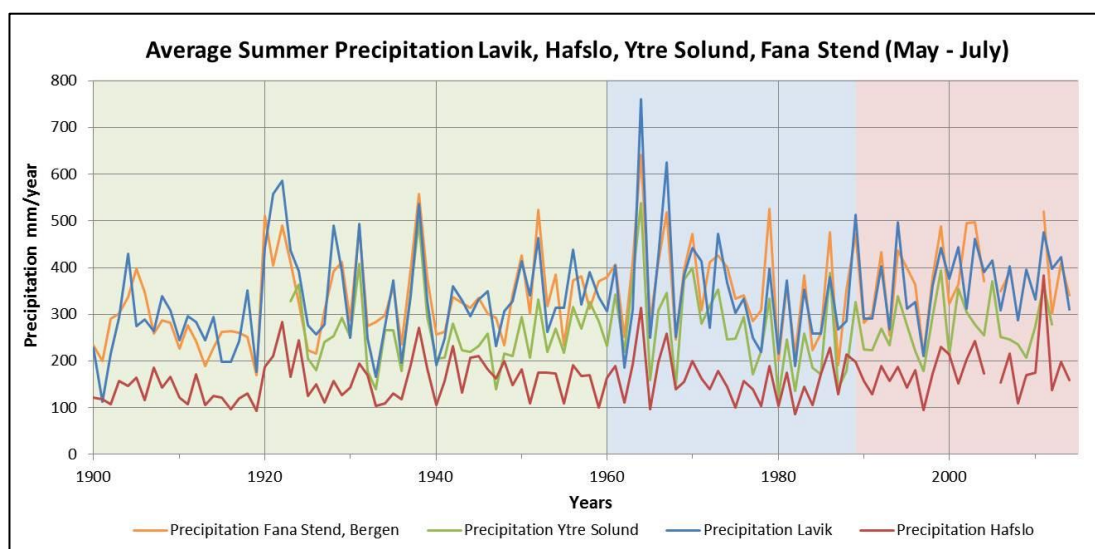
Precipitation [mm/year]: Winter Period					
	1. Period 1900-1960	2. Period 1961-1989	3. Period 1990-2014	Change 1. to 3.	Change in %
Fana Stend, Bergen	439,77	436,66	596,18	156,41	35,57%
Ytre Solund	432,37	456,65	515,79	83,42	19,29%
Lavik	522,90	491,02	682,53	159,63	30,53%
Hafslø	264,68	241,72	348,54	83,86	31,68%

Table 2: Average winter precipitation in mm/year for Fana Stend, Ytre Solund, Lavik and Hafslø, calculated for the three pre-defined periods, as well as the difference between period 1 and 3 in mm/year and %. The three colors depict the different periods: green = pre-impact period, blue = transitional period, red = full-impact period.

Graph 2 shows the annual winter precipitation values, depicting a general level of fluctuations that is ranging between 100 mm/year and 1000 mm/year with only one interruption due to a large peak around 1990. As seen, there are relatively large fluctuations in winter precipitation at all climate stations during the entire period (Graph 2). Thus there are high peaks at all stations during the years 1921, between 1934 and 1949 and especially in the period after the highest peak in 1989.

Beside that there is also a slight increase in precipitation measurable at the different stations (Table 2), showing the calculated differences between period one and three. At Lavik and Fana Stend this increase is the largest, regarding the absolute values. Thus it is

accounting for 156.41 mm/year at Fana Stend and 159.63 mm/year more precipitation at Lavik. Beside that the increase at Ytre Solund and Hafslø is smaller, only around 83 mm/year more at both stations. However, considering the relative values, Fana Stend and Hafslø depict the largest increase in precipitation, of more than 30%. Regarding the Inner parts of the Sognefjord and hence Ytre Solund, Lavik and Hafslø, the average increase in precipitation accounts for 27.2%, being strongest at Hafslø. Overall the general trend seems to show an increase in winter precipitation.



Graph 3: Average summer precipitation in mm/year at the four climate stations at Fana Stend, Ytre Solund, Lavik and Hafslø from 1900 to 2013. The x-axis shows the years and the y-axis the precipitation in mm/year. The three background colors depict the different periods: green = pre-impact period, blue = transitional period, red = full-impact period.

Precipitation [mm/year]: Summer Period					
	1. Period 1900-1960	2. Period 1961-1989	3. Period 1990-2014	Change 1. to 3.	Change in %
Fana Stend, Bergen	320,76	362,91	376,90	56,14	17,50%
Ytre Solund	259,54	270,15	270,41	10,87	4,19%
Lavik	319,49	350,45	365,37	45,87	14,36%
Hafslø	155,18	163,17	180,44	25,25	16,27%

Table 3: Average summer precipitation in mm/year for Fana Stend, Ytre Solund, Lavik and Hafslø, calculated for the three pre-defined periods, as well as the difference between period 1 and 3 in mm/year and %. The three background colors depict the different periods: green = pre-impact period, blue = transitional period, red = full-impact period.

Graph 3 represents the summer precipitation values for all stations, with Table 3 adding the calculated averages. Overall the fluctuations of all stations are leveling within a range of

100 mm/year and 500 mm/year, only interrupted by some large peaks around the years 1920, 1940, 1964 and 1967.

At Lavik a strong increase in precipitation is visible by comparing the measuring periods, depicting a rise in the amount of rain of 45.87 mm/year. Beside that there are huge peaks visible around 1920, 1940, 1964 and 1967. A similar rising trend is shown at Fana Stend, Bergen, where the average precipitation rises at 56.14 mm/year. The measurements at Bergen show even more very strong peaks, indicating high summer precipitation in 1920, 1938, 1952, 1964, 1967 and 1979. In the period after 1979 the high number of peaks seems to represent the general rise in average precipitation of 17.5% (Table 3).

Considering the %-values, like in the winter period the increase in average precipitation is second largest at Hafslø, accounting for 16.27 % (Table 3). Thus the inner part of the fjord again features the largest increase in %. Beyond that it is visible that there are also peaks in precipitation at Hafslø during the years 1922, 1938, 1965 and 2011. Regarding the precipitation values measured at Ytre Solund, there is in general a slight rise of 10.87 mm/year noticeable, as well as some big peaks in 1931, 1938 and 1964. Overall this indicates a significant increase in precipitation at all four climate stations. The calculated average of Ytre Solund, Lavik and Hafslø thereby shows a rise of 11.6%, thus showing the largest increase in precipitation to occur in wintertime.

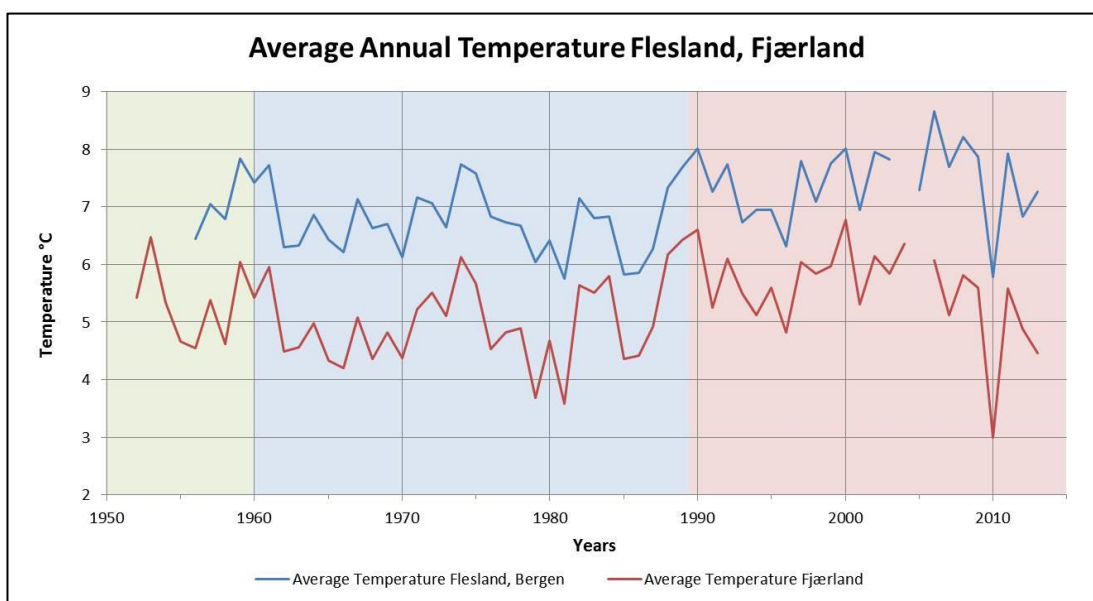
3.1.2 Temperature

The following Graphs 4 until 6 show the annual and seasonal temperatures in °C, measured at the climate stations at Flesland and Fjærland. The x-axes thereby depict the measuring period from 1952 until 2013, ranging from 1950 till 2015. Beside that the y-axes show the temperature in °C. The three background colors depict the different periods, before, while and after building of the water power plants.

The Tables 4 until 6 represent the calculated average temperatures for the three periods at Flesland and Fjærland. Additionally they show the difference between the first and the last period in °C and %. The tables also feature the three background colors for the three defined periods.

3.1.2.1 Annual

Graph 4 shows the entire data set of annual temperature values measured for the two climate stations. Thereby the level of temperature fluctuations at Flesland is ranging between 6.0°C and 8.0°C, while the variations at Fjærland range between 4.5°C and 6.5°C with only few exceptions. Thus the temperatures at Flesland are about 1.5°C higher than the measured temperatures at Fjærland. Above that both stations show similar peaks and troughs, indicating the same temperature trend, only increased at 1.5°C.



Graph 4: Average annual temperature in °C, measured at the climate stations at Flesland and Fjærland during the period from 1952 until 2013. The y-axis represents the temperature in °C, while the x-axis shows the years. The three background colors depict the different periods: green = pre-impact period, blue = transitional period, red = full-impact period.

Temperature [°C]: Annual					
	1. Period 1952-1960	2. Period 1961-1989	3. Period 1990-2013	Change 1. to 3.	Change in %
Flesland, Bergen	7,11	6,72	7,43	0,32	4,50%
Fjærland	5,32	4,97	5,56	0,24	4,45%

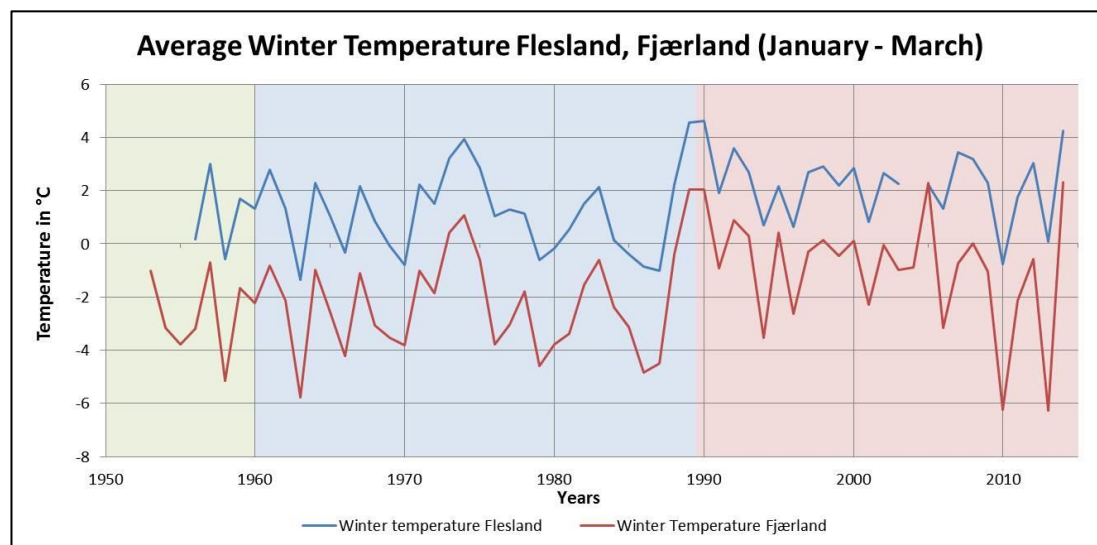
Table 4: Average annual temperature in °C at Flesland and Fjærland for the three pre-defined periods, as well as the difference between period 1 and 3 in °C and %. The three background colors depict the different periods: green = pre-impact period, blue = transitional period, red = full-impact period.

By comparing the three measuring periods, the temperatures decline from the first to the second period (Table 4). Thus the temperatures drop from 7.11°C to 6.72°C at Flesland and from 5.32°C to 4.97°C at Fjærland. However, there is a significant increase in temperature noticeable at both stations during the third period. Overall this causes a rise in temperature

of 0.32°C at Flesland and 0.24°C at Fjærland from the first to the third period, exceeding the initial temperatures with approximately 4.5% at both stations.

However, this increasing trend is not continuous, as the temperatures seem to slightly drop after 2005 (Graph 4). Additionally the rising trend is interrupted by a big trough in 2010, representing a year with very low temperatures.

3.1.2.2 Seasonal



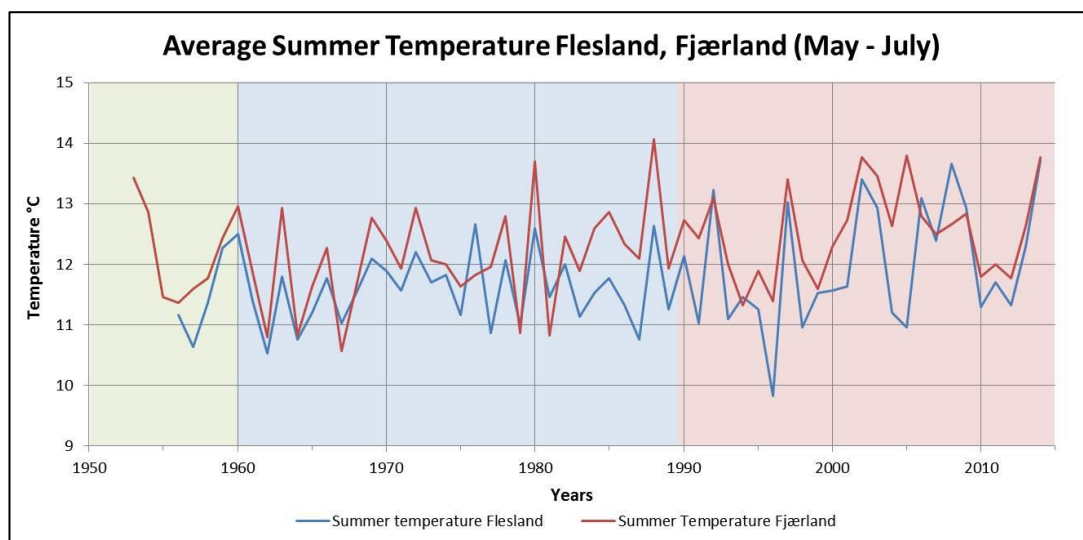
Graph 5: Average winter temperature in °C, measured at the climate stations at Flesland and Fjærland during the period from 1952 until 2013. The y-axis represents the temperature in °C, while the x-axis shows the years. The three background colors depict the different periods: green = pre-impact period, blue = transitional period, red = full-impact period.

Temperature [°C]: Winter Period					
	1. Period 1953-1960	2. Period 1961-1989	3. Period 1990-2014	Change 1. to 3.	Change in %
Flesland	1,13	1,14	2,23	1,11	98,10%
Fjærland	-2,61	-2,26	-0,95	1,67	-63,76%

Table 5: Average winter temperature in °C at Flesland and Fjærland for the three pre-defined periods, as well as the difference between period 1 and 3 in °C and %. The three background colors depict the different periods: green = pre-impact period, blue = transitional period, red = full-impact period.

Graph 5 shows the average winter temperature at the two stations, with variations at Fjærland leveling between -5.0°C and +1.0°C while Flesland represents variations within a range of -1.0°C and 4.0°C. Additionally it can be seen that again both stations show a similar behavior regarding peaks and troughs during the entire measuring period. However, what is even more apparent is a significant rise in temperature at both stations, Flesland and Fjærland, starting around 1988. This causes the temperatures to increase with 1.11°C at

Flesland and 1.67°C at Fjærland from period one to period three (Table 5). Even though there are some marked minima around 2010, the overall trend indicates a general increase in average winter temperatures. By comparing the summer and the winter period, the largest increase is visible at Fjærland in winter time, rising from -2.61 to -0.95. Thus there is a significant increase in winter temperature at both stations.



Graph 6: Average annual temperature in °C, measured at the climate stations at Flesland and Fjærland during the period from 1952 until 2013. The y-axis represents the temperature in °C, while the x-axis shows the years. The three background colors depict the different periods: green = pre-impact period, blue = transitional period, red = full-impact period.

Temperature [°C]: Summer Period					
	1. Period 1953-1960	2. Period 1961-1989	3. Period 1990-2014	Change 1. to 3.	Change in %
Flesland	11,59	11,57	11,99	0,40	3,49%
Fjærland	12,24	12,09	12,54	0,30	2,45%

Table 6: Average summer temperature in °C at Flesland and Fjærland for the three pre-defined periods, as well as the difference between period 1 and 3 in °C and %. The three background colors depict the different periods: green = pre-impact period, blue = transitional period, red = full-impact period.

Graph 6 now shows the average summer temperature and Table 6 the therefor calculated averages. The overall level of both stations is fluctuating between 10.5°C and 13.5°C. Regarding the entire graph it is visible, that the temperatures measured at both stations are more similar during the summer season than they are by considering annual values.

Fjærland seems to show bigger variations in temperature, indicating stronger differences between maxima and minima temperature. Additionally there seems to be an increase in temperature during the last period at both stations, starting around 1985. Thus the average temperatures are rising at 0.40°C at Flesland and at 0.30°C at Fjærland (Table 6). In both

cases this increase causes the overrun of the initial temperatures. Moreover it can be seen that Fjærland is warmer in summer and colder in winter, compared to Flesland, thus depicting a larger range of fluctuations.

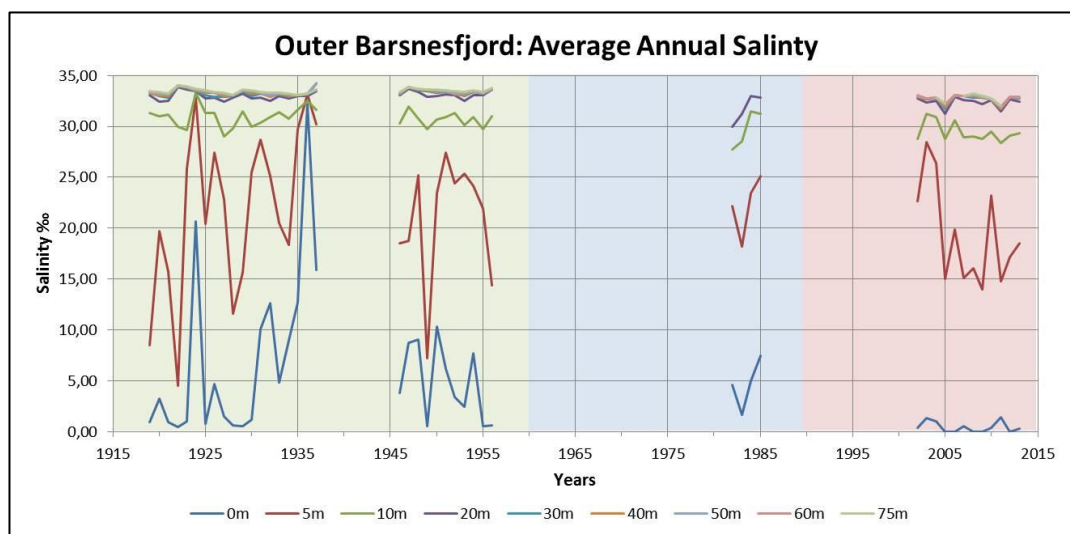
3.2 Hydrography Outer Barsnesfjord

3.2.1 Salinity

The subsequent Graphs 7 until 9 are showing the average salinity in ‰ measured in the Outer Barsnesfjord for annual and seasonal situations. Thereby the x-axes depict the time in years from 1915 until 2015 in steps of ten years, while the y-axes show the salinity in ‰ in steps of 5‰. The three background colors depict the different periods, before, while and after building of the water power plants. Thereby the depths of 0 m, 5 m, 10 m, 20 m, 30 m, 40 m, 50 m, 60 m and 75 m have been measured. It additionally has to be pointed out, that the 0 m layer represents the lowest salinity and thus is located at the bottom of the graph, with increasing salinities and deep layers on top.

The Tables 7 to 9 depict the calculated annual salinity averages in ‰ for the three periods for the Outer Barsnesfjord. Additionally they show the difference between period one and three in ‰ and %. The blue colors thereby show the different kinds of water masses, however, the transition zones can be slightly variable as the water masses blend into each other.

3.2.1.1 Annual



Graph 7: Average annual salinity in ‰ measured at the Outer Barsnesfjord in the depths from 0 m to 75 m. The x-axis thereby shows the years from 1915 until 2015 in steps of ten years, while the y-axis depicts the salinity in ‰, ranging from 0‰ to 35‰ in steps of 5‰. The three background colors depict the different periods: green = pre-impact period, blue = transitional period, red = full-impact period.

Salinity [‰]: Outer Barsnesfjord Annual						
Depth [m]	1. Period 1916-1960	2. Period 1961-1989	3. Period 1990-2013	Change 1. to 3.	Change in %	
0	6,06	5,48	0,45	-5,61	-92,61 %	Brackish Water
5	21,35	22,23	19,26	-2,10	-9,81 %	Compensation Current
10	30,86	29,66	29,44	-1,42	-4,60 %	Intermediate Water
20	33,03	32,25	32,36	-0,67	-2,02 %	Threshold Turbulence
30	33,27	34,13	32,64	-0,63	-1,88 %	Basin Water
40	33,35	n.d.	32,68	-0,67	-2,01 %	
50	33,41	34,52	32,74	-0,66	-1,99 %	
60	33,43	34,52	32,82	-0,61	-1,82 %	
75	33,47	34,52	32,76	-0,71	-2,13 %	

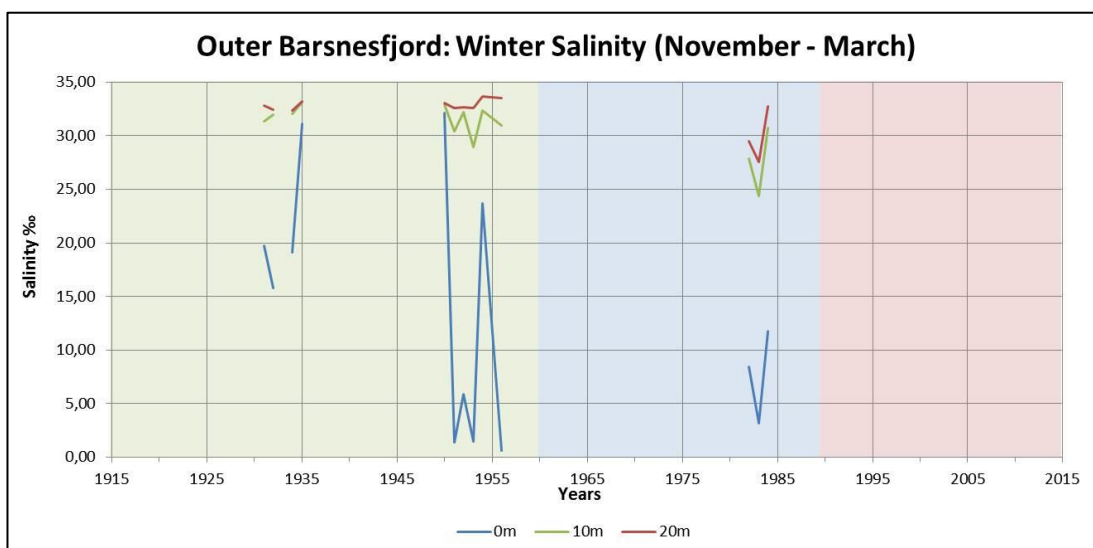
Table 7: Average annual salinity in ‰ at the Outer Barsnesfjord for the three pre-defined periods as well as the difference between period 1 and 3 in ‰ and %. The blue colors depict the different kinds of water masses, however, the transition zones can slightly vary.

Graph 7 shows the average annual salinities in ‰. Especially the 0 m layer thereby shows huge fluctuations, ranging from nearly 0.0‰ to almost 35.0‰. Against that the 5 m layer is leveling between 7.5‰ and 30.0‰, while the 10 m layer ranges between 27.5‰ and 32.5‰. In the 20 m to 75 m layers, the fluctuations are laying very close, ranging between 31.0‰ and 34.0‰.

Beside that it can be seen that all layers show a slight decline in salinity during the three periods. The decline is largest in the 0 m surface layer, causing a drop from 6.06‰ to 0.45‰ (Table 7). However, due to the high amount of data included in this graph detailed statements are difficult.

3.2.1.2 Seasonal

Graph 8 represents the average winter salinities in ‰ at the Outer Barsnesfjord, however, just depicting the period from 1931 until 1984. The measured depths comprise 0 m, 5 m, 10 m, 20 m, 30 m, 40 m, 50 m, 60 m and 70 m. Additionally it has to be pointed out, that only the period before and during the building of the water power plants are visible, due lack of data. Overall the average level of the 5 m to 70 m layers is ranging between 27.5‰ and 34.0‰ before 1960 and between 20.0‰ and 32.5‰ after 1980. Against that the 0 m layer displays the most significant fluctuations, ranging from 0.0‰ to around 30.0‰.

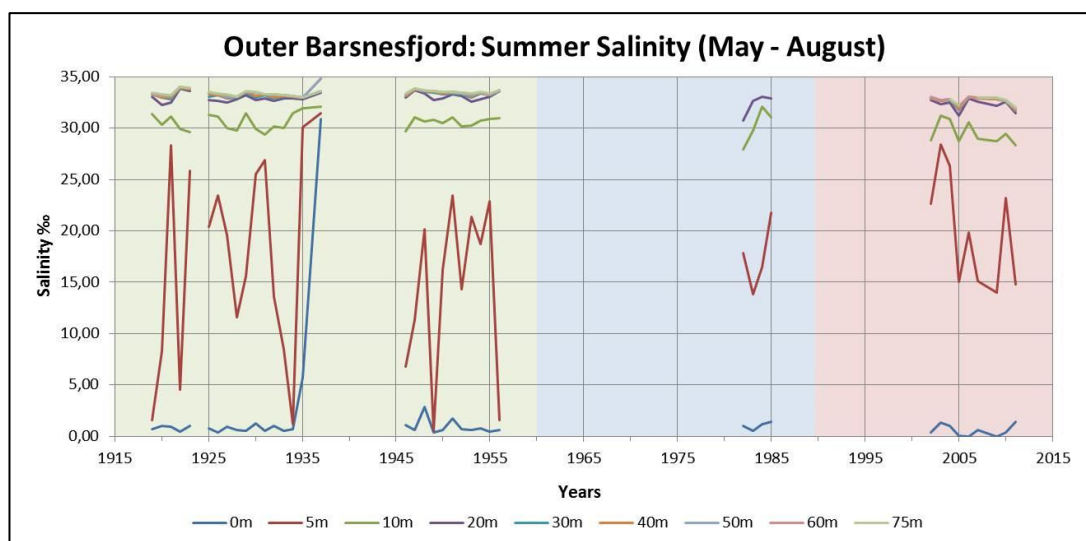


Graph 8: Average winter salinity in ‰ measured at the Outer Barsnesfjord between 1931 and 1984. The x-axis shows the years from 1915 until 2015, while the y-axis depicts the salinity in ‰. The three background colors depict the different periods: green = pre-impact period, blue = transitional period, red = full-impact period.

Salinity [‰]: Outer Barsnesfjord Winter Period						
Depth [m]	1. Period 1931-1960	2. Period 1961-1984		Change 1. to 2.	Change in %	
0	14,48	7,76		-6,72	-46,39%	Brackish Water
5	30,50	25,39		-5,11	-16,75%	Compensation Current
10	31,51	27,64		-3,87	-12,27%	Intermediate Water
20	32,93	29,91		-3,02	-9,18%	Threshold Turbulence
30	33,26	n.d.				Basin Water
40	33,19	n.d.				
50	33,29	n.d.				
60	33,42	n.d.				
75	33,45	n.d.				

Table 8: Average winter salinity in ‰ at the Outer Barsnesfjord for the three pre-defined periods as well as the difference between period 1 and 2 in ‰ and %. The blue colors depict the different kinds of water masses, however, the transition zones can slightly vary.

Despite relatively large periods without data, regarding the entire time period there is a strong decline in salinity visible in all layers (Graph 8). This reduction is most pronounced in the uppermost 0 m layer, thus depicting a huge decline of 46.39% (Table 8). Beside that the 10 m and 20 m layers show a less extreme but still significant drop of 16.75% and 12.27% (Table 8). Overall it thereby depicts a large decrease in salinity in winter time. However, despite adding more months there are still big gaps without data, making it difficult to interpret the progress of the salinity during these periods.



Graph 9: Average summer salinity in ‰ measured at the Outer Barsnesfjord between 1916 and 2011. The x-axis shows the years, while the y-axis depicts the salinity in ‰. The three background colors depict the different periods: green = pre-impact period, blue = transitional period, red = full-impact period.

Salinity [‰]: Outer Barsnesfjord Summer Period						
Depth [m]	1. Period 1916-1990	2. Period 1961-1989	3. Period 1990-2011	Change 1. to 3.	Change in %	
0	2,04	1,03	0,57	-1,47	-72,19 %	Brackish Water
5	16,18	17,48	19,93	3,75	23,21 %	Compensation Current
10	30,67	30,21	29,54	-1,12	-3,66 %	Intermediate Water
20	33,01	32,34	32,30	-0,72	-2,17 %	Threshold Turbulence
30	33,27	n.d.	32,58	-0,70	-2,09 %	Basin Water
40	33,38	n.d.	32,61	-0,76	-2,28 %	
50	33,44	n.d.	32,68	-0,76	-2,26 %	
60	33,43	n.d.	32,74	-0,69	-2,06 %	
75	33,47	n.d.	32,66	-0,81	-2,43 %	

Table 9: Average summer salinity in ‰ at the Outer Barsnesfjord for the three pre-defined periods as well as the difference between period 1 and 3 in ‰ and %. The blue colors depict the different kinds of water masses, however, the transition zones can slightly vary.

Graph 9 depicts the average summer salinity during the period from 1916 until 2011. The 0 m layer thereby fluctuates in the range between 0.0‰ and 2.5‰, only interrupted once by a very large peak in 1937, going up to 30.0‰. This is the only big peak in salinity within the 0 m layer, while otherwise there is only a relatively constant drop of in total 72.19% visible. This is approved by Table 9, showing a decline from 2.04‰ to 0.57‰. Beside that the 5 m layer displays the largest fluctuations, varying between 0.0‰ and 30.0‰ until 1960 and between 13.0‰ and 29.0‰ after 1980. While the 10 m layer levels between 27.5‰ and 32.5‰, the 20 m to 75 m layers show quite close values, ranging between 31.0‰ and 35.0‰ (Table 9).

Furthermore it is visible, that there are big fluctuations in salinity, especially in the 0 m and 5 m layers, ranging from 0.0‰ to more than 30.0‰ (Graph 9). Regarding the entire period there is a slight decline in salinity visible in all layers, except for 5 m depth, which displays an increase of 3.75‰ (Table 9). However, the long period without data between 1957 and 1981 makes solid statements difficult.

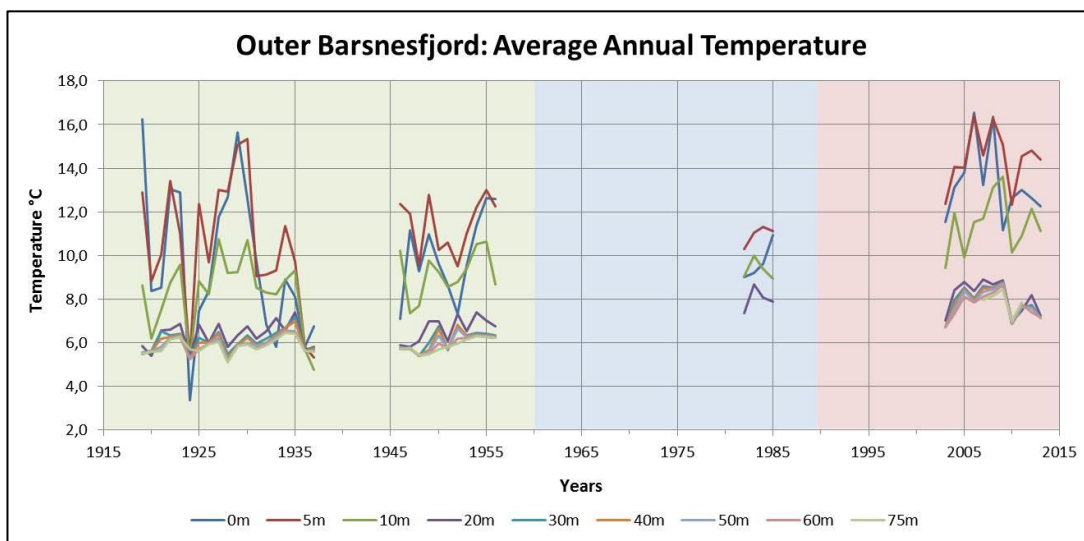
3.2.2 Temperature

The subsequent Graphs 10 to 12 depict the average temperature in °C at the Outer Barsnesfjord during the period from 1916 until 2013. While the x-axes depict the time in years in steps of ten years, the y-axis shows the temperature in °C, in steps of 2°C. Thereby the depths of 0 m, 5 m, 10 m, 20 m, 30 m, 40 m, 50 m, 60 m and 75 m have been measured.

Again the background colors show the three periods, pre-impact, transitional and full-impact period.

The Tables 10 to 12 represent the calculated average temperatures in °C for the periods before, during and after building of the water power plants, as well as the difference between the first and the last period in °C and %. The blue colors thereby depict the different kinds of water masses, however, the transition zones can slightly differ, as the water masses blend into each other.

3.2.2.1 Annual



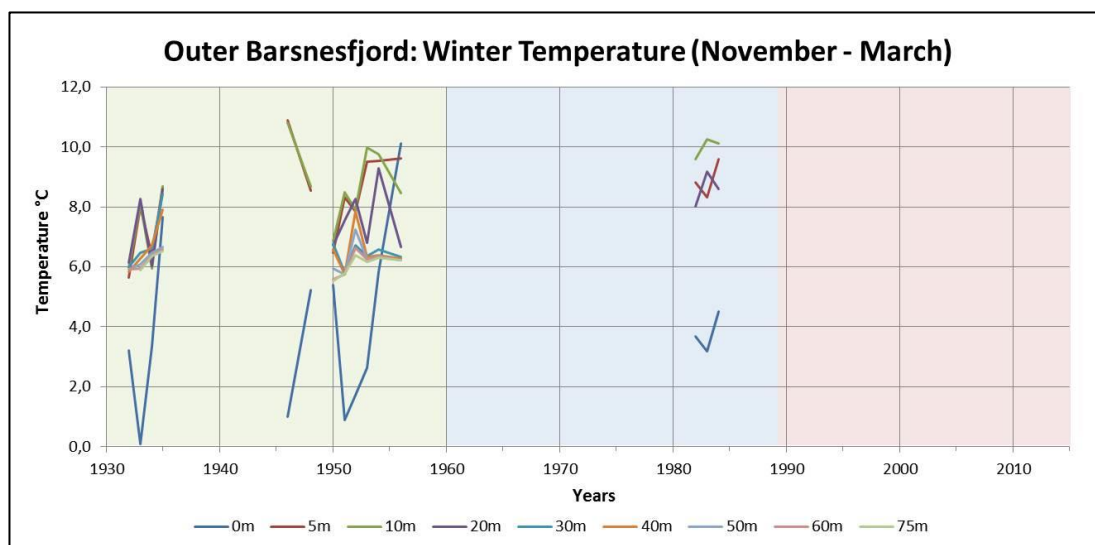
Graph 10: Average annual temperature in °C measured at the Outer Barsnesfjord during the period from 1916 till 2013. While the x-axis shows the years, the y-axis depicts the temperature in °C. The three background colors depict the different periods: green = pre-impact period, blue = transitional period, red = full-impact period.

Temperature [°C]: Outer Barsnesfjord Annual						
Depth [m]	1. Period 1916-1960	2. Period 1961-1989	3. Period 1990-2013	Change 1. to 3.	Change in %	
0	9,90	10,05	12,79	2,90	29,26 %	Brackish Water
5	10,90	10,94	14,46	3,56	32,71 %	Compensation Current
10	8,53	9,62	11,59	3,06	35,87 %	Intermediate Water
20	6,39	7,92	8,07	1,68	26,31 %	Threshold Turbulence
30	6,08	6,91	7,86	1,78	29,37 %	Basin Water
40	5,99	n.d.	7,80	1,80	30,10 %	
50	5,90	6,75	7,73	1,83	30,94 %	
60	5,84	n.d.	7,61	1,77	30,26 %	
75	5,83	6,57	7,61	1,79	30,71 %	

Table 10: Average annual temperature °C at the Outer Barsnesfjord for the three pre-defined periods and additionally the difference between period 1 and 3 in °C and %. The blue colors depict the different kinds of water masses, however, the transition zones can slightly vary.

Graph 10 shows the annual temperature at the Outer Barsnesfjord, with the layers from 20 m to 75 m fluctuating in the range of 5.0°C to 7.0°C before 1960 and between 7.0°C and 9.0°C in the time after 1980. This noticeable increase is also confirmed by the Table 10. Beside that the 0 m to 10 m layers show larger fluctuations, ranging between 7.0°C and 13.0°C before 1985 and between 10.0°C and 16.0°C after 2000. Additionally it can be seen that there is a general rising temperature trend visible in all layers causing an increase of around 30% in all layers (Table 10).

3.2.2.2 Seasonal



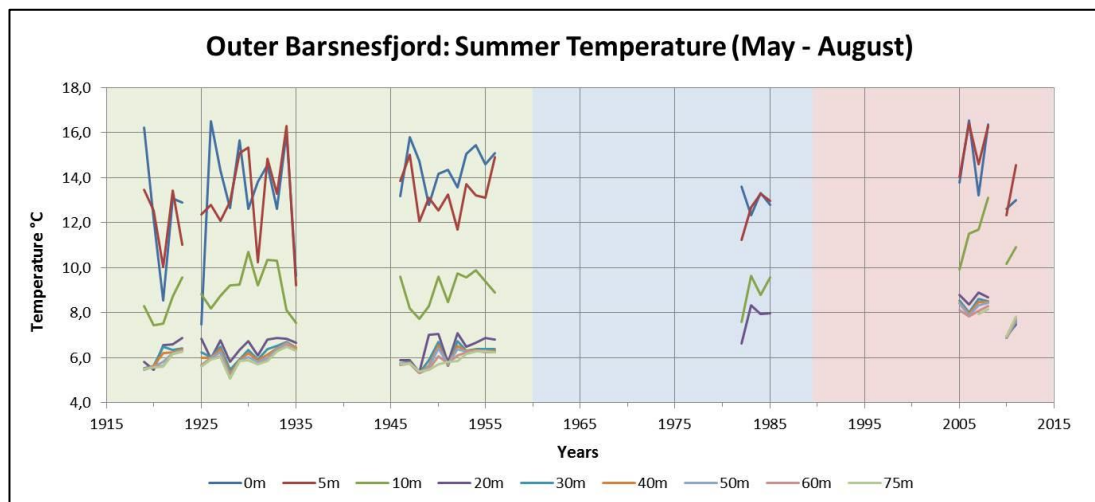
Graph 11: Average winter temperature in °C measured at the Outer Barsnesfjord during the period from 1932 till 1984. While the x-axis shows the years, the y-axis depicts the temperature in °C. The three background colors depict the different periods: green = pre-impact period, blue = transitional period, red = full-impact period.

Temperature [°C]: Outer Barsnesfjord Winter Period						
Depth [m]	1. Period 1932-1960	2. Period 1961-1984		Change 1. to 2.	Change in %	
0	3,93	3,80		-0,13	-3,33 %	Brackish Water
5	8,29	8,91		0,62	7,48 %	Compensation Current
10	8,30	9,99		1,68	20,25 %	Intermediate Water
20	7,39	8,60		1,21	16,38 %	Threshold Turbulence
30	6,51	n.d.				Basin Water
40	6,50	n.d.				
50	6,23	n.d.				
60	6,11	n.d.				
75	6,13	n.d.				

Table 11: Average winter temperature °C at the Outer Barsnesfjord for the three pre-defined periods and additionally the difference between period 1 and 2 in °C and %. The blue colors depict the different kinds of water masses, however, the transition zones can slightly vary.

Graph 11 shows the winter temperatures, however again only representing the period before and during building of the water power plants, from 1932 until 1984. In general the 30 m to 75 m layers are fluctuating in the range of 6.0°C to 8.0°C, while the 5 m to 20 m layers level in the range of 6.0°C to 10.0°C (Graph 11). Beside that the 0 m layer shows the largest fluctuations, ranging from 0.0°C up to 8.0°C. Overall there is a rise in the upper 5 m to 20 m layers visible, which is most pronounced in the 10 m layer, causing an increase of

20.25% (Table 11). The 0 m layer represents a drop in temperature, accounting for 3.33%. However, changes are only visible in the layers from 0 m to 20 m, as there are no data available for the deeper layers after 1956.



Graph 12: Average summer temperature in °C measured at the Outer Barsnesfjord during the period from 1916 till 2013. While the x-axis shows the years, the y-axis depicts the temperature in °C. The three background colors depict the different periods: green = pre-impact period, blue = transitional period, red = full-impact period.

Temperature [°C]: Outer Barsnesfjord Summer Period						
Depth [m]	1. Period 1916-1960	2. Period 1961-1989	3. Period 1990-2011	Change 1. to 3.	Change in %	
0	13,51	13,00	13,96	0,45	3,34 %	Brackish Water
5	12,80	12,54	14,69	1,88	14,72 %	Compensation Current
10	8,76	8,89	11,42	2,66	30,40 %	Intermediate Water
20	6,37	7,71	8,14	1,77	27,88 %	Threshold Turbulence
30	6,10	n.d.	7,98	1,88	30,89 %	Basin Water
40	6,01	n.d.	7,94	1,93	32,18 %	
50	5,93	n.d.	7,88	1,94	32,76 %	
60	5,87	n.d.	7,75	1,88	32,01 %	
75	5,84	n.d.	7,73	1,89	32,43 %	

Table 12: Average summer temperature °C at the Outer Barsnesfjord for the three pre-defined periods and additionally the difference between period 1 and 3 in °C and %. The blue colors depict the different kinds of water masses, however, the transition zones can slightly vary.

Graph 12 depicts the summer temperature at the Outer Barsnesfjord, again for the period from 1916 until 2011. Thereby the 20 m to 75 m layers are fluctuating within a range of 5.5°C and 9.0°C, showing slightly higher values in the last period. Beside that the 0 m and 5 m layers are ranging between 10.0°C and 16.0°C, also depicting the highest values after

2005. The 10 m layer levels between 7.5°C and 11.0°C until 1985 and between 10.0°C and 13.0°C in the time afterwards, indicating an overall strong increase.

Furthermore the given data indicate a rising temperature trend in all layers. While this increase in the uppermost 0 m layer only accounts for 3.34% and in the 5 m layer for 14.72%, there is a stronger rise visible in the deeper layers, making up for more than 30% rise in all depths (Table 12). The only exception is the 20 m layer, showing a rise of 27.88%. Furthermore especially in the uppermost surface water big fluctuations are apparent, pointing out huge differences between maxima and minima temperatures.

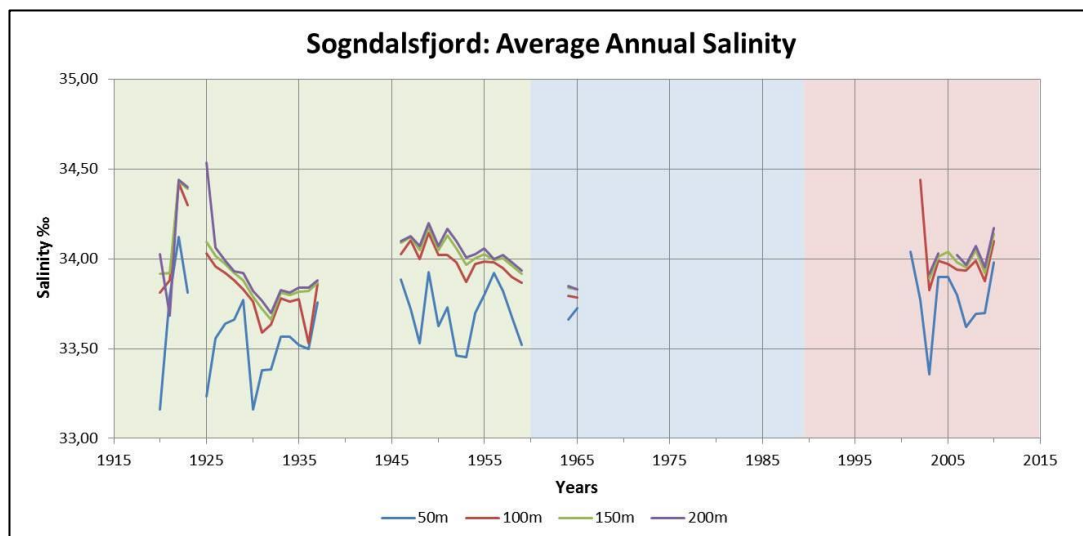
3.3 Sognalsfjord

3.3.1 Salinity

The Graphs 13 until 15 represent the salinity values in ‰ at the Sogndalsfjord for annual, summer and winter situations. While the annual and summer values only comprise the depths of 50 m, 100 m, 150 m and 200 m, the winter values are measured for 0 m, 5 m, 10 m, 20 m, 30 m, 40 m, 50 m, 100 m, 150 m and 200 m. The x-axes depict the time in years from 1915 until 2015 in steps of ten years and the y-axes the salinity in ‰. The different background colors show the periods before, while and after building of the large power plants.

The Tables 13 until 15 represent the calculated average salinities in ‰ for the three single periods in all depths. Additionally they depict the difference between the first and the third period, showing the variation before and after building of the water power plants. This difference is shown in ‰ as well as in %. Again the blue colors depict the different kinds of water masses, however, the transition zones can slightly differ, as the water masses blend into each other.

3.3.1.1 Annual



Graph 13: Average annual salinity in ‰ measured at the Sogndalsfjord for the period from 1916 until 2013. The x-axis shows the years, while the y-axis depicts the salinity in ‰ for the depths from 50 m to 200 m. The three background colors depict the different periods: green = pre-impact period, blue = transitional period, red = full-impact period.

Salinity [‰]: Sogndalsfjord Annual						
Depth [m]	1. Period 1916-1960	2. Period 1961-1989	3. Period 1990-2010	Change 1. to 3.	Change in %	
50	33,62	33,71	33,76	0,14	0,43 %	Basin Water
100	33,91	33,59	34,00	0,10	0,29 %	
150	33,98	34,42	34,00	0,02	0,07 %	
200	34,01	34,27	34,02	0,01	0,03 %	

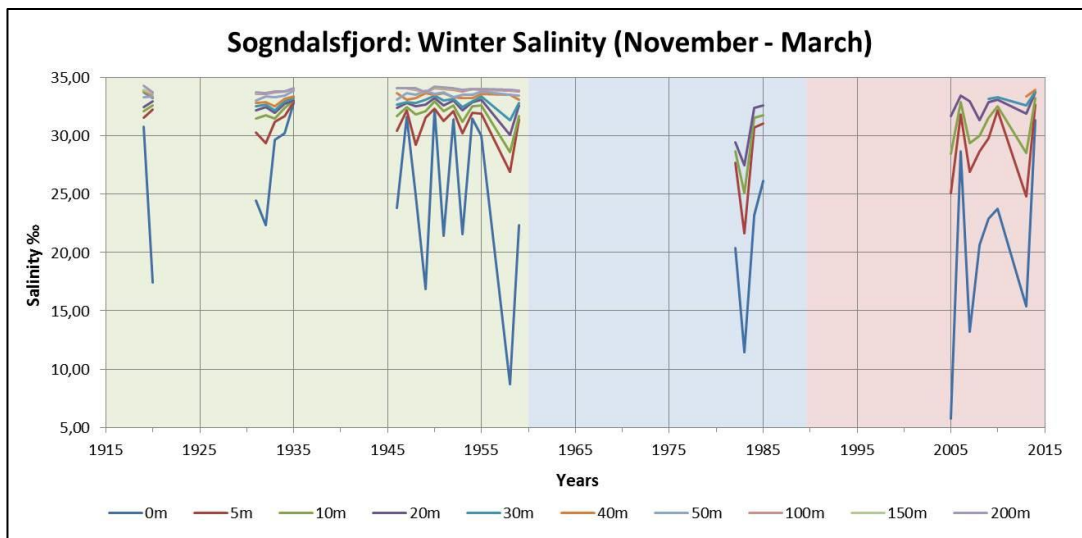
Table 13: Average annual salinity values in ‰ at the Sogndalsfjord for three pre-defined periods and additionally the difference between period 1 and 3 in ‰ and %. The blue color depicts the kind of water mass.

Graph 13 shows the entire data set about the annual salinity at the Sogndalsfjord. The salinity fluctuations are ranging between 33.4‰ and 34.4‰. Beside that a slight increase is visible during the three periods in all layers, most pronounced in the uppermost 50 m layer, accounting for 0.43% (Table 13). Additionally it depicts an increase in salinity with growing depth in the first and third period, while the values decline in the second period.

However, regarding the entire graph, it is difficult to make a reliable statement about the salinity progress, due to the low number of values between 1956 and 2001. As the data set only depicts the depths between 50 m and 200 m it is necessary to get some more values, also including the upper water layers, showing changes from the outside more directly. Beyond that further data are important to allow a comparison of the Sogndalsfjord data with the ones from the other measuring stations. Thus, by subdividing the graphs into

summer and winter seasons an additional data set is used, also supplying values of the upper layers.

3.3.1.2 Seasonal



Graph 14: Average winter salinity in ‰ measured at the Sogndalsfjord for the period from 1916 until 2013. The x-axis shows the years, while the y-axis depicts the salinity in ‰ for the depths from 0 m to 200 m. The three background colors depict the different periods: green = pre-impact period, blue = transitional period, red = full-impact period.

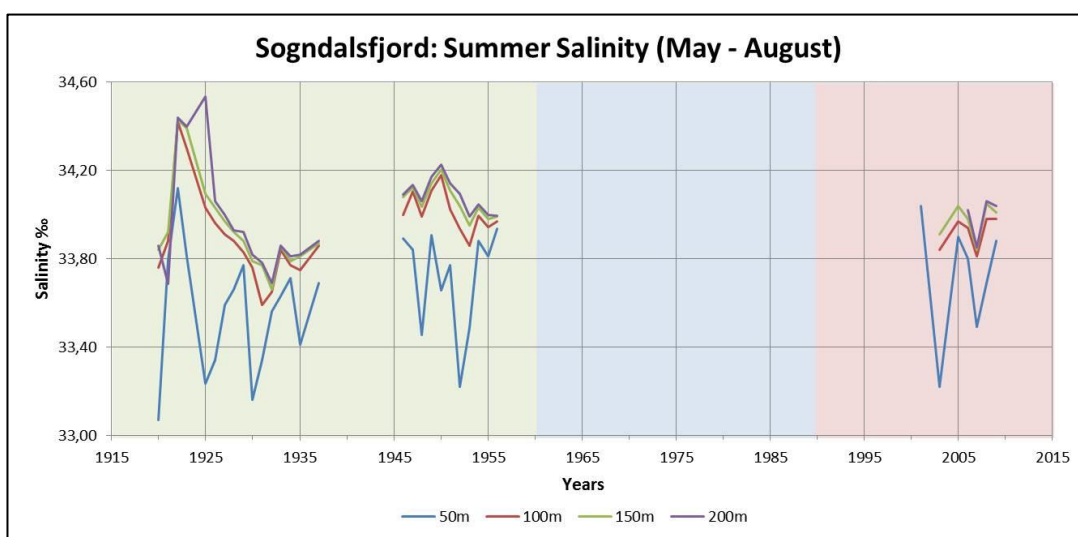
Salinity [‰]: Sogndalsfjord Winter Period						
Depth [m]	1. Period 1919-1960	2. Period 1961-1989	3. Period 1990-2014	Change 1. to 3.	Change in %	
0	25,48	20,31	20,21	-5,27	-20,68 %	Brackish Water
5	31,10	27,81	29,02	-2,09	-6,71 %	Compensation Current ----- Intermediate Water
10	31,98	29,28	30,82	-1,16	-3,63 %	
20	32,55	30,51	32,65	0,11	0,33 %	
30	32,90	n.d.	33,31	0,41	1,24 %	Treshhold ----- Turbulence
40	33,32	n.d.	33,55	0,23	0,71 %	
50	33,51	n.d.	n.d.			Basin Water
100	33,89	n.d.	n.d.			
150	33,94	n.d.	n.d.			
200	33,98	n.d.	n.d.			

Table 14: Average winter salinity in ‰ at the Sogndalsfjord for the three pre-defined periods and additionally the difference between period 1 and 3 in ‰ and %. The blue colors depict the different kinds of water masses, however, the transition zones can slightly differ.

Graph 14 shows the winter salinity values from 1919 until 2014, also including depths representing the surface and intermediate water layers. Thus it also allows taking a closer

look on these highly influenced layers. The 5 m to 200 m layers are thereby fluctuating in the range from 27.5‰ to 35.0‰ before 1960 and between 22.5‰ and 32.5‰ after 1980. Beside that the 0 m layer displays much larger variations, leveling between 7.5‰ and 32.5‰ during the entire period.

As can be clearly seen, the 0 m and thus surface layer has the largest fluctuations, ranging from around 5.0‰ to more than 30.0‰. Thus, especially in the years around 1958, 1983 and 2005 the salinity reaches very deep troughs. Furthermore a decrease in salinity is visible in the uppermost 0 m to 10 m, accounting for 20.68% in the 0 m surface layer (Table 14). Against that a slight rise is visible in the 20 m layer, increasing at 0.11‰. Beside that the deeper layers show a decrease in fluctuations, as well as in average salinity.



Graph 15: Average summer salinity in ‰ measured at the Sogndalsfjord for the period from 1916 until 2009. The x-axis shows the years, while the y-axis depicts the salinity in ‰ for the depths from 50 m to 200 m. The three background colors depict the different periods: green = pre-impact period, blue = transitional period, red = full-impact period.

Salinity [‰]: Sogndalsfjord Summer Period						
Depth [m]	1. Period 1916-1960	2. Period 1961-1989	3. Period 1990-2009	Change 1. to 3.	Change in %	
50	33,61	33,66	33,72	0,11	0,32 %	Basin Water
100	33,92	33,79	33,92	0,00	0,00 %	
150	33,99	33,84	33,97	-0,02	-0,05 %	
200	34,02	33,85	33,98	-0,04	-0,11 %	

Table 15: Average summer salinity in ‰ at the Sogndalsfjord for the three pre-defined periods and additionally the difference between period 1 and 3 in ‰ and %. The blue color depicts the kind of water mass.

Graph 15 represents the data set of summer salinity values at the Sogndalsfjord, representing deeper water masses than the layers that have been viewed before. Thus the

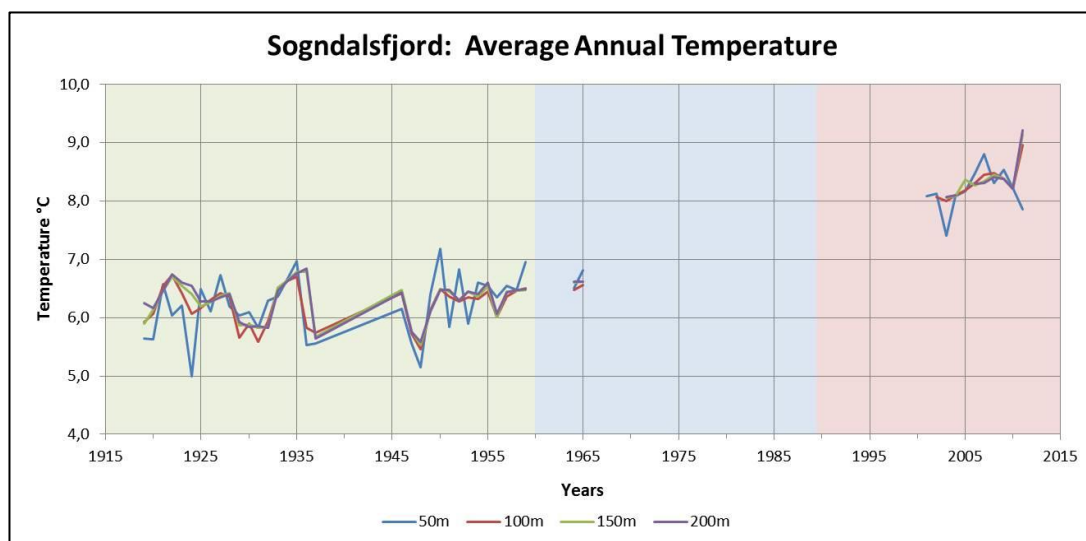
100 m to 200 m layers are leveling between 33.6‰ and 34.4‰, while the 50 m layer ranges between 33.2‰ 34.0‰. Beside that a slight rise in salinity is visible during the entire measuring period within the 50 m layer, counting for 0.11‰ (Table 15). Additionally it can be noticed that the highest fluctuations also seem to occur in this layer. It is also visible that the values, especially in 100 m to 200 m depth, are relatively similar (Graph 15). However, as the depths only range from 50 m to 200 m, the water layers do not exactly represent the mostly influenced uppermost surface water.

3.3.2 Temperature

The subsequent Graphs 16 until 19 depict the average temperature in °C, measured at the Sogndalsfjord for the period from 1916 until 2011. While the x-axes depict the time in years from 1915 until 2015 in steps of ten years, the y-axes show the temperature in °C. Thereby the annual and summer data depict the depths of 50 m, 100 m, 150 m and 200 m, while the winter data comprise 0 m, 5 m, 10 m, 20 m, 30 m, 40 m, 50 m, 100 m, 150 m and 200 m. The different background colors depict the three periods, before, while and after building of the large water power plants.

The Tables 16 until 19 depict the calculated average temperatures during the three periods in °C, as well as the difference between period one and three in °C and %. The blue colors show the different kinds of water masses, however, the transition zones can slightly differ, as the water masses blend into each other.

3.3.2.1 Annual



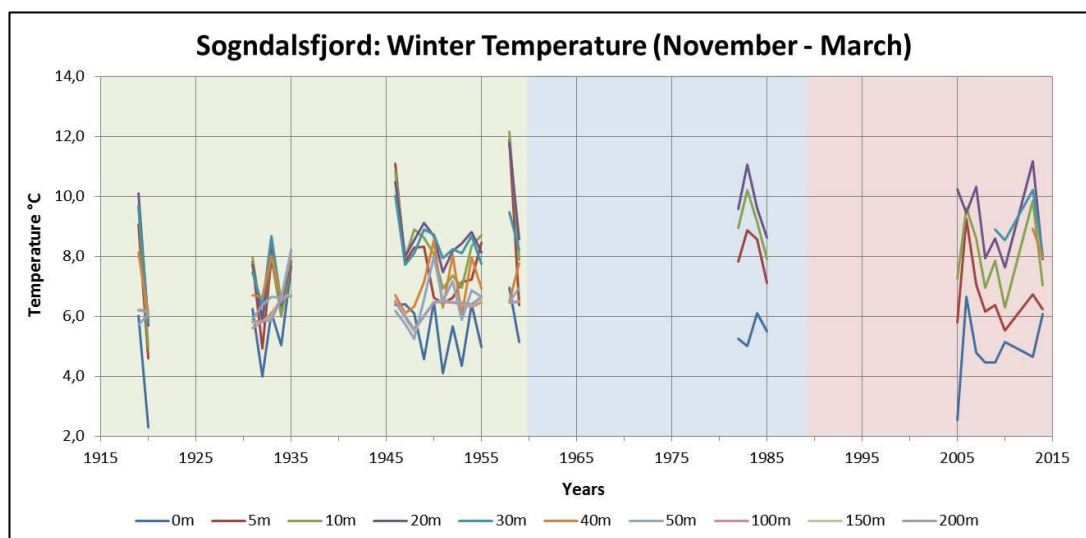
Graph 16: Average annual temperature in °C at the Sogndalsfjord in the depths from 50 m to 200 m from 1916 till 2009. The x-axis shows the years, while the y-axis depicts the temperature in °C. The three background colors depict the different periods: green = pre-impact period, blue = transitional period, red = full-impact period.

Temperature [°C]: Sogndalsfjord Annual						
Depth [m]	1. Period 1916-1960	2. Period 1961-1989	3. Period 1990-2011	Change 1. to 3.	Change in %	
50	6,15	6,93	8,15	2,00	32,49 %	Basin Water
100	6,21	6,93	8,27	2,06	33,20 %	
150	6,28	6,91	8,37	2,08	33,17 %	
200	6,31	6,62	8,31	2,00	31,76 %	

Table 16: Average annual temperature in °C, measured at the Sogndalsfjord for the three pre-defined periods and additionally the difference between period 1 and 3 in % and %. The blue color depicts the kind of water mass.

Graph 16 shows the annual temperatures at the Sogndalsfjord, which is divided by a break in measurement between 1965 and 2002. These two periods of measurement show strongly different levels of average temperatures. While the temperature in the first part fluctuates between the range of 5.0°C and 7.0°C, in the second part the averages level between 7.5°C and 9.0°C. Thus there is a huge increase in temperature in 50 m to 200 m visible during the entire period within all layers. This causes a rise in average temperature from around 2.04°C in all layers (Table 16).

3.3.2.2 Seasonal



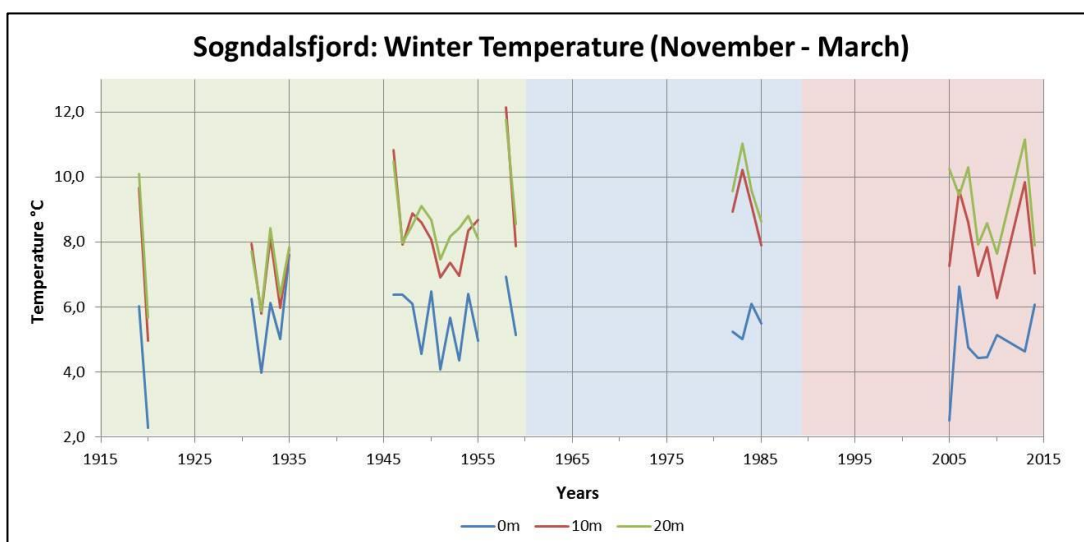
Graph 17: Average winter temperature in °C at the Sogndalsfjord for the depths from 0 m to 200 m from 1916 until 2009. The x-axis shows the years, while the y-axis depicts the temperature in °C. The three background colors depict the different periods: green = pre-impact period, blue = transitional period, red = full-impact period.

Temperature [°C]: Sogndalsfjord Winter Period						
Depth [m]	1. Period 1919-1960	2. Period 1961-1989	3. Period 1990-2014	Change 1. to 3.	Change in %	
0	5,52	5,46	4,84	-0,68	-12,31 %	Brackish Water
5	7,60	8,09	6,64	-0,95	-12,56 %	Compensation Current
10	8,05	9,05	7,93	-0,12	-1,50 %	Intermediate Water
20	8,32	9,71	9,15	0,83	9,96 %	Treshhold Turbulence
30	8,13	n.d.	8,99	0,86	10,58 %	
40	7,07	n.d.	8,60	1,53	21,63 %	Basin Water
50	6,51	n.d.	8,76	2,25	34,53 %	
100	6,24	n.d.	8,44	2,19	35,10 %	
150	6,27	n.d.	8,44	2,17	34,58 %	
200	6,27	n.d.	8,43	2,16	34,43 %	

Table 17: Average winter temperature in °C at the Sogndalsfjord, calculated for the three pre-defined periods and additionally the difference between period 1 and 3 in % and %. The blue colors depict the different kinds of water masses, however, the transition zones can slightly vary.

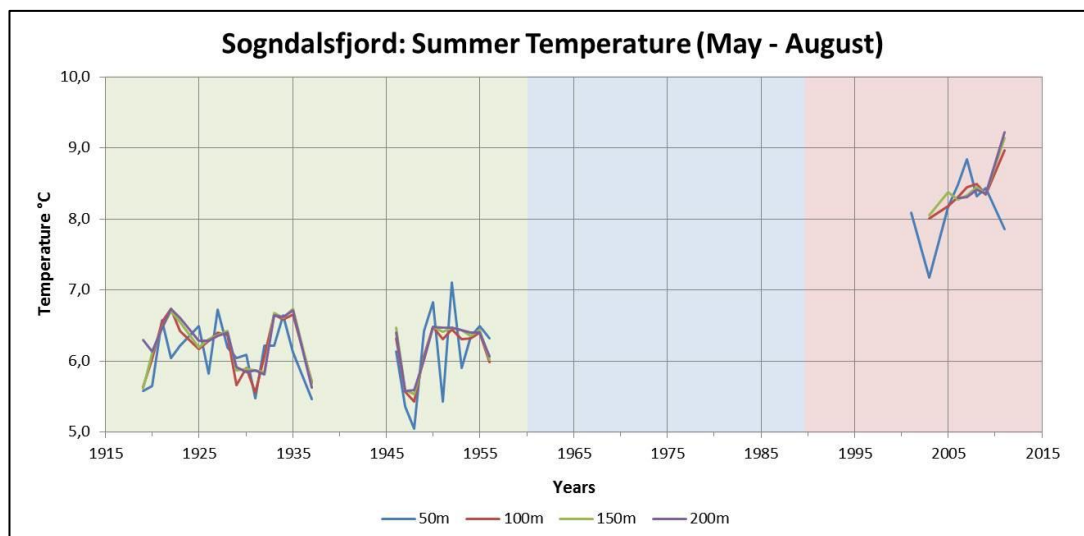
Graph 17 shows the average winter temperatures, comprising the depths of 0 m, 5 m, 10 m, 20 m, 30 m, 40 m, 50 m, 100 m, 150 m and 200 m. Thereby the temperatures fluctuate within a range of 4.0°C and 8.5°C in the period before 1960, with some single peaks and troughs standing out. Beside that the fluctuations in the period afterwards range between 4.5°C and 10.0°C, thus showing a larger range.

Additionally a decreasing trend in the upper 0 m to 10 m is shown, being strongest at 5 m depth with a drop of 12.56% (Table 17). The lower depths display an increasing trend. The average rise in temperature within the basin water, from 50 m to 200 m depth accounts for 2.19°C. Overall the periods with data missing subdivide the graph into six parts, which can be used to examine the course of the temperature. However, the gaps without measurements during the entire period are relatively large, making it difficult to track the entire development and progress of the various layers. To get a closer look on the most interesting depths, a further subdivision of the graph is used.



Graph 18: Average winter temperature in °C at the Sogndalsfjord, focusing on the depths from 0 m to 20 m during the period from 1916 to 2009. The x-axis shows the years, while the y-axis depicts the temperature in °C. The three background colors depict the different periods: green = pre-impact period, blue = transitional period, red = full-impact period.

Graph 18 represents the average winter temperatures, however focusing only on the depths of 0 m, 10 m and 25 m. As can now be seen, while the 0 m depth is leveling in the range of 4.0°C and 6.5°C, the 10 m and 20 m depths show higher averages, ranging between 6.0°C and 10.0°C. Additionally again a drop in temperature is visible in the 0 m and 10 m layer, accounting for a 12.31% and 1.50% reduction (Table 17). Thus, by comparing the first and the third measured period, a drop of temperature of 0.68°C at 0 m and of 0.12°C at 10 m is shown. The 20 m layer displays a reversed trend, increasing at 0.83°C, which makes 9.96% more. Overall the fluctuations in all three depths are very large, representing big differences between the temperature maxima and minima within the layers.



Graph 19: Average summer temperature in °C at the Sogndalsfjord for the depths from 0 m to 200 m from 1916 until 2009. The x-axis shows the years, while the y-axis depicts the temperature in °C. The three background colors depict the different periods: green = pre-impact period, blue = transitional period, red = full-impact period.

Temperature [°C]: Sogndalsfjord Summer Period						
Depth [m]	1. Period 1916-1960	2. Period 1961-1989	3. Period 1990-2011	Change 1. to 3.	Change in %	
50	6,06	6,50	8,17	2,11	34,88 %	Basin Water
100	6,18	6,47	8,39	2,21	35,79 %	
150	6,23	6,60	8,42	2,20	35,24 %	
200	6,26	6,62	8,44	2,18	34,91 %	

Table 18: Average Summer temperature in °C at the Sogndalsfjord, calculated for the three pre-defined periods and additionally the difference between period 1 and 3 in % and %. The blue color depicts the water mass.

Graph 19 depicts the average summer temperature at the Sogndalsfjord, again divided by periods without measurements, residing in the period before 1960 and after 2000. While the temperature in all layers in the period before 1960 levels in a range of 5.5°C and 7.8°C, the layers show larger temperatures in the second period. Thus they are leveling in a range of 7.5°C and 9.0°C after 2000.

Nevertheless, despite adding one more month there are only data for the deep water layers available, including the depths of 50 m, 100 m, 150 m and 200 m. As can be seen there is a remarkable increase in temperature of more than 30% in all layers (Table 18). By comparing the period from 1916 until 1960 with the period from 1990 till 2011, the average rise accounts for more than 2.18°C in all layers.

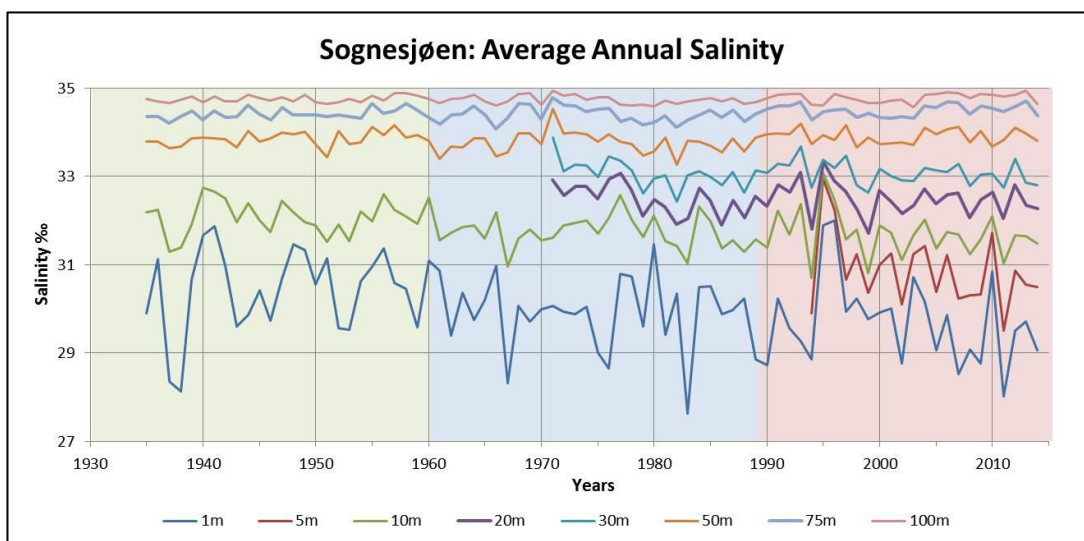
3.3 Sognesjøen

3.3.1 Salinity

The subsequent Graphs 20 to 24 depict the average salinity in ‰ at the Sognesjøen, measured in the period 1935 until 2014. The measured depths comprise 1 m, 5 m, 10 m, 20 m, 30 m, 50 m, 75 m and 100 m. While the x-axes show the years from 1930 until 2015 in steps of ten years, the y-axes represent the salinity in ‰. The three colors thereby depict the three periods, before, while and after building of the large water power plants

The Tables 19 to 21 depict the average annual salinities in ‰, calculated for the three defined periods before, while and after building of the water power plants. Additionally they show the difference between period one and three in ‰ and ‰. The blue colors show the kinds of water masses, however, the transition zones can slightly differ, as the water masses blend into each other.

3.3.1.1 Annual



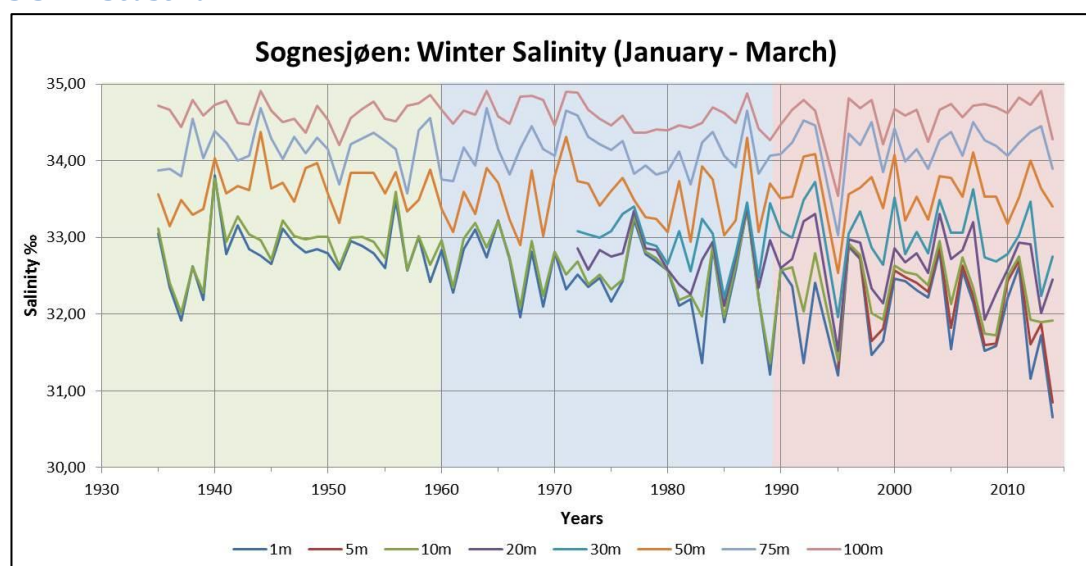
Graph 20: Average annual salinity in ‰ measured at the Sognesjøen for the period from 1935 until 2014. The x-axis shows the years, while the y-axis depicts the salinity in ‰ for the depths from 1 m to 100 m. The three background colors depict the different periods: green = pre-impact period, blue = transitional period, red = full-impact period.

Salinity [‰]: Sognesjøen Annual						
Depth [m]	1. Period 1935-1960	2. Period 1960-1989	3. Period 1989-2014	Change 1. to	Change in %	
1	30,43	29,90	29,70	-0,74	-2,42 %	Surface Water
5	n.d.	29,86	30,86			
10	32,08	31,74	31,68	-0,40	-1,24 %	
20	n.d.	32,49	32,49			
30	n.d.	33,07	33,08			
50	33,85	33,77	33,91	0,05	0,16 %	Deep Water
75	34,41	34,40	34,50	0,09	0,25 %	
100	34,75	34,73	34,78	0,03	0,08 %	

Table 19: Average annual salinity in ‰ at the Sognesjøen, calculated for the three pre-defined periods and additionally the difference between period 1 and 3 in ‰ and %. The blue colors depict the different kinds of water masses, however, the transition zones can slightly vary.

Graph 20 shows the average annual salinity measured at the Sognesjøen, depicting a different behavior at the different water depths. Especially apparent is the decrease in salinity in the upper 1 m and 10 m layers, accounting for -2.42% and -1.24% (Table 19). Against that a slight rise in the 50 m to 100 m layers is shown. Furthermore it can be seen, that the largest fluctuations occur in the upper depths, especially in the 1 m layer. The largest peak thereby happened in 1995, also visible in the 5 m to 20 m layers.

3.3.1.2 Seasonal



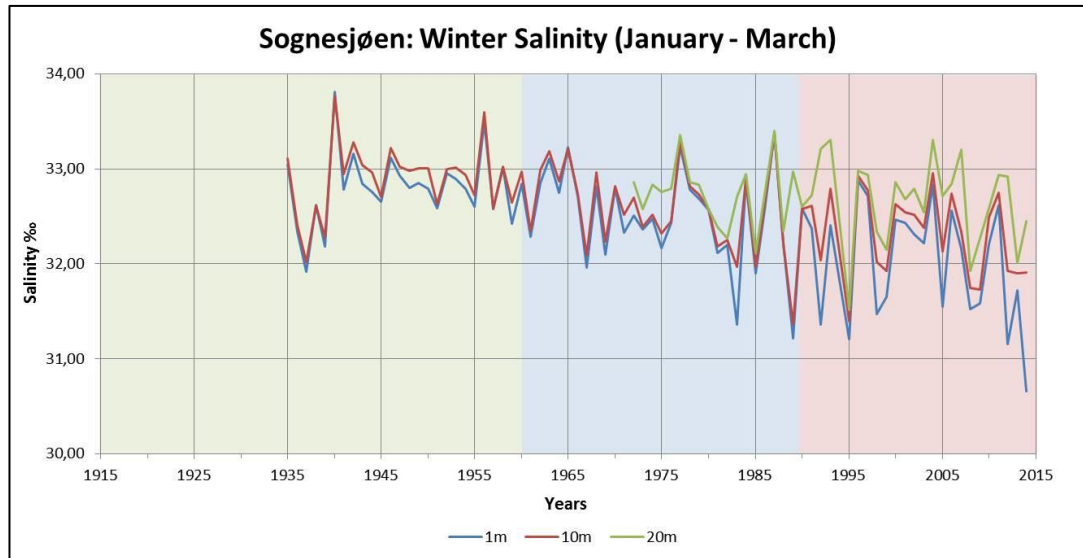
Graph 21: Average winter salinity in ‰ measured at the Sognesjøen for the period from 1935 until 2014. The x-axis shows the years, while the y-axis depicts the salinity in ‰ for the depths from 1 m to 100 m. The three background colors depict the different periods: green = pre-impact period, blue = transitional period, red = full-impact period.

Salinity [‰]: Sognesjøen Winter Period						
Depth [m]	1. Period 1935-1960	2. Period 1960-1989	3. Period 1990-2014	Change 1. to 3.	Changes in %	
1	32,80	32,48	32,03	-0,77	-2,36 %	Surface Water
5	n.d.	n.d.	32,12			
10	32,90	32,57	32,32	-0,58	-1,76 %	
20	n.d.	32,74	32,66			
30	n.d.	32,98	33,01			
50	33,64	33,51	33,59	-0,05	-0,14 %	Deep Water
75	34,15	34,13	34,19	0,03	0,10 %	
100	34,62	34,59	34,60	-0,02	-0,07 %	

Table 20: Average winter salinity in ‰ at the Sognesjøen, calculated for the three pre-defined periods and additionally the difference between period 1 and 3 in ‰ and %. The blue colors depict the different kinds of water masses, however, the transition zones can slightly vary.

Graph 21 shows the entire data set of winter salinity values measured at the Sognesjøen. The uppermost water layers from 1 m to 30 m are ranging between 31.50‰ and 33.00‰, while the lowermost 50 m to 100 m are separated, leveling between 33.00‰ and 35.00‰.

Overall there is a decreasing trend visible in all layers, except at 75 m depth. This trend is most pronounced in the 1 m layer, showing 2.36% less salinity (Table 20). Additionally there seems to be a significant change in the range of fluctuations, especially within the uppermost layers from 0 m to 20 m. Thus the fluctuations become remarkably larger and lower in average after around 1980, in particular in the layers of 0 m, 5 m, 10 m and 20 m depth. However, in general there are again too many depth lines within this graph for reliable statements about the development of the salinity in specific layers. Thus a further subdivision is used, to give more information.

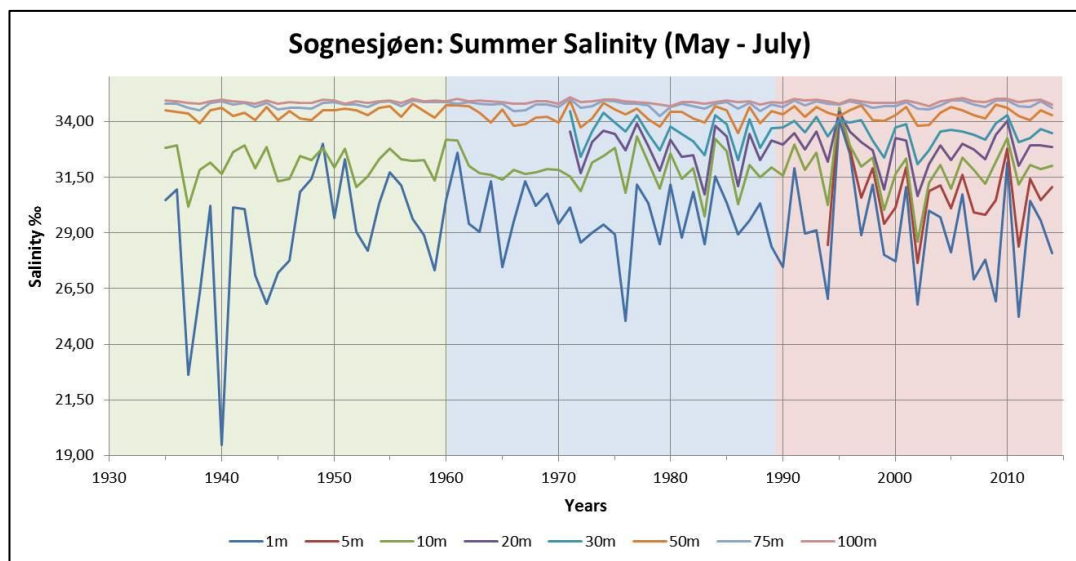


Graph 22: Average winter salinity in ‰ measured at the Sognesjøen for the period from 1935 until 2014, focusing on the upper 1 m to 20 m layers. The x-axis shows the years, while the y-axis depicts the salinity in ‰. The three background colors depict the different periods: green = pre-impact period, blue = transitional period, red = full-impact period.

Graph 22 shows the average winter salinity at the Sognesjøen, focusing on the 1 m, 10 m and 25 m layers. Even though there seem to be higher fluctuations than in the Nordic Sea, covering a wider range of salinity values, there are no significant peaks or troughs visible during the entire period.

However, striking is the general decline in salinity after around 1980, visible in all layers. This drop is especially large in the uppermost 1 m layer, accounting for 0.77‰ (Table 20). At 10 m depth a similar drop is apparent, accounting for 0.58‰ until the last period. As the measurement of the 20 m layer first started in 1973, only the change between the second and third period is visible.

Beside that also the width of the fluctuations becomes remarkably larger after 1980, indicating stronger minima and maxima during that time. In average the 1 m and 10 m layers are leveling between 33.2‰ and 32.2‰ until around 1980. In contrast the average range is between 33.0‰ and 31.5‰ in the period after 1980, showing significantly larger fluctuations as well as lower average salinities.

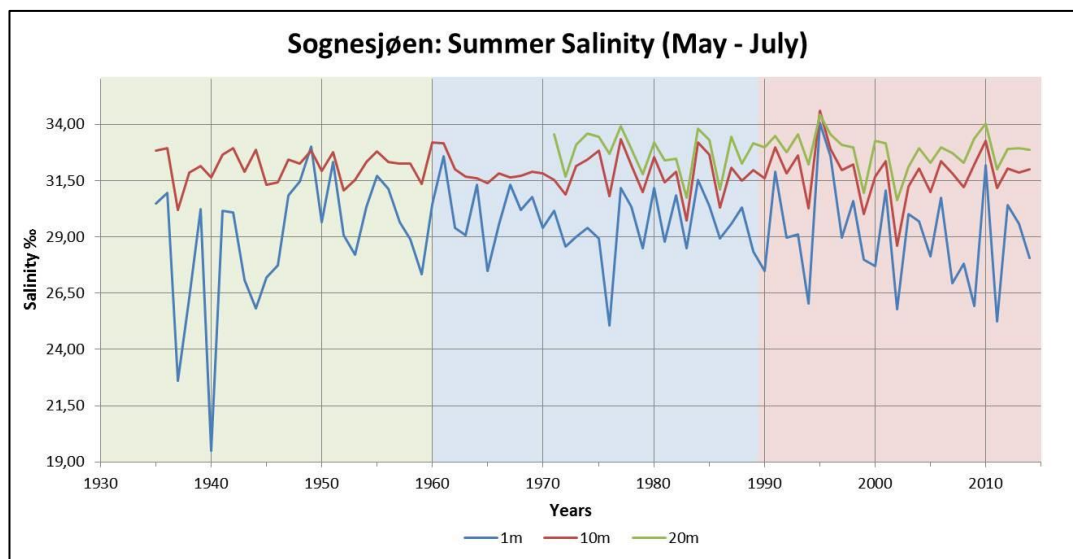


Graph 23: Average summer salinity in ‰ measured at the Sognesjøen for the period from 1935 until 2014. The x-axis shows the years, while the y-axis depicts the salinity in ‰ for the depths from 1 m to 100 m. The three background colors depict the different periods: green = pre-impact period, blue = transitional period, red = full-impact period.

Salinity [‰]: Sognesjøen Summer Period						
Depth [m]	1. Period 1935-1960	2. Period 1960-1989	3. Period 1990-2014	Change 1. to	Change in %	
1	28,93	29,68	29,08	0,15	0,51 %	Surface Water
5	n.d.	29,86	30,72			
10	32,16	31,84	31,84	-0,32	-0,99 %	
20	n.d.	32,77	32,82			
30	n.d.	33,51	33,54			Deep Water
50	34,41	34,28	34,37	-0,04	-0,10 %	
75	34,76	34,73	34,78	0,02	0,05 %	
100	34,90	34,89	34,91	0,02	0,05 %	

Table 21: Average summer salinity in ‰ at the Sognesjøen, calculated for the three pre-defined periods and additionally the difference between period 1 and 3 in ‰ and %. The blue colors depict the different kinds of water masses, however, the transition zones can slightly vary.

Graph 23 shows the entire data set of summer salinity values at the Sognesjøen. Thereby the 1 m to 30 m layers fluctuate between the range of 27.50‰ and 34.00‰, while the 50 m to 100 m layers are very similar, ranging only between 34.00‰ and 35.00‰. Thus it can be seen that the highest salinity values occur in the deepest parts of the Sognesjøen, while the salinity becomes lower when getting closer to the surface. The uppermost layers also show extremely stronger fluctuations. Regarding the overall trend, there are different developments visible in the single layers (Table 21). However, as the graph is containing many depth-lines, reliable statements about specific layers are difficult. For that reason a further subdivision is used, to get more information about the most interesting depths.



Graph 24: Average summer salinity in ‰ measured at the Sognesjøen for the period from 1935 until 2014, focusing on the upper 1 m to 20 m layers. The x-axis shows the years, while the y-axis depicts the salinity in ‰. The three background colors depict the different periods: green = pre-impact period, blue = transitional period, red = full-impact period.

Graph 24 now depicts the average summer salinity in ‰ measured at the Sognesjøen in 1 m, 10 m and 20 m depth. The measuring period from the 1 m and 10 m layer is from 1935 until 2014 while the measurement of 20 m first starts 1971. The overall range of the three water layers is between 26.5‰ and 34.00‰, however with some exceptions, especially in the 1 m layer.

By only showing the depths of 1 m, 10 m and 20 m, the graph displays small changes within the salinity values. Beside the largest fluctuations visible within the 1 m layer in 1937 and 1940, there is also a slight rise in the average salinity measurable, accounting for 0.58% (Table 21). Thus the salinity values increased at 0.17‰. At 20 m depth a rise of 0.04‰ is apparent. Additionally the 10 m layer shows a reversed trend with salinity values declining at 0.31‰, making up for 0.97%.

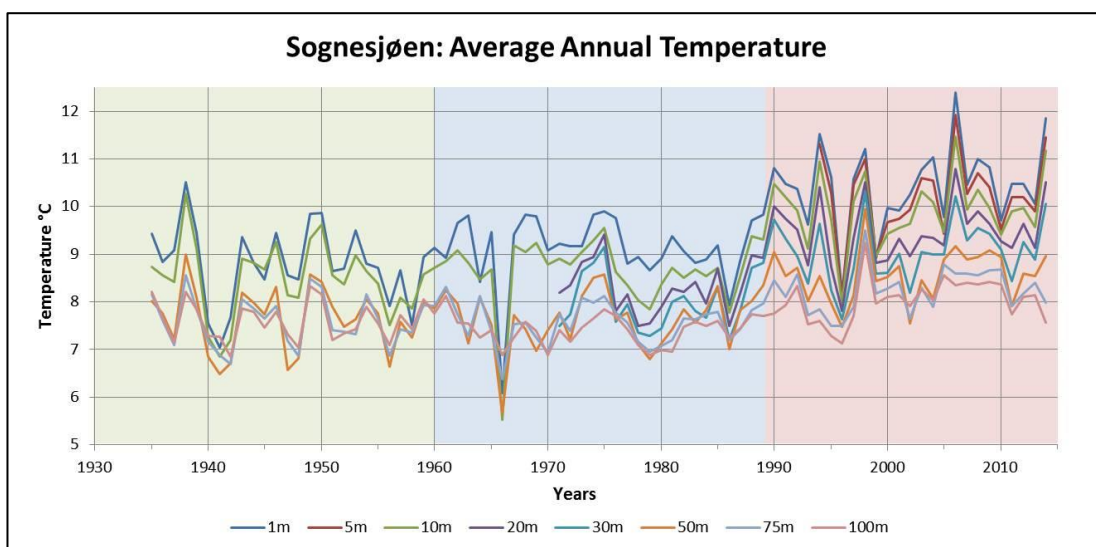
There are also some large fluctuations within the measuring period in the 1 m layer visible, showing very low salinities. The most pronounced minima are seen during the first years of measurement in 1937 and 1940, showing values less than 20.0‰ (Graph 24). Furthermore there are some smaller but still very low troughs, reducing the salinity to around 25.0‰ in 1976, as well as during the period from 1994 until 2014.

3.3.2 Temperature

The subsequent Graphs 25 to 29 depict the average temperatures at the Sognesjøen in °C, for the period from 1935 until 2014. Thereby they show the depths 1 m, 5 m, 10 m, 20 m, 30 m, 50 m, 75 m and 100 m. The x-axes depict the years in steps of ten years, while the y-axis represents the temperature in °C. The colored background depicts the different periods, the pre-impact period, the transitional period and the full-impact period.

The Tables 22 to 24 depict the average temperature values in °C, calculated for the three defined periods as well as the difference between period one and three in °C and %. The blue colors thereby show the different kinds of water masses, however, the transition zones can slightly vary, as the water masses blend into each other.

3.3.2.1 Annual



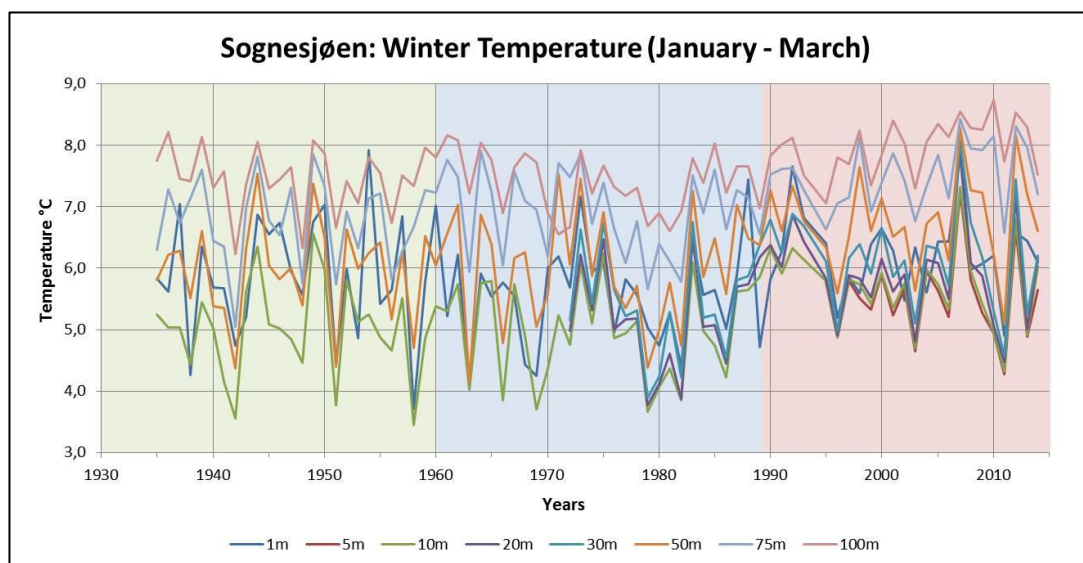
Graph 25: Average annual temperature in °C measured at the Sognesjøen during the period from 1935 until 2014. The x-axis shows the years, while the y-axis depicts the temperature in °C for 1 m to 100 m depths. The three background colors depict the different periods: green = pre-impact period, blue = transitional period, red = full-impact period.

Temperature [°C]: Sognesjøen Annual						
Depth [m]	1. Period 1935-1960	2. Period 1960-1989	3. Period 1989-2014	Change 1. to	Change in %	
1	8,81	9,12	10,45	1,64	18,66 %	Surface Water
5	n.d.	9,41	10,22			
10	8,50	8,64	9,94	1,44	16,91 %	
20	n.d.	8,31	9,46			
30	n.d.	8,00	9,06			
50	7,65	7,62	8,56	0,91	11,94 %	Deep Water
75	7,61	7,55	8,25	0,64	8,42 %	
100	7,61	7,41	8,04	0,43	5,68 %	

Table 22: Average annual temperature in °C at the Sognesjøen, calculated for the three pre-defined periods and additionally the difference between period 1 and 3 in °C and %. The blue colors depict the different kinds of water masses, however, the transition zones can slightly vary.

Graph 25 depicts the average annual temperature at the Sognesjøen. The values are ranging between 7.0°C and 11.0°C, however showing a rising trend mainly in the end of the period and one exception through a trough in 1966. Beside that the graph shows a rising trend in all layers. This increase is largest in the 1 m layer, accounting for 1.64°C or 18.66% (Table 22). Additionally a large trough is noticeable around 1966 in the upper 1 m to 50 m layers. What is also visible is a similar trend, especially in the upper 1 m to 30 m layers. Against that the deeper layers, from 50 m to 100 m show a slightly different behavior. Regarding the entire period, the general range of fluctuations seems to have changed around 1985, causing higher average values as well as larger fluctuations.

3.3.2.2 Seasonal

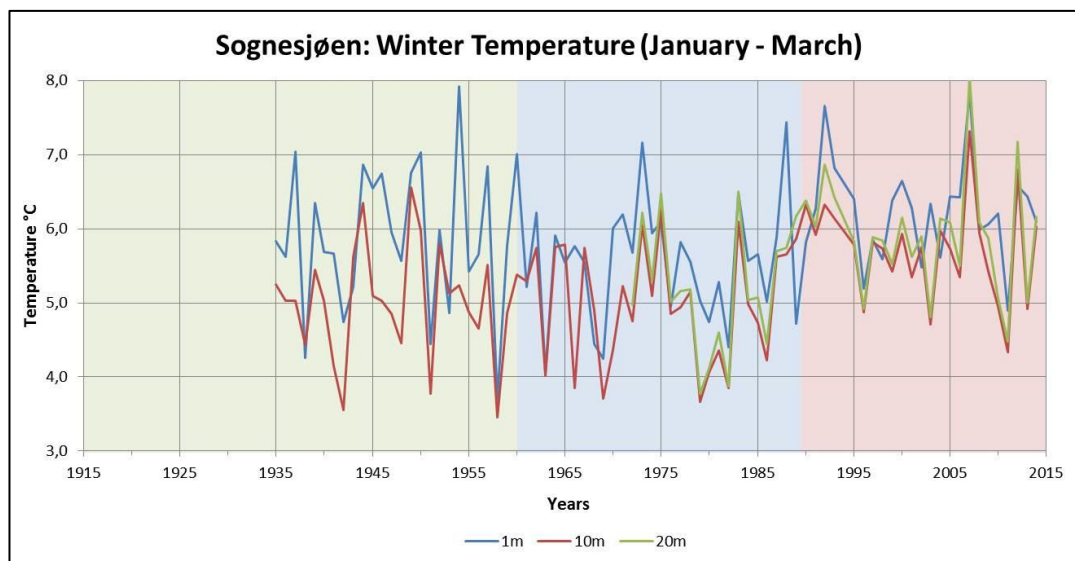


Graph 26: Average winter temperature in °C measured at the Sognesjøen during the period from 1935 until 2014. The x-axis shows the years, while the y-axis depicts the temperature in °C for 1 m to 100 m depths. The three background colors depict the different periods: green = pre-impact period, blue = transitional period, red = full-impact period.

Temperature [°C]: Sognesjøen Winter Period						
Depth [m]	1. Period 1935-1960	2. Period 1960-1989	3. Period 1990-2014	Change 1. to 3.	Change in %	
1	5,90	5,54	6,22	0,32	5,39 %	Surface Water
5	n.d.	n.d.	5,51			
10	5,02	4,99	5,70	0,68	13,60 %	
20	n.d.	5,19	5,91			
30	n.d.	5,19	5,91			
50	5,96	6,01	6,77	0,81	13,62 %	Deep Water
75	6,76	6,91	7,51	0,74	10,99 %	
100	7,46	7,38	7,98	0,52	7,03 %	

Table 23: Average winter temperature in °C at the Sognesjøen, calculated for the three pre-defined periods and additionally the difference between period 1 and 3 in °C and %. The blue colors depict the different kinds of water masses, however, the transition zones can slightly vary.

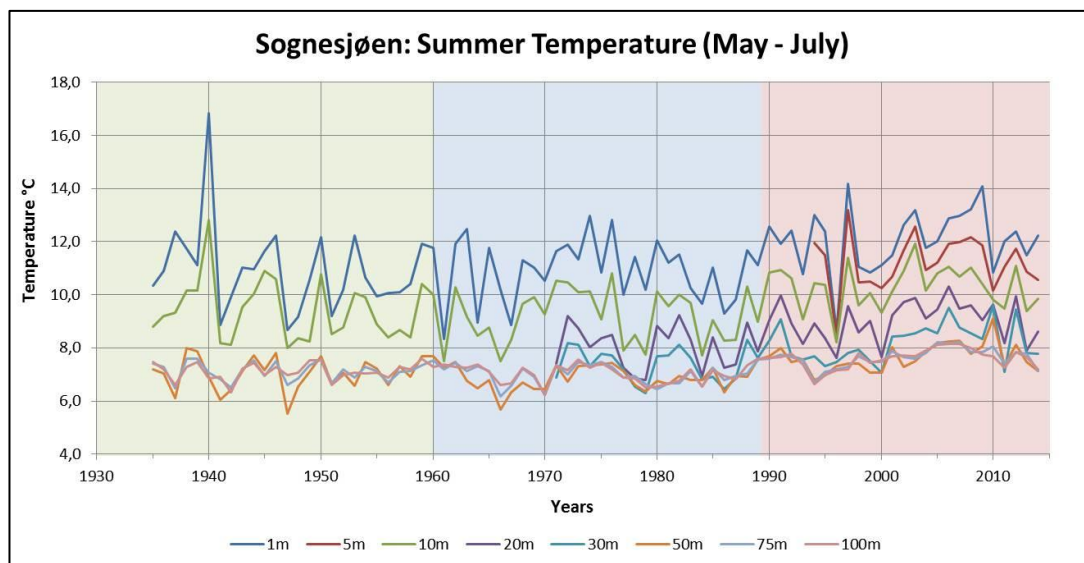
The figure above shows the entire dataset of winter temperature values in °C. Overall it is visible that the fluctuations of all layers level within a range of 4.0°C to 8.0°C. However, this range seems to become lifted after 1990, then fluctuating between 5.0°C and 8.5°C. Beside that the graph seems to show a general rise in temperature within all layers. Thus the largest change of 0.81°C appears in the 50 m layer (Table 23). However, owing to the high number of temperature-lines a general trend is not clearly visible. Nevertheless the graph enables to take a deeper look on the most significant upper layers through a further subdivision.



Graph 27: Average winter temperature in °C measured at the Sognesjøen during the period from 1935 until 2014, focusing on the upper 1 m to 20 m layers. The x-axis shows the years, while the y-axis depicts the temperature in °C. The three background colors depict the different periods: green = pre-impact period, blue = transitional period, red = full-impact period.

Graph 27 depicts the winter temperatures measured at the Sognesjøen, however focusing on the depths of 1 m, 10 m and 20 m. In general the three layers show fluctuations in the range of 4.0°C to 7.0°C, including some exceptions protruding this range. Especially in the 10 m layer are many high peaks but also various lows, indicating big differences between the maxima and minima as well as the most pronounced changes at all. Additionally it is visible that the largest fluctuations have occurred before 1970.

Furthermore there is a strong change in temperature visible in all layers after around 1985. Thus, within the entire measuring period the temperature increases at 5.39% at 0 m and 13.6% at 10 m depth (Table 23). This is also depicting the overall trend, which shows a rise in temperature in all layers.



Graph 28: Average summer temperature in °C measured at the Sognesjøen during the period from 1935 until 2014 for the 1 m to 100 m layers. The x-axis shows the years, while the y-axis depicts the temperature in °C. The three background colors depict the different periods: green = pre-impact period, blue = transitional period, red = full-impact period.

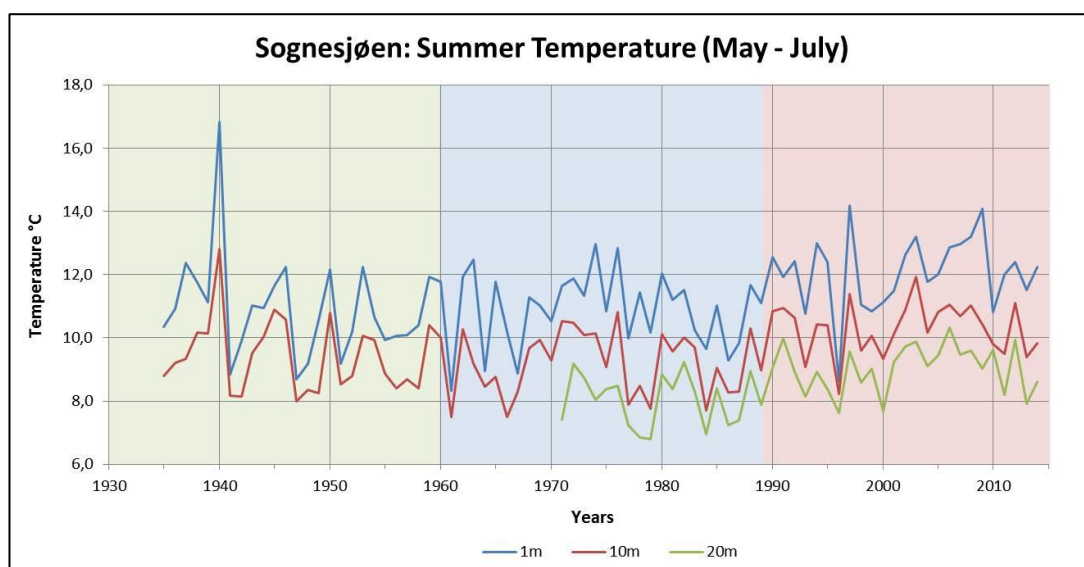
Temperature [°C]: Sognesjøen Summer Period						
Depth [m]	1. Period 1935-1960	2. Period 1960-1989	3. Period 1990-2014	Change 1. to 3.	Change in %	
1	10,97	10,90	12,08	1,12	10,18 %	Surface Water
5	n.d.	9,41	11,22			
10	9,43	9,18	10,31	0,87	9,24 %	
20	n.d.	8,04	9,04			
30	n.d.	7,38	8,20			Deep Water
50	7,06	6,86	7,65	0,59	8,31 %	
75	7,13	7,00	7,64	0,51	7,21 %	
100	7,12	7,03	7,60	0,48	6,71 %	

Table 24: Average summer temperature in °C at the Sognesjøen, calculated for the three pre-defined periods and additionally the difference between period 1 and 3 in °C and %. The blue colors depict the different kinds of water masses, however, the transition zones can slightly vary.

Graph 28 depicts the average summer temperatures, leveling within the range of 6.0°C and 12.0°C with some exceptions. One big peak is visible in the 1 m and 10 m layer in 1940, causing the temperatures to rise from about 11.0°C to around 17.0°C. Another very obvious increase of temperature in all water layers occurred in 1998, shown by a huge peak there. This causes an enormous rise in temperature within all layers, increasing these at around 5.0°C. Furthermore it is visible that there are higher fluctuations within the 1 m and 10 m depth in the period until 1970, while the variations are smaller in the deeper layers.

In general there seems to be a slight rise in temperature in all of the water layers, starting in the second measuring period. This causes the temperature to rise more than 1.0°C in the

upper 1 m to 20 m layers, as well as more than 0.6°C in the lowermost 30 m to 100 m layers (Table 24). Compared to the summer period the data depict a larger overall temperature increase at 1 m and 10 m depth. However, due to the high number of different water-depths shown in the graph a reliable statement is difficult. Therefore a further classification into more detailed graphs showing only specific water layers can be useful.



Graph 29: Average summer temperature in °C measured at the Sognesjøen during the period from 1935 until 2014, focusing on 1 m to 20 m depth. The x-axis shows the years while the y-axis depicts the temperature in °C. The three background colors depict the different periods: green = pre-impact period, blue = transitional period, red = full-impact period.

Graph 29 again depicts the average summer temperature, however focusing on the 1 m, 10 m and 25 m layers. The average level of fluctuations is ranging between 8.0°C and 13.0°C, only interrupted by some exceptions. The graph now clearly shows the big peak in temperature around 1940 in the 1 m and 10 m water layers. The 20 m layer is excluded, as the measurement of this depth first started in 1971. Also the second peak in 1998 is clearly visible, even though it is smaller than the first peak. In general the temperature of all depths shows an increasing trend within the last part of the measured period, starting around 1985. This causes an overall rise in temperature of 1.27°C at 1 m and 1.03°C at 10 m depth (Table 24). Beside that the 20 m layer still shows an increase at 1.16°C from the second to the third period.

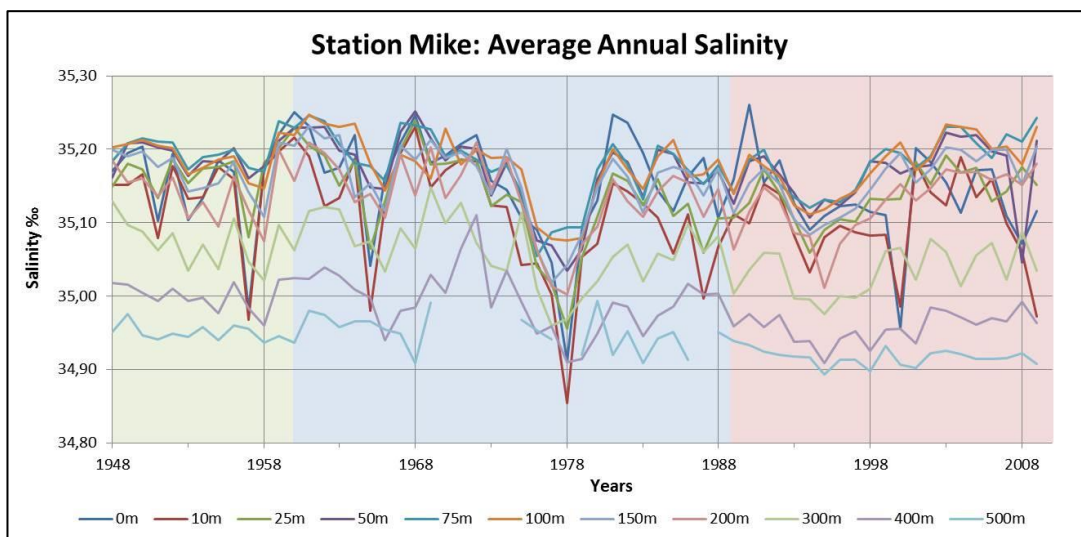
3.4 Station Mike

3.4.1 Salinity

The subsequent Graphs 30 to 34 depict the average salinity in ‰ for annual and seasonal situations, measured at Station Mike in the Nordic Sea. The measured depths include 0 m, 10 m, 25 m, 50 m, 75 m, 100 m, 150 m, 200 m, 300 m, 400 m and 500 m. While the x-axes depict the time in years from 1948 until 2010 in steps of ten years, the y-axes show the salinity in ‰. The three background colors depict the three defined periods before, while and after building of the large water power plants.

The Tables 25 to 27 depict the calculated average salinities in ‰ for the three periods before, while and after water power plant building. Additionally they show the difference in salinity between the first and the third period in ‰ and ‰. The blue colors show the different kinds of water masses, however, the transition zones can slightly vary, as the water masses blend into each other.

3.4.1.1 Annual



Graph 30: Average annual salinity in ‰ measured at Station Mike for the period from 1949 until 2008 and the depths from 0 m to 500 m. The x-axis shows the years, while the y-axis depicts the salinity in ‰. The three background colors depict the different periods: green = pre-impact period, blue = transitional period, red = full-impact period.

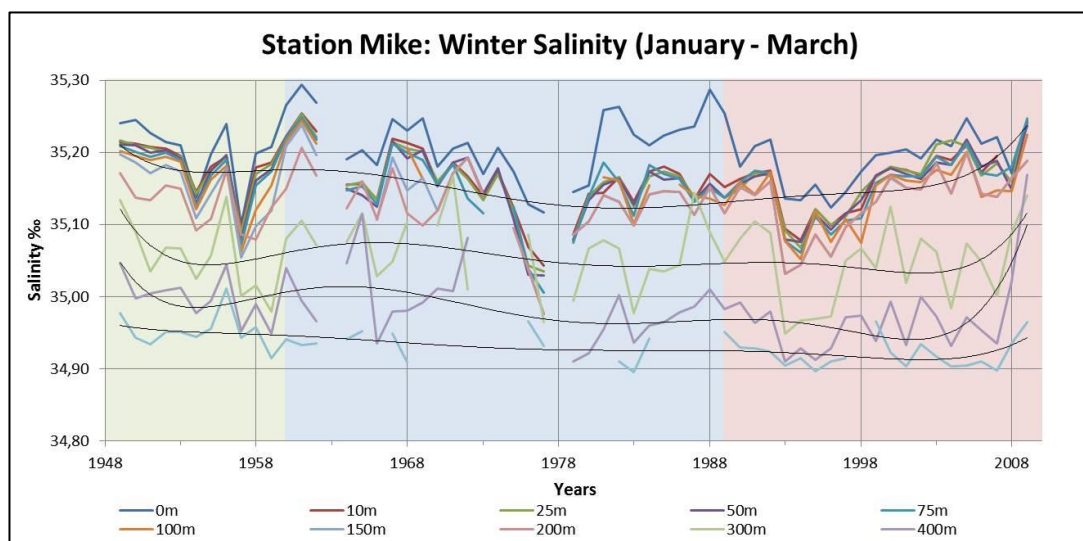
Salinity [‰]: Station Mike Annual						
Depth [m]	1. Period 1948-1960	2. Period 1960-1989	3. Period 1989-2009	Change 1. to 3.	Change in %	
0	35,16	35,15	35,13	-0,03	-0,08 %	Surface Water
10	35,15	35,10	35,10	-0,05	-0,13 %	
25	35,17	35,13	35,14	-0,03	-0,09 %	
50	35,19	35,17	35,17	-0,02	-0,07 %	Deep Water
75	35,20	35,17	35,18	-0,02	-0,05 %	
100	35,19	35,17	35,18	-0,01	-0,03 %	
150	35,17	35,15	35,16	-0,01	-0,04 %	
200	35,14	35,13	35,13	-0,01	-0,04 %	
300	35,07	35,06	35,04	-0,04	-0,11 %	
400	35,00	34,99	34,96	-0,04	-0,13 %	
500	34,95	34,95	34,92	-0,03	-0,10 %	

Table 25: Average annual salinity in ‰ at the Nordic Sea, calculated for the three pre-defined periods and additionally the difference between period 1 and 3 in ‰ and %. The blue colors depict the different kinds of water masses, however, the transition zones can slightly vary.

Graph 30 shows the entire data set of annual salinity data in ‰, measured at Station Mike. Thereby the graph depicts a huge amount of data, giving information about salinity fluctuations within the surface but also the deep ocean water. The range of the y-axis also perfectly depicts the typical salinity values for sea water, which usually fluctuates around 35‰. Regarding the Nordic Sea, the salinity values also give information about the source of the water. Hence salinity values higher than 35.0‰ is indicator of Gulf Stream water. The upper layers of 0 m to 200 m are mainly leveling in the range of 35.10‰ and 35.25‰, thus showing the highest salinity values at all. However there are some significant exceptions due to remarkable troughs within the entire period. Beside that the lowermost layers from 300 m to 500 m are occurring in the range of 34.90‰ and 35.10‰.

In general big fluctuations are visible, especially pronounced in the upper water layers, showing differences up to 0.4‰ (Table 25). Beside that all layers depict a slight decline in salinity, ranging between 0.0% and 0.13%. However, do to the high number of depth-lines shown in the graph it is difficult to figure out the progress of specific layers. For that reason a further fragmentation of the graph is used, to get a closer look on specifically the seasons as well as on the surface water layers.

3.4.1.2 Seasonal



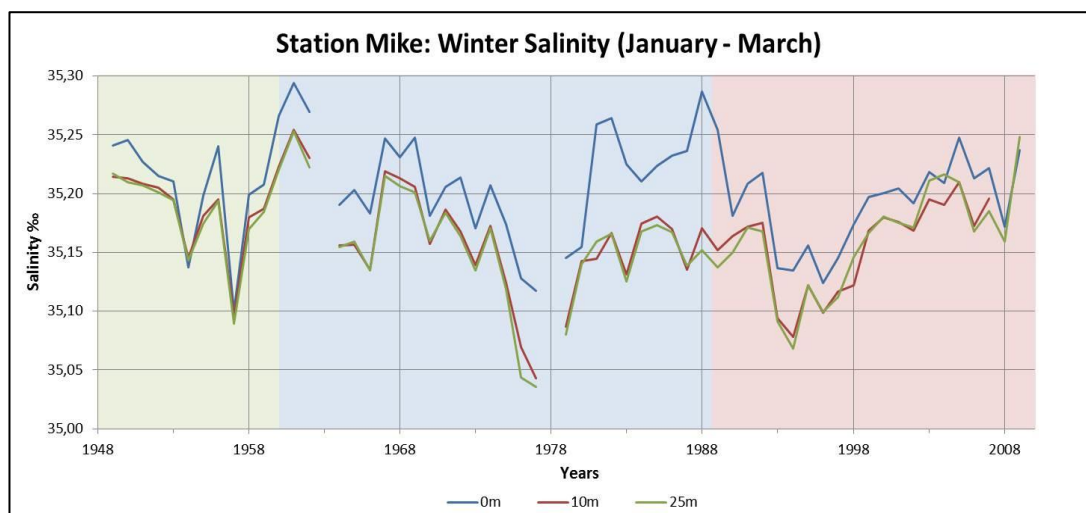
Graph 31: Average winter salinity in ‰ measured at Station Mike for the period from 1949 until 2008 and the depths from 0 m to 500 m. The x-axis shows the years, while the y-axis depicts the salinity in ‰. Additionally trend lines have been added. The three background colors depict the different periods: green = pre-impact period, blue = transitional period, red = full-impact period.

Salinity [‰]: Station Mike Winter Period						
Depth [m]	1. Period 1949-1960	2. Period 1960-1989	3. Period 1990-2009	Change 1. to 3.	Change in %	
0	35,19	35,19	35,17	-0,02	-0,06 %	Surface Water
10	35,17	35,14	35,15	-0,02	-0,05 %	
25	35,19	35,16	35,17	-0,02	-0,07 %	
50	35,20	35,18	35,17	-0,02	-0,07 %	Deep Water
75	35,19	35,17	35,18	-0,02	-0,04 %	
100	35,18	35,17	35,17	-0,01	-0,04 %	
150	35,16	35,15	35,15	-0,01	-0,04 %	
200	35,13	35,14	35,15	0,01	0,04 %	
300	35,06	35,06	35,04	-0,02	-0,06 %	
400	35,00	35,00	34,97	-0,03	-0,08 %	
500	34,95	34,95	34,92	-0,03	-0,09 %	

Table 26: Average winter salinity in ‰ at the Nordic Sea, calculated for the three pre-defined periods and additionally the difference between period 1 and 3 in ‰ and %. The blue colors depict the different kinds of water masses, however, the transition zones can slightly vary.

Graph 31 represents the average winter salinity in ‰ at Station Mike. As can be seen, only two of the gaps with missing data are visible within the winter period, indicating the other two periods to occur during the summer season. The upper layers from 0 m to 200 m are leveling within the range of 35.05‰ and 35.25‰. Beside that the 300 m to 500 m layers are different, fluctuating in the range of 34.90‰ and 35.10‰. Overall the general fluctuations of all of the layers are quite small, only accounting from 34.9‰ to 35.3‰.

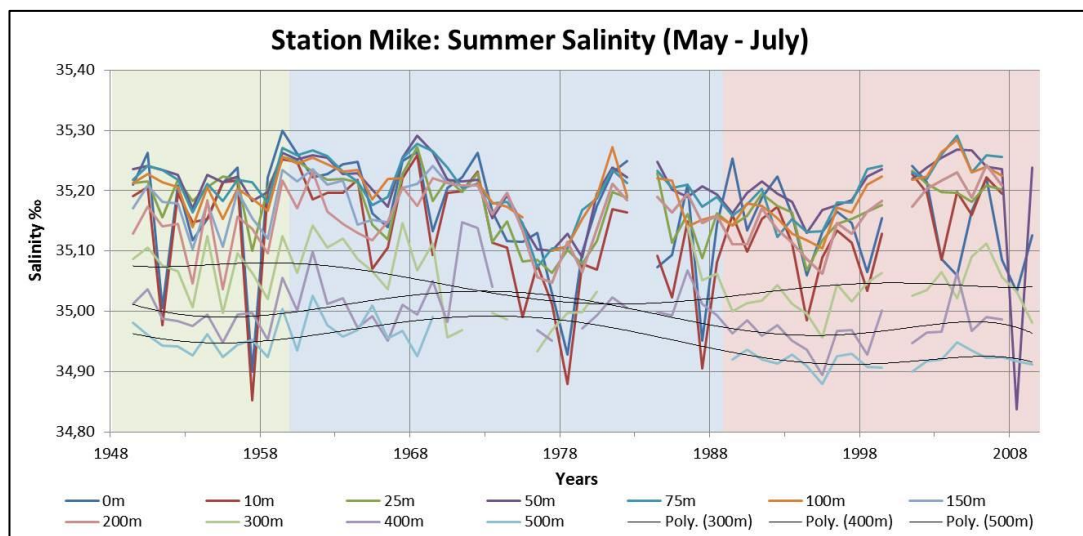
Regarding all depths there are slight drops in salinity in all layers. Thereby the 500 m layer is showing the strongest decline of 0.03‰ (Table 26). Beside that the 200 m layer displays a reversed trend with an increase in salinity of 0.01‰. However, a closer look on specifically the significant upper surface water layers might reveal more information about potential changes.



Graph 32: Average winter salinity in ‰ measured at Station Mike for the period from 1949 until 2008, focusing on the depths from 0 m to 25 m. The x-axis shows the years, while the y-axis depicts the salinity in ‰. The three background colors depict the different periods: green = pre-impact period, blue = transitional period, red = full-impact period.

Graph 32 now depicts the winter salinity in ‰, focusing on the depths of 0 m, 10 m and 25 m. As the graph shows, there is a marked minimum visible around 1978, even though the data from the year itself are missing. During that time the salinity also reaches its absolute minimum within the entire measuring period. As seen in Graph 32 this phenomenon of very low salinity values occurred more often. Thus there was already a low around 1957, but also around 1993 emerging in the Nordic Sea.

Overall, by comparing the period before the water power plants, from 1949 until 1960, and after the building, from 1990 till 2009, there are only small changes in salinity apparent in all three layers. Thus there is a reduction of 0.02‰ in all layers (Table 26). The largest drop thereby occurs in the 25 m layer, accounting for 0.07%. Beside that the salinity declined at 0.06% in 0 m and 0.05% in 10 m depth.



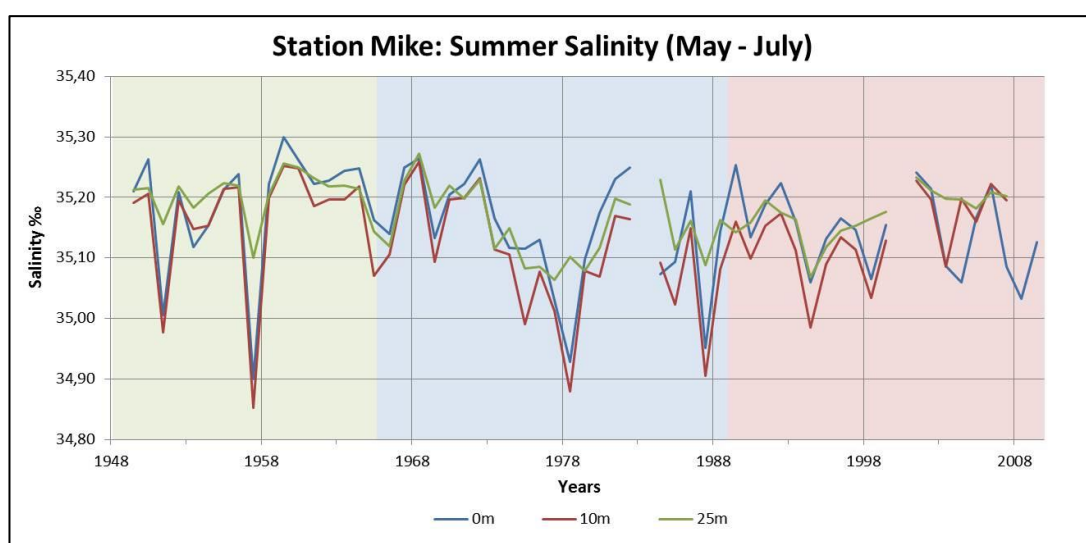
Graph 33: Average summer salinity in ‰ measured at Station Mike for the period from 1949 until 2008 and the depths from 0 m to 500 m. The x-axis shows the years, while the y-axis depicts the salinity in ‰. The three background colors depict the different periods: green = pre-impact period, blue = transitional period, red = full-impact period. Trend lines have been added.

Salinity [‰]: Station Mike Summer Period						
Depth [m]	1. Period 1949-1960	2. Period 1960-1989	3. Period 1990-2009	Change 1. to 3.	Change in %	
0	35,19	35,19	35,17	-0,02	-0,07 %	Surface Water
10	35,17	35,13	35,14	-0,03	-0,07 %	
25	35,19	35,16	35,17	-0,02	-0,07 %	
50	35,20	35,17	35,18	-0,02	-0,07 %	Deep Water
75	35,20	35,17	35,18	-0,02	-0,04 %	
100	35,18	35,17	35,17	-0,01	-0,04 %	
150	35,16	35,15	35,15	-0,01	-0,04 %	
200	35,13	35,14	35,15	0,02	0,05 %	
300	35,06	35,05	35,04	-0,02	-0,06 %	
400	35,00	35,00	34,97	-0,03	-0,08 %	
500	34,95	34,95	34,92	-0,03	-0,09 %	

Table 27: Average summer salinity in ‰ at the Nordic Sea, calculated for the three pre-defined periods and additionally the difference between period 1 and 3 in ‰ and %. The blue colors depict the different kinds of water masses, however, the transition zones can slightly vary.

Graph 33 shows the entire dataset of summer salinity values measured at the Nordic Sea. There are two gaps without data visible around 1983 and 2000, however not big enough to significantly disturb making statements about the salinity progress. Overall the upper 0 m to 200 m layers range between 35.10‰ and 35.25‰, while the 300 m to 500 m layers are separated, ranging between 34.90‰ and 35.10‰. Especially in the upper layers the graph shows huge fluctuations beyond the average range, indicating differences between maxima and minima salinities from around 0.4‰.

Beside that almost all layers show a slight decline in salinity, accounting for a reduction between 0.04% and 0.09% (Table 27). While the 0 m to 50 m layers show a drop in salinity of around 0.07%, this only accounts for 0.04% in the depths between 75 m and 150 m. The strongest drop occurs in the lowermost 300 m, 400 m and 500 m layers, causing a decline of 0.06%, 0.08% and 0.09% (Table 27). This trend is also confirmed by the trend lines through the three layers. Within the 200 m layer there is again a reversed trend visible, depicting a rise in salinity of 0.05%. However, due to the high number of depth-lines, it is difficult to make more precise statements. Thus a further subdivision is used to take a closer look on single depths.



Graph 34: Average summer salinity in ‰ measured at Station Mike for the period from 1949 until 2008, focusing on 0 m to 25 m depth. The x-axis shows the years, while the y-axis depicts the salinity in ‰. The three background colors depict the different periods: green = pre-impact period, blue = transitional period, red = full-impact period.

Graph 34 represents the average summer salinities for the 0 m, 10 m and 25 m layers of the surface water. As now clearly visible, there are large fluctuations in the salinity in all three layers during the first two periods. However, these extreme episodes of very low salinities seem to be missing in the third period.

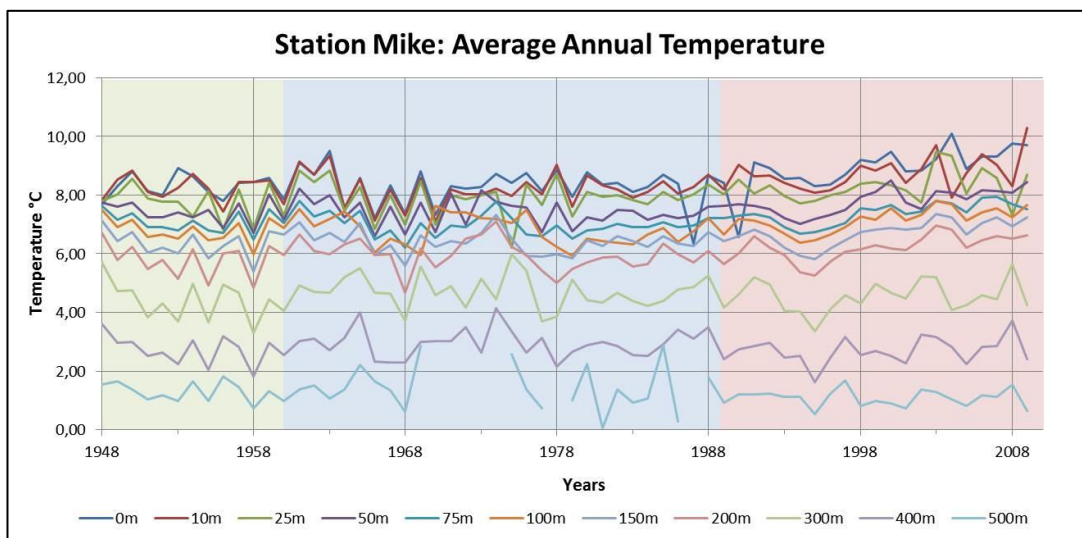
Furthermore it is obvious, that the salinity scale on the y-axis now needs a wider range than during the winter season. Regarding the overall trend, there is a slightly decreasing trend visible in all layers, accounting for 0.07% (Table 27).

3.4.2 Temperature

The following Graphs 35 to 39 depict the average temperature in °C at the Nordic Sea during the period from 1948 until 2009. The measured depths comprise 0 m, 10 m, 25 m, 50 m, 75 m, 100 m, 150 m, 200 m, 300 m, 400 m and 500 m. While the x-axes depict the time in years from 1948 until 2010 in steps of ten years, the y-axes show the temperature in °C. The background colors depict the three periods, before, while and after building of the large water power plants.

The Tables 28 to 30 depict the calculated average temperatures in °C for the three periods before, while and after building of the water power plants. Beside that they show the difference between the first and the third period in °C and %. The blue colors show the different kinds of water masses, however, the transition zones can slightly vary, as the water masses blend into each other.

3.4.2.1 Annual



Graph 35: Average annual temperature in °C measured at the Nordic Seas in the depths from 0 m to 500 m for the period from 1948 until 2009. The x-axis shows the years from 1948 to 2010, while the y-axis depicts the temperature in °C. The three background colors depict the different periods: green = pre-impact period, blue = transitional period, red = full-impact period.

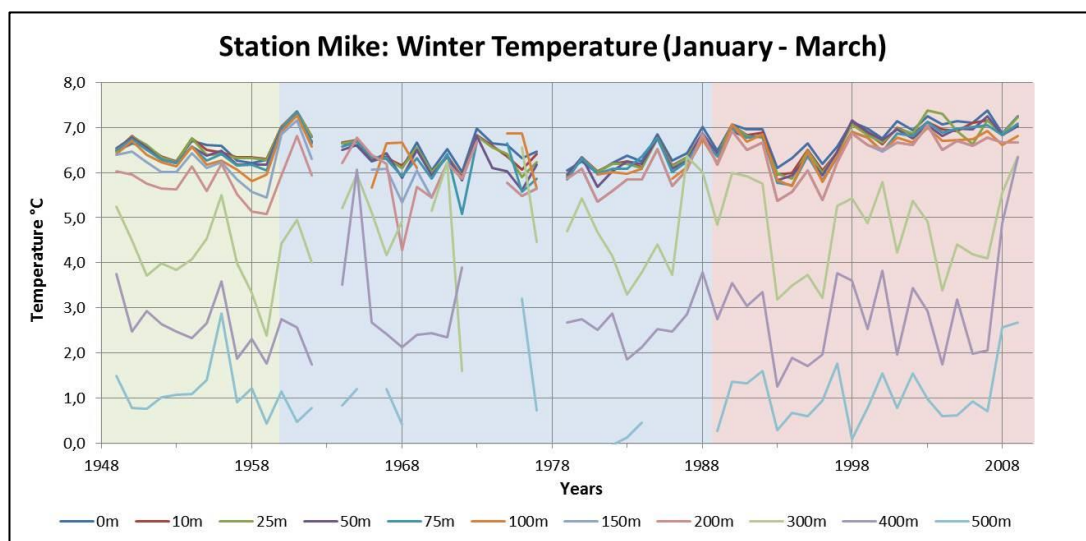
Temperature [°C]: Station Mike Annual						
Depth [m]	1. Period 1948-1960	2. Period 1960-1989	3. Period 1989-2009	Change 1. to 3.	Change in %	
0	8,29	8,30	8,95	0,66	7,94 %	Surface Water
10	8,23	8,21	8,77	0,54	6,55 %	
25	7,76	7,91	8,30	0,54	7,01 %	
50	7,40	7,43	7,79	0,39	5,30 %	Deep Water
75	7,07	7,00	7,38	0,31	4,35 %	
100	6,80	6,80	7,17	0,37	5,41 %	
150	6,36	6,41	6,73	0,36	5,69 %	
200	5,80	5,96	6,24	0,44	7,56 %	
300	4,39	4,70	4,55	0,16	3,68 %	
400	2,72	2,94	2,70	-0,02	-0,80 %	
500	1,28	1,48	1,09	-0,19	-15,00 %	

Table 28: Average annual temperature in °C at the Nordic Sea, calculated for the three pre-defined periods and additionally the difference between period 1 and 3 in °C and %. The blue colors depict the different kinds of water masses, however, the transition zones can slightly vary.

Graph 35 shows the entire dataset of annual temperatures in °C. Overall it is visible that the uppermost 0 m to 200 m level within the range of 5.5°C and 10°C. Beside that the deepest layers from 300 m to 500 m are separated, fluctuating within the range of 0.0°C to 5.0°C. Despite the high number of different depth lines shown in the graph, a slight rise in temperature in the upper 200 m is visible (Table 28). Against that only a very small increase is seen at the 300 m layer as well as a temperature decline in the 400 m and 500 m layers. Overall the largest absolute increase is visible in the surface layer at 0 m depth, accounting for 0.66°C.

Furthermore the graph depicts several peaks and troughs, which are partly visible at all depths. Especially in the uppermost 200 m the temperature progress seems to be similar, showing likewise peaks and troughs in the different layers. Very obvious are thereby two big troughs, only occurring in the 0 m layer during the years 1987 and 1990. In general this figure gives a good overview over the entire set of data measured at Station Mike, enabling a further subdivision into more detailed graphs. This is necessary, to allow a more detailed look on the significant surface water layers and time periods, potentially giving more information.

3.4.2.2 Seasonal



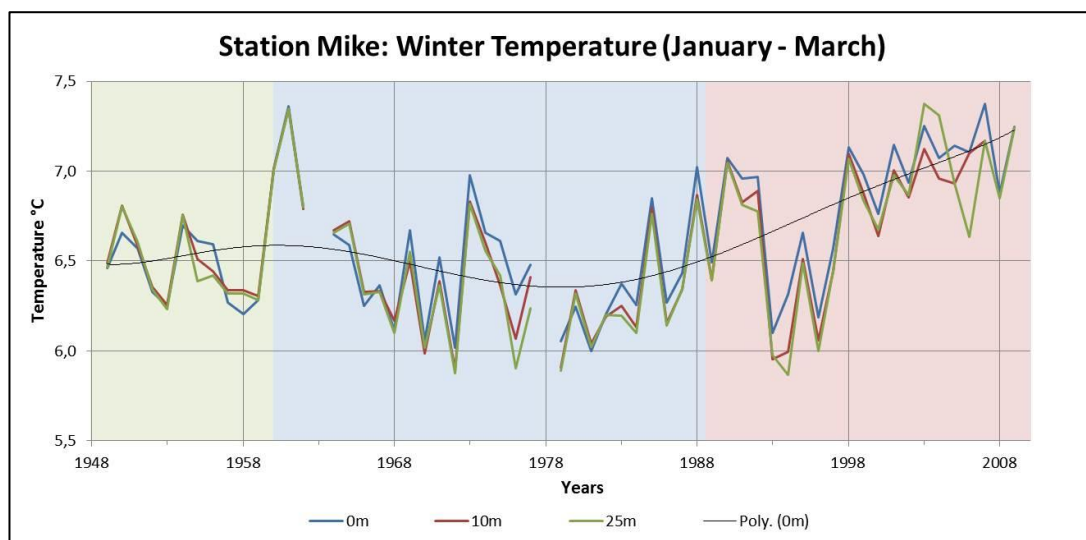
Graph 36: Average winter temperature in °C measured at the Nordic Seas in the depths from 0 m to 500 m for the period from 1949 until 2009. The x-axis shows the years from 1948 to 2010, while the y-axis depicts the temperature in °C. The three background colors depict the different periods: green = pre-impact period, blue = transitional period, red = full-impact period.

Temperature [°C]: Station Mike Winter Period						
Depth [m]	1. Period 1949-1960	2. Period 1960-1989	3. Period 1990-2009	Change 1. to 3.	Change in %	
0	7,63	7,83	8,36	0,73	9,63 %	Surface Water
10	7,56	7,69	8,06	0,50	6,60 %	
25	7,28	7,42	7,63	0,35	4,83 %	
50	6,89	6,91	7,24	0,35	5,07 %	Deep Water
75	6,64	6,64	7,01	0,37	5,60 %	
100	6,43	6,54	6,81	0,38	5,98 %	
150	6,10	6,21	6,49	0,39	6,42 %	
200	5,62	6,12	6,49	0,87	15,47 %	
300	4,21	4,63	4,70	0,49	11,73 %	
400	2,67	2,99	2,95	0,28	10,34 %	
500	1,25	1,33	1,19	-0,06	-4,63 %	

Table 29: Average winter temperature in °C at the Nordic Sea, calculated for the three pre-defined periods and additionally the difference between period 1 and 3 in °C and %. The blue colors depict the different kinds of water masses, however, the transition zones can slightly vary.

Graph 36 shows the entire dataset of winter temperature values at Station M. Overall the temperatures of the 0 m to 200 m layers are leveling in the range of 5.5°C and 7.5°C. Beside that the 300 m to 500 m depths are ranging between 0.0°C and 5.5°C. There are also two periods without measurements visible around 1963 and 1978. Overall, the given winter values show a slight rise in temperature within the entire measuring period. This causes the highest increases in the 0 m, 200 m, 300 m and 400 m layers. The 0 m, 300 m and 400 m

layers show a rise between 9% and 12%, while the 200 m layer displays 15.47% more (Table 29). Against that the 500 m layer decreases at 4.63%. In general the upper layers are more expressive as they contain more complete data sets with fewer measurements missing. Due to the main focus on the upper surface layers, a further classification is used to provide more detailed information.

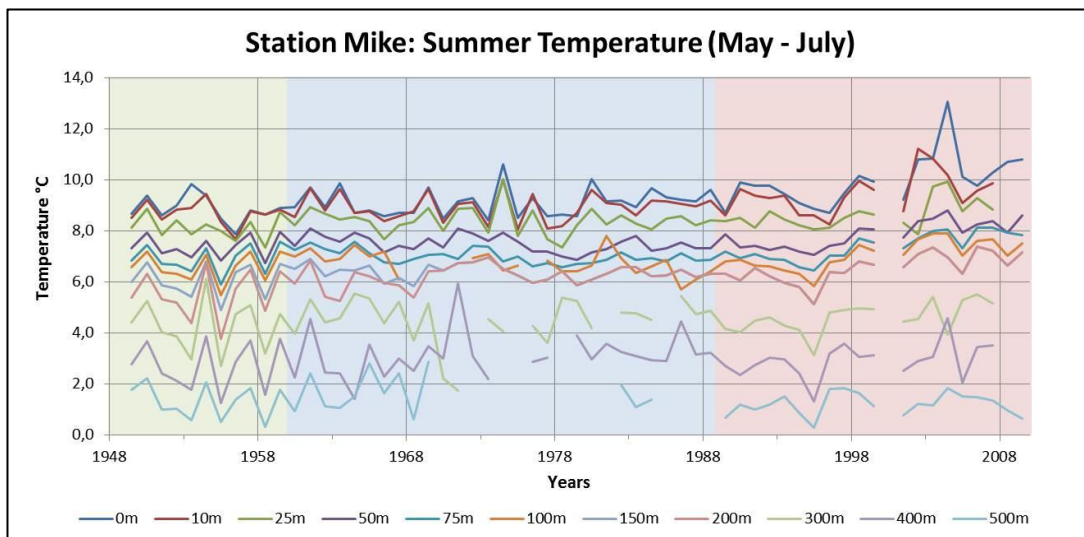


Graph 37: Average winter temperature in °C measured at the Nordic Seas, focusing on the 0 m to 25 m layers for the period from 1949 until 2009. The x-axis shows the years from 1948 to 2010, while the y-axis depicts the temperature in °C. Additionally a trend line has been added. The three background colors depict the different periods: green = pre-impact period, blue = transitional period, red = full-impact period.

Graph 37 depicts again the average winter temperature values, now focusing on the upper layers of 0 m, 10 m, and 25 m. Overall the fluctuations in all layers range between 6.0°C and 7.5°C. However, regarding the period after 1990, the range seems to change, showing variations between 6.75°C and 7.25°C, only interrupted by two very large troughs in 1993 and 1996.

As can be seen there has been a huge peak in the 10 m and 25 m layers around 1961, followed by a general decline until around 1980. In the period afterwards a rise in temperature is visible. This reflects the overall trend of the graph, showing a general temperature increase. Thus a rise in the temperature of 0.73°C at 0 m, of 0.50°C at 10 m and of 0.35°C at 25 m depth is visible (Table 29). However, there has been a cold period interrupting that rising temperature trend, lasting from around 1983 until 1997, including two especially big troughs in 1993 and 1996. These show a drop in temperature from 7.1°C to about 5.9°C, marking a period with very cold winter temperatures.

Furthermore there is a difference between the periods before and after 1982 visible. While in the period before 1982 the temperatures of the 10 m and 25 m layers are often higher than the temperature of the 0 m layer, this is only the case once after 1982, when the 25 m layer is crossing the 0 m layer during the period from 2003 to 2005.



Graph 38: Average summer temperature in °C measured at the Nordic Seas in the depths from 0 m to 500 m for the period from 1949 until 2009. The x-axis shows the years from 1948 to 2010, while the y-axis depicts the temperature in °C. The three background colors depict the different periods: green = pre-impact period, blue = transitional period, red = full-impact period.

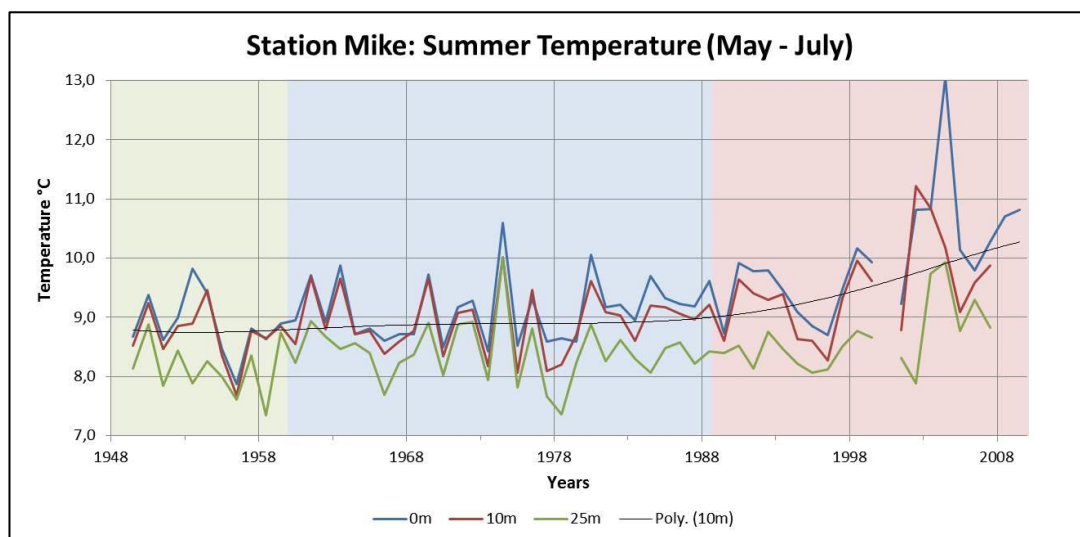
Temperature [°C]: Station Mike Summer Period						
Depth [m]	1. Period 1949-1960	2. Period 1960-1989	3. Period 1990-2009	Change 1. to 3.	Change in %	
0	7,74	7,85	8,46	0,72	9,37 %	Surface Water
10	7,65	7,71	8,16	0,51	6,62 %	
25	7,36	7,44	7,70	0,34	4,64 %	
50	6,93	6,92	7,29	0,36	5,12 %	Deep Water
75	6,67	6,64	7,03	0,36	5,42 %	
100	6,46	6,53	6,83	0,37	5,73 %	
150	6,10	6,19	6,49	0,39	6,43 %	
200	5,62	6,11	6,50	0,88	15,66 %	
300	4,15	4,61	4,63	0,48	11,67 %	
400	2,60	3,00	2,89	0,28	10,84 %	
500	1,22	1,34	1,17	-0,05	-4,28 %	

Table 30: Average summer temperature in °C at the Nordic Sea, calculated for the three pre-defined periods and additionally the difference between period 1 and 3 in °C and %. The blue colors depict the different kinds of water masses, however, the transition zones can slightly vary.

Graph 38 shows the entire dataset of summer temperature values measured at Station Mike. Overall the fluctuations of the 0 m to 200 m depths are leveling within a range of

5.0°C to 11.0°C. Beside that the 300 m to 500 m layers show variations between 1.0°C and 5.0°C.

During the period of 1999 until 2001 there is a lack of data visible in all depths, as already seen in a similar way in Graph 36, showing the winter period at the Nordic Sea. Nevertheless and despite the high number of depth lines in the graph, a general trend of increasing temperatures is visible in the layers from 0 m to 400 m depth. Thus, except for the 500 m layer showing a decline of 4.28%, there is a rise in temperature noticeable in all other layers (Table 30). The strongest increase is thereby measured in the 200 m to 400 m layers. Overall the increase in summer temperature is quite similar to the rise in winter. Again this graph gives a good overview over the entire set of summer data from Station Mike and thus provides the opportunity to take a more detailed look on the single layers.



Graph 39: Average summer temperature in °C measured at the Nordic Seas, focusing on the depths of 0 m to 25 m for the period from 1949 until 2009. The x-axis shows the years from 1948 to 2010, while the y-axis depicts the temperature in °C. The three background colors depict the different periods: green = pre-impact period, blue = transitional period, red = full-impact period. A trend line has been added.

Graph 39 represents the average summer temperature focusing on the 0 m to 25 m layers. The average range of fluctuations is between 7.5°C and 11.0°C, only interrupted by one extreme peak in the 0 m layer in 2004. This peak is also marking the highest temperature measured in the entire period. Overall there is a rising temperature trend visible in all layers within the measuring period. The increase seems to be strongest in the years after around 1990, however starting already around 1988. In total it causes an increase in temperature of 0.72°C at 0 m, 0.51°C at 10 m and 0.34°C at 25 m depth (Table 30). The rising trend is also confirmed by the trend line focusing on the 10 m layer.

4. Discussion

4.1 Discussion Objective 1

Are data available to examine potential changes in temperature and salinity in the Nordic Sea, as well as in the Sognefjord and especially the tributaries Sogndalsfjord and Barsnesfjord?

4.1.1 Discussion

As the main topic of this bachelor thesis is the examination of the hydrographical factors salinity and temperature in the Sognefjord region, sufficient data are essential. Thereby it is not only significant to have continuous measurements, but also similar periods and conditions to be able to finally also compare the data. However, as can be seen in Chapter "3. Results" and in the raw data in Chapter "8. Appendix", there are huge amounts of data available for all the different water bodies. Overall the largest data set has been measured at the Nordic Sea by Station Mike, shown in Chapter 8, Appendix V. Thus there is an enormous series of continuous data present that can be used for further examinations. Beside that the Sognesjøen also delivers a large series of data, enabling to have a closer look on the border zone between the Nordic Sea and the entrance of the Sognefjord. The extent of the thereby delivered data can also be seen in Chapter "3. Results" and in the raw data in Chapter 8, Appendix IV. Regarding the inner part of the Sognefjord and thus especially the Sogndalsfjord and the Inner and Outer Barsnesfjord, there are also data available, also shown in Chapter 8 in the Appendices II and III. However, these data are mainly sampled in the frame of different scientific works, dealing with the hydrographic factors of these regions water bodies. Additionally it has to be mentioned that more data exist, especially for 0 m to 40 m depth in the Sogndalsfjord, however they were not presented by the supervisor.

Regarding the climate data, there is a large amount of measurements available from different climate stations within the Sognefjord region. Due to the continuous data supplied by the Norwegian Meteorological Institute the usage of these values is possible. The raw data of these can also be found in Chapter 8, Appendix I.

Overall the main basis for this thesis is delivered by a previous work, already dealing with the hydrography in the Barsnesfjord (Kaufmann, 2014). In the frame of this work, many data have already been analyzed for seasonal trends, however mainly focusing on the

Barsnesfjord region. Main reason for this previous work was the examination of the influence of the open ocean on the Barsnesfjord hydrography. Thus, this work partly serves as the basis for this thesis. However some seasonal definitions have been changed in the frame of this work, for the purpose of the topic focusing more on the potential influence through the water power plants, now.

Hence, within this work a further subdivision of the available data into the defined seasons will be implemented, to allow a closer look on the potential changes in salinity and water temperature. Beside that tables and graphs will be made, enabling a comparison and analyses of the hydrographical development within the different regions.

4.1.2 Conclusion

According to Chapter “3. Results” huge amounts of data are available, which can be used for further studies regarding these water bodies. Through the additional existence of climate data, covering the affected regions, there is also the chance to figure out potential connections and correlations. Thus, overall there are sufficient data available for an investigation of temperature and salinity patterns of the different regions.

4.2 Discussion Objective 2

Are water power plants or climatic variations capable of causing significant changes in the fjords hydrography?

4.2.1 Discussion

Most water power plants in Norway are using dams to store large amounts of water. Thereby they are able to produce energy accommodating the demand. However, as already mentioned in Chapter “1.3.3.1 Hydroelectric Power Production in Norway”, this rhythm counteracts with the natural flow regime of the Norwegian rivers. Thus the usage of water power plants with damming systems can change the natural flow of water and thereby the amount of freshwater entering the fjord system during different times of the year. Thereby it can possibly change the thickness of the brackish water layer, enabling more or less heat to be added to the compensation current. Especially regarding the seasonal water inflow it

seems likely that hydroelectric power production may also change the patterns of the fjords surface salinity.

These influences of changed water runoff have been demonstrated by Opdal et al. (2013). This can also be seen in Figure 9 in Chapter “1.3.3.1 Hydroelectric Power Production in Norway”, which is taken from that paper, showing the change in water inflow in a regulated and unregulated environment. Overall Figure 9 depicts a strong change in water inflow, confirming the previously mentioned potential consequences. Thus there is a larger release of water visible during the winter months, especially from January to March. On the other hand a much weaker water release is apparent in summer time, mainly from May to July. The functionality of water power plants, as well as the former researches by other papers seem to indicate a strong connection and a possible influence of water power plants on the fjord hydrography and hence on salinity and temperature values.

Beside that the climate can also have an influence on the salinity and temperature conditions within the fjords. Especially the upper water layers have a close connection with the surrounding climate. As water has a very high heat capacity, it is storing large amounts of heat, mainly dependent on the surrounding air temperature and solar radiation (Dale, pers. com.). With overall rising air temperatures due to global warming, this can also affect the temperature of water bodies like of the Nordic Sea or of the fjords. However, beside the overall change in average temperature also seasonal, local and episodic temperature changes can cause effects. Temperature changes are thereby mainly and strongest visible in the uppermost water layers. With respect to changes in precipitation, this is most likely to have the strongest influence on the salinity values of especially the upper water masses. As changes in precipitation also influence the water inflow into the fjords, this can contribute to higher or lower salinities, depending on more or less rain. The same is valid for increased melting of land ice, causing more water inflow into the fjords and thus lower surface salinities.

4.2.2 Conclusion

Especially water power plants that are using dams may have strong effects on the surface water masses due to changes in the seasonal water inflow. Equally a change in climate and thus in temperature and precipitation can cause variations in the upper water masses.

Thus, both factors potentially have the ability to cause verifiable changes in the fjord hydrography and therefore in salinity and water temperature.

4.3 Discussion Objective 3

Does the hydrographical data show any yearly changes at the Sognesjøen as well as in its tributaries Sogndalsfjord and Barsnesfjord during the last 50 to 100 years?

4.3.1 Outer Barsnesfjord

4.3.1.1 Salinity

The annual salinity values of the Outer Barsnesfjord show an overall declining trend in all layers (Graph 7) with a contemporary rise in precipitation (Table 1). This rise in precipitation might have contributed to this phenomenon. The decline is largest in the 0 m surface layer, causing a decline from 6.06‰ to 0.45‰ (Table 7). As the 0 m layer is mainly influenced by rivers and outside influences, this could depict more precipitation into the Barsnesfjord. This theory is also confirmed by the visible increase in precipitation, most likely having caused this average drop in salinity (Table 1). This result has already been figured out by Opdal et al. (2013), however showing less decrease in salinity compared to this work's results. Nevertheless, the data used in this work have been sampled in the inner part of the Sognefjord which has experienced the highest increase in precipitation in % (Table 1). Thus the rise in precipitation most likely has caused this stronger decline in salinity than investigated by Opdal et al. (2013), who was sampling further outside the fjord.

Additionally it also has to be kept in mind that the last period's values have been sampled mainly in August, thus potentially representing a time with less water inflow as it is the end of the summer season. Thus it points towards salinity values being higher. This would discount with the visible drop in salinity, thus indicating further influencing factors.

The basin water at 10 m to 75 m depths in the Barsnesfjord is exchanged during winter time with water transported inwards by the compensation current and intermediate water from the Sognefjord (Dale, pers. com.). Thus the Barsnesfjords basin water represents the 10 m winter water of the Sognefjord, which has replaced the bottom water of the Outer Barsnesfjord. Due to the drop in salinity visible in these water masses, a large decline in

salinity at 10 m depth in the Sognefjord must have occurred. Reason for this could have been the overall rise in average precipitation (Table 1), increased glacier melting or alternatively increased water runoff from the power plants, which would all influence the Sognefjords 10 m layer.

Beside that especially in the 0 m and 5 m layers large fluctuations are visible, ranging from nearly 0.0‰ to almost 35.0‰ (Graph 7). However, the enormous peak in the 0 m layer around 1936 can be explained by only one winter value available for that year. Thus the peak represents only this single winter value. Yet it has to be kept in mind that this single peak also increases the average value of this period, thus indicating a higher than usual salinity. In general the 0 m layer represents the uppermost surface water, which is influenced the most by changes in water inflow, precipitation, snow accumulation and melting, but also by climatic changes. Regarding these factors, an increase in precipitation or snow melt during spring and summer can explain the huge variations in salinity.

4.3.1.2 Temperature

At the Outer Barsnesfjord a temperature increase is visible in all layers, causing an increase of around 30% (Table 10). However, it has to be taken into account that the last values from 2003 to 2013 have been sampled mainly during August while the previous data have been taken during July and August. Thus the average air temperature was higher while taking these values. This could also have influenced the water temperature especially in the upper layers, causing higher temperatures. However, there is already an increase visible in the second period, from 1960 until 1989, indicating a rise in water temperature despite the late sampling time in the last period. Regarding the temperature (Table 4), there is no rise visible between the first and the second period, thus indicating another factor to have caused the change in hydrography.

What is also conspicuous is the increase in water temperature at the deeper layers from 40 m to 75 m (Table 10). As the basin water of the Barsnesfjord is renewed in winter time, these water masses represent the winter water of the Sognefjord at sill depth, which is around 10 m. This increase in the temperature in the water mass from 10 m depth could reflect the global rise of temperature. Regarding the development from the first to the third period, a rise in both, average air temperature as well as water temperature at 10 m depth is visible. However, taking the change from the first to the second period into account, a decline in air temperature can be seen, while the 10 m layer shows a rise. This indicates an

additionally influencing factor, which might be the building of the water power plants in this transitional period.

Beside that the 0 m and 10 m layers are showing larger fluctuations than the deeper water masses (Graph 10). This can be related to the influence of air temperature and water inflow, which is strongest on the uppermost water layers.

4.3.2 Sogndalsfjord

4.3.2.1 Salinity

The annual salinity values of the Sogndalsfjord only show the depths from 50 m to 200 m and thus the signals from the summer water in the Sognefjord at 25 m depth (Graph 13) (Dale, pers. com.). As there is a small rise in salinity visible in all layers, this also indicates a rise in salinity at 25 m depth in the Sognefjord in summer (Table 13). Usually the summer salinity values feature a decreasing trend due to high snow melt and precipitation. As the precipitation values also increased (Table 1), an additional factor seems to have influenced the 25 m water at the Sognefjord, strongly pointing towards an effect through the water power plants. Furthermore it has to be kept in mind, that weak signals at 25 m depth most probably would be stronger at shallower depths in the Sognefjord. Thus, there seem to be significant changes within these water masses, recommending a further investigation.

4.3.2.2 Temperature:

Again only the water depths from 50 m to 200 m at the Sogndalsfjord are shown (Graph 16). These water masses represent the summer temperature in the Sognefjord at 25 m depth. This is due to the basin water in the Sogndalsfjord being renewed in summer time. Thus changes in the basin water of the Sogndalsfjord indicate changes in about 25 m depth at the Sognefjord in summer.

Additionally there is a strong rise in temperature shown, accounting for more than 30% in all layers (Table 16). Reason for that can be on the one hand the simultaneous increase in air temperature (Graph 4). However, this rise is only small, accounting for 0.32°C at Flesland and 0.24°C at Fjærland (Table 4). Thus it most likely only contributed little to the heating in the water mass at 25 m of the Sognefjord. Beside that the inflow of 4°C cold dammed water

from the water power plants would mainly cause a cooling in the surface of the fjord water, thus not being responsible for the rise. Even though the data were collected in August, as the basin water values represent the summer values of the Sognefjord at 25 m depth, they are not influenced by different air temperatures due to that. However, as the data depict the annual situation this might indicate a stronger overall effect of the warming factors like air temperature, than of the cooling ones like the water power plants.

4.3.3 Sognesjøen

The Sognesjøen has accumulated climate signals and hydrographical signals from the water power plants upstream. Thus it shows signals from, beside others, the Hardangerfjord area and also the Sognefjord.

4.3.3.1 Salinity:

The annual salinity measured at the Sognesjøen shows a different behavior at the different water depths. While there is a decrease in the upper 1 m and 10 m layers, there is an increase at 50 m to 100 m depth (Table 19). The drop in salinity in the upper water layers can be related to the simultaneous increase in precipitation at Ytre Solund, which mainly represents this region (Table 1). However, also the increase in precipitation at the other climate stations and thus in the rest of the area contributes to this drop. Reason for that is the transport of the fjords surface water outwards, where it is mixed into the coastal current and where the Sognesjøen station is found. As the uppermost water layers reflect changes from outside most pronounced and fastest there is a connection possible. This connection was already shown by Opdal et al. (2013). However, also inflowing colder dammed water could be the reason. Beside that the rise in the deeper layers seems to indicate an influence from the Nordic Sea, potentially showing a different inflow of water masses. As there are increasing values visible, the water seems to mainly consist of warm, high salinity Atlantic water mixing in.

Furthermore it can be seen, that the largest fluctuations occur in the upper water layers, especially in the 1 m layer (Graph 19). However, by comparing it with the annual precipitation it is shown that there are also large fluctuations visible at Ytre Solund (Graph 1). Additionally the fluctuations can be caused by increased snow melt in summer and larger snow accumulation in winter time.

4.3.3.2 Temperature

The annual temperatures at the Sognesjøen show an overall rising trend in all layers, ranging between 18.66% and 5.68% (Table 22). This increase is largest in the 1 m layer, accounting for 1.64°C. At the same time a rise in air temperature is visible of around 0.3°C to 0.5°C, might supporting this water temperature increase (Table 4). Against that the inflow of 4°C cold dammed water from the power plants would counteract this rise.

Also noticeable is one large trough in the temperature around 1966 in the upper 1 m to 50 m layers (Graph 25). By comparing it with the coincident air temperature (Graph 4) there is only a small low visible. Thus there seems to be another influencing factor, potentially pointing towards the water power plants. Beside that the general range of fluctuations seems to have changed around 1985, causing higher average values as well as larger fluctuations. However, this rise can also be seen in the overall air temperature. Nevertheless, while the air temperatures are showing a decline in the very last end of the measured period, this cannot be seen at the Sognesjøen (Graph 25), pointing out that there might be an additional influencing factor. Regarding the time period of the change, this can potentially be correlated with the building of the water power plants.

Furthermore it can be seen, that especially the upper water layers from 1 m to 30 m are following similar variations. Reason for this can be the origin and mixing of the water masses. Due to the close connection with the Nordic Sea, this similarity might reveal the inflow of similar water masses. Against that the 50 m to 100 m layers seem to represent different water masses, due to their separated position in the graph.

4.3.4 Conclusion

Overall the graphs and tables show significant changes in both, water temperature and salinity at all three parts of the Sognefjord. However, an accurate attribution to the main reasons is not yet possible, as both, climate changes and water power plant influences can cause these effects. Nevertheless, there are remarkable hydrographical changes visible within the last 50 to 100 years, suggesting a further examination.

4.4 Discussion Objective 4

Is it possible to determine seasonal effects and thus direction of the changes in salinity and temperature?

4.4.1 Outer Barsnesfjord

4.4.1.1 Salinity:

As can be seen in the winter salinity values of the Outer Barsnesfjord, there is an overall strong decline visible in the 0 m to 20 m layers (Table 8). However, due to a lack of data only period one and two are visible. There has also been a slight drop in precipitation at Hafslo from the first to the second period, which might have caused a rise in salinity values in that region (Table 2). However, the Outer Barsnesfjord depicts a general drop in salinity in all layers, mostly pronounced in the surface 0 m layer (Graph 8). Thus the decline in salinity indicates a second influencing factor, finally causing this change. Overall this seems to show a combined influence through increased precipitation in winter time and increased inflow of freshwater due to water power plants. Hence it seems to depict a strong connection to the building of the large water power plants, starting in that second, transitional period.

Beside that there are very large fluctuations in surface salinity in the 0 m layer visible, ranging from 0.0‰ to around 30.0‰. This is due to the fact that the strong influences of changed water inflows, precipitation and climatic changes are mainly seen in the uppermost layers. Especially during the years between 1950 and 1955 there seem to have been strong changes in the salinity values within that layer. According to the climate data from Hafslo these years also show relatively high amounts of precipitation, potentially contributing to the large fluctuations.

The summer salinity values of the Outer Barsnesfjord show an overall drop in all layers, except for 5 m depth (Table 9). Parts of this drop can be related to a contemporary rise in precipitation at Hafslo (Table 3). However, overall Hafslo only has a relatively small average amount of precipitation. Regarding the extremely strong drop at 0 m depth, this can at least partly be related to the single peak in 1936, causing the salinity to rise from 0.0‰ to more than 30‰. Reason for that peak in the 0 m layer is only one winter value available for the year 1936. Thus it can be related to a lack of data. Nevertheless, this strong rise in salinity also influences the calculated average of this period by making it larger than usual. Furthermore, some of the increase might occur due to the increased summer precipitation

as well as land ice melting. The 0 m layer thereby represents the water layer, mainly influenced by the lake Hafslavatnet water. Besides that the last period contains values mainly sampled in late August. Consequently these values could reflect reduced fresh water flow to the Sognefjord in summer time, which could cause lower salinity values. This also explains the larger fluctuations in the first period. Thus the data before 1960 also include May and July values, thus showing the peaks in water runoff.

Beside that there is an increase in salinity visible in the 5 m layer, which also shows the largest fluctuations at all (Graph 9). This can also be related to the data after 1980, being mainly sampled in August. According to that the data are missing the main part of the snow melting that causes a 5 m thick freshwater layer. A thinner brackish water layer would make the 5 m layer more saline, a mechanism discussed by Venneman (2014). As a part of the compensation current the layer brings in water from the Sognefjord, thus potentially showing effects from the water power plants. The rise in salinity at 5 m could reflect less fresh water inflow to the Sognefjord, finally causing higher salinity water to flow in with the compensation current at 5 m to 10 m. Hence, again an influence through the water power plants in the Inner Sognefjord seems to be seen, due to less fresh water possibly causing a thinner brackish water layer in the Sognefjord.

Against that the 20 m to 75 m layers show quite similar values. Reason for this is the origin of this basin water, coming from 10 m depth from the Sognefjord in winter. Hence, the visible drop in salinity in this water from 10 m depth can be explained by a simultaneous increase in winter precipitation (Table 3). Additionally a larger freshwater inflow caused by the power plants can also contribute to this decline in salinity in the 10 m layer.

4.4.1.2 Temperature:

Regarding the winter temperature values of the Outer Barsnesfjord, only data for the first, pre-impact, and second, transitional period, are shown (Graph 11). However it is visible that the largest fluctuations appear in the 0 m layer. This is due to the strongest influence of outside factors on the uppermost layers, especially on the surface water. Thus in the 0 m layer changes in precipitation, water runoff or air temperature are visible directly and mostly pronounced. Overall these fluctuations probably represent variations between cold and warm years.

Additionally it can be seen, that there is a rise in the temperature in the 5 m to 20 m layers, while the temperature at the surface 0 m layer drops at 3.33% (Table 11). While the uppermost 0 m layer is mostly influenced from outside, by sun, air and river inflow, the deeper layers also show these effects, however less strong and slightly more stable. Regarding the air temperature development, there is a rise at Flesland in winter, while the temperatures drop at Fjærland, making a global change difficult as explanation (Table 5). Thus especially the rise in water temperature in the 5 m to 20 m layers might indicate a change in the hydrography of the inflowing water and thus in the inflow through the compensation current, possibly related to the building of the water power plants.

Considering the summer temperature at the Outer Barsnesfjord an overall increasing trend is visible in all layers (Graph 12). In the depths below sill level, from 30 m to 75 m this rise is quite strong, accounting for more than 30% in all layers (Table 12). Again these water masses represent the winter water of the Sogndalsfjord and Sognefjord at 10 m depth, due to the basin water exchange occurring in winter time. The reason for the increase of temperature at 10 m depth in the Sognefjord can be an overall rise in air temperature. Regarding influence through the water power plants, potentially inflowing dammed water would have a temperature of around 4°C. An increased inflow of this water would lead to a cooling of the fjord, thus not being able to have caused the rise. However, there is also a rise in air temperature visible at both stations (Table 6). It is therefore assumed that the water temperature is stronger influenced by climatic changes than by water runoff.

Beside the basin water, the 10 m layer in summer time shows the largest increase of 30.40% regarding the water masses above sill level (Table 12). Reason for this can be a combination of less cold meltwater inflow, rising air temperatures due to the sampling time of the third periods values in August and more heat absorption in shallower water masses. Latter occurs due to the darkening of the coastal water masses from increased river run-off. The darkening of coastal water has already been shown by Aksnes et al. (2009). Due to the fact that freshwater has a lower density than seawater, this inflow is most pronounced in the surface layers. Nevertheless, a final explanation for the rise being strongest at 10 m could not be found.

Additionally large fluctuations are visible, especially in the upper 0 m to 10 m layers (Graph 12). These variations which are mostly pronounced in the surface water are related to influences from outside. Thus factors like a change in air temperature and water runoff can be seen directly and strongest in the surface water.

4.4.2 Sogndalsfjord

4.4.2.1 Salinity:

The winter salinity at the Sogndalsfjord shows a decrease in the uppermost 0 m to 10 m depths while there is a rise in the deeper layers (Table 14). Reason for the drop can be the simultaneous increase in precipitation at Hafslo, which mainly represents this region (Table 2). This would also explain the reduction being largest in the uppermost layers, while it becomes less with increasing depth. However, also an increased inflow of dammed river water can cause this significant drop in salinity. As the decline is very large, accounting for 20.68% in the 0 m layer (Table 14), this indicates an influence beyond the rise in precipitation, thus pointing towards additional release of fresh water in winter time. However, regarding the overall change it has to be kept in mind that the last periods values have been sampled at the Aqua Culture Station and thus closer to the shore than the previous data. Hence they could be stronger influenced by freshwater runoff through the Sogndalsriver than the regular mid-fjord sampling stations. Nevertheless, usually the Sogndalsriver is not large in winter time.

Beside that very high fluctuations are visible in the 0 m surface water layer ranging from around 5.0‰ to more than 30.0‰. Thus the salinity reaches very deep troughs down to nearly 5.0‰, especially in the years around 1958, 1983 and 2005 (Graph 14). Reason for that is the direct influence through precipitation, snow melt and snow accumulation on the uppermost water layer. Changes of these factors are strongest in the upper surface water and hence most visible at 0 m depth. There are also several large peaks and troughs apparent in the precipitation progress that can be reason for the fluctuations in salinity (Graph 2).

The summer salinity values at the Sogndalsfjord only contain the basin water from 50 m to 200 m depth, thus representing the summer water from the 25 m layer at the Sognefjord. Overall a slight rise in salinity is visible during the measuring period at the 50 m layer, counting for 0.11‰ (Table 15). This layer also depicts very high fluctuations especially in the period before 1960. Regarding the time period of the largest fluctuations, occurring in the pre-impact period, this could indicate a more stable water inflow afterwards, due to damming by the water power plants (Graph 15). Beside that it has to be kept in mind that the last period's values are sampled mainly in late August, thus depicting higher average air temperatures and maybe less water inflow as it is the end of the summer period.

Against that the 100 m layer shows stable conditions, while the 150 m and 200 m layers depict slight declines. Overall the 100 m to 200 m layers show pretty similar trends, possibly related to a common influence through deep water circulations and hence suggesting minor changes in salinities in the Sognefjord at 25 m in summer time.

4.4.2.2 Temperature:

The winter temperature values in the Sogndalsfjord show a decrease in the upper 0 m to 10 m layers (Table 17). However, it is also apparent that the temperatures only constantly dropped at 0 m depth, while they have been rising from the first to the second period at 5 m to 10 m depth, before finally declining. The rise in temperature from the first to the second period at 5 m and 10 m might occur due to a contemporary increase in air temperature (Graph 5 and Table 5). Due to mixing these effects finally reach the deeper layers down to 10 m. Against that the cooling trend from the second to the third period seems to indicate a higher inflow of cold freshwater due to the damming through the water power plants and increased runoff from precipitation. As can be seen, this drop in temperature already starts earlier in the surface layer, which shows a decline from the first period on (Table 17). Reason for that might be that signals caused by outside factors are first visible in the uppermost layer, before expanding into the deeper parts by mixing processes. As the formation of the large water power plants started in the second period from 1961 until 1989, changes are first visible in the uppermost 0 m layer. With ongoing time the continuous mixing processes might have transported these signals in the deeper water masses, too.

Beside this decrease in temperature in the upper water masses, an overall rise is visible in the water layers from 20 m to 200 m (Graph 17). The 20 m layer thereby still belongs to the intermediate water mass, while the 30 m to 200 m represent the basin water. As the bottom water exchange takes place in summer, this basin water represents the 25 m summer water of the Sognefjord outside the sill. The increase in temperature in the 25 m layer of the Sognefjord can mainly be related to overall higher air temperatures as well as again the darkening of the coastal water, which has been shown by Aksnes et al. (2009). As there is a strong increase in air temperature visible at both stations, this potentially contributes to the warmer water temperatures (Table 5). An influence through the water power plants is thereby less likely, as an increased water inflow in this way would cause a

drop in temperature. Reason for that is the average temperature of the dammed water, leveling at around 4°C due to its origin from deeper parts of the lakes.

Moreover, there are also large fluctuations visible, which seem to become stronger during the last periods (Graph 17). However, this might be related to differences in the way of sampling in the last period, as these data have been taken by the “From Mountain to Fjord”-students, unlike the previous values.

Since the summer values of the Sogndalsfjord just include the depths of 50 m to 200 m, they only show the basin water of the fjord (Graph 19). Thus there is hardly any difference compared to the winter basin water. Especially the 100 m to 200 m layers are almost the same, as the water masses are stagnant during that time period. Only the 50 m layer might show slight changes, due to influences of seasonal turbulence at that depth, transmitted by tidal currents at the sill. However, by comparing the winter and summer temperatures (Table 17 and 19) it is visible that even the 50 m layer is almost equal and thus not giving any new information.

4.4.3 Sognesjøen

4.4.3.1 Salinity:

As seen before in Chapter “4.3.3.2 Salinity” of the Sognesjøen, regarding the yearly averages there is a decrease in salinity visible. This also coincides with the work of Opdal et al. (2013).

The average winter salinity at the Sognesjøen depicts a decreasing trend in all layers, except for 75 m depth (Table 20). This trend is most pronounced in the 1 m and 10 m layers, showing 2.36% and 1.76% less salinity. As can be seen there is also a rise in winter precipitation visible at all of the climate stations in the Sognefjord and Bergen area within that period (Table 2), potentially having contributed to the drop in salinity. However, also hydroelectric power production could be responsible for the decline. Through the damming more water is released in winter time compared to natural floating regimes, thus leading to a drop in salinity values. This also fits with the strongest decline occurring in the uppermost 1 m layer, as the surface reflects changes through water inflow and climate variations the most.

Additionally there seems to be a significant change in the range of fluctuations in winter, especially within the uppermost layers from 0 m to 20 m (Graph 26). Thus the fluctuations become remarkably larger and lower in average after 1980, especially in the layers of 0 m, 5 m, 10 m and 20 m depth. This drop is especially large in the uppermost 1 m layer, accounting for 0.77‰ by comparing the first and the third measuring period (Table 20). Taking the amount of precipitation into account, there seems to also be at least a slight increase, potentially contributing to the change (Table 2). Thus, especially the deep troughs in the period after 1980 seem to fit with simultaneous events of high precipitation (Graph 2). Nevertheless, the reduction in fluctuations as well as the lower average salinities indicate an additional influence, might pointing towards effects from the water power plants. Regarding the time period of the phenomenon, a potential connection with the building of these also seems to be likely.

Regarding the summer salinity values of the Sognesjøen, there are different developments visible in the single layers (Graph 28). However, all changes are very small, accounting for less than 1% change. Overall this seems to show that there are no remarkable changes in summer salinity. Considering the working hypothesis, the summer salinity values are supposed to be higher after building of the power plants due to less water inflow. However, this is maybe difficult to see, as the increase in precipitation and glacier melting could counteract the effect of summer damming. Thus there has been a significant increase in precipitation during the measured period, which should usually be visible, at least in the upper water layers (Table 3). Hence, the only small changes in surface salinity at 1 m depth, accounting for 0.58%, potentially reflect this situation, as they do not show the strong increase in precipitation. Overall, the only small changes seem to reveal the net effect of reduced inflow of fresh water from the water power plants together with increased precipitation and glacier melting.

Beside that overall trend, there are strong fluctuations visible, especially in the uppermost 1 m layer (Graph 29). Thus there are large troughs in the 1 m layer around 1937 and 1940, depicting salinities from around 20‰ (Table 21). However, these can be related to some events of very high precipitation between 1930 and 1940 (Graph 3). Furthermore there are some smaller, but still very low troughs, reducing the salinity to around 25.0‰ in 1976, as well as during the period from 1994 until 2014. These periods of very low salinities can be explained by relatively high precipitation values around 1970 as well as around 1985. Additionally there have been relatively high temperatures during the years 1976 and 1997, too, possibly also contributing through high evaporation.

4.4.3.2 Temperature

The winter temperatures measured at the Sognesjøen show an overall rise in temperature in all layers (Table 23). This increase can be related to the general rise in temperature (Table 5). The main increase in water temperature occurs between 1980 and 1990, however the same trend being visible regarding the air temperature (Graph 26). Additionally also the fluctuations become lifted at that time, especially in the uppermost 0 m to 20m. Thus the maxima as well as the minima values seem to increase, showing less cold temperatures after around 1990. At first appearance this higher level seems to indicate water power influences. Overall the similar trend of water and air temperature indicates a close correlation. Influences through the additionally inflowing water by the water power plants are however unlikely, as this water would have an average temperature of around 4°C, thus having a cooling effect on the more than 5°C warm fjord water. Even though the main change in variations occurs in the third, full-impact period, this change in water temperature seems to be caused by increased average air temperatures (Table 5).

Additionally it is noticeable that there is a similar trend in the 10 m and 20 m layers (Graph 27). This can be due to the general winter mixing within these layers, causing likewise progresses. Against that the 0 m layer features much more variability as it is directly influenced by precipitation, rivers and dams. Overall the largest fluctuations seem to occur at 0 m and 10 m depth and in the period before 1970, mainly the pre-impact period. During that time all upper layers from 0 m to 20 m show large peaks, however, most pronounced in the surface water at 0 m. Regarding the air temperatures at Flesland and Fjærlund, it is clearly visible that the surface waters are following the temperature progress (Graph 5). Hence the large fluctuations particularly in 1954 and 1960 can be related to very mild winters.

Regarding the summer temperature data of the Sognesjøen, a big peak in 1940 in the 1 m and 10 m layer is noticeable, causing a rise from 11.0°C to around 17.0°C (Graph 28). However, this peak is caused by only one measurement available for the defined summer month, depicting only the very high temperature in July. Beside that there is another peak visible in 1997 in the 1 m to 20 m layers, causing a rise in temperature of around 4.0°C. The reason for that can be seen in the temperature progress, showing a large peak in temperature during this year (Graph 6). As the change in water temperature is mainly seen in the upper 1 m to 20 m layers, this indicates to be caused by the average rise in air temperature. The effects thereby have most probably been transported into the deeper layers by typical surface mixing processes.

Furthermore it is visible that there are higher fluctuations in summer within the 1 m and 10 m layers before 1970, while the variations are smaller in the deeper layers (Graph 29). This can be related to more variations in the local climate, causing large fluctuations in the upper water layers while the deeper water masses are less affected. This theory seems to be confirmed by the temperature progress, showing similar trends within this period indicating direct effects on the upper layers (Graph 6). The overall temperature increase in the 1 m to 10 m layers during summer is moreover much larger compared to the winter period, even though there is a larger increase in air temperature in winter. Thus it indicates less inflow of cold snow meltwater, causing the surface temperatures to rise.

Beside that the 50 m to 100 m layers in summer show quite similar progresses, however strongly different from the 1 m to 30 m layers due to colder temperatures (Graph 28). This seems to indicate the inflow of different water masses from the Nordic Sea, causing colder temperatures in the lower layers. Additionally there are also differences in the development of the 10 m and 20 m layers visible, however, not possible to be explained.

Besides that there is an overall rise in summer temperature visible in all layers during the entire period (Table 24). This rise becomes most pronounced in the second period around 1985. However, there is also an increase in temperature visible at both climate stations, thus indicating to be the reason for the increased water temperature (Table 6). However, the rise in water temperature could also point towards less inflow of 4°C-cold, dammed water through the hydroelectric power production, thus leading to less cooling and hence even warmer water temperatures in summer.

4.4.4 Nordic Sea

4.4.4.1 Salinity:

Regarding the annual data from Station Mike, there is a slight reduction in salinity visible in all layers (Table 25). This could indicate increased melting of land ice, causing more water inflow into the Nordic Sea and hence lower salinities. Nevertheless, compared with the fjords, the changes in the Nordic Sea are very small.

The winter salinity values of the Nordic Sea show a slight decline in all layers (Table 26). The strongest drop thereby occurs in the 300 m to 500 m layers, which seem to be separated from the upper 0 m to 200 m depths. Reason for that can be the inflow of a new water

mass featuring lower salinities. The Nordic Sea is meeting place of the warmer, high salinity Atlantic current and of the colder, low salinity Arctic current. These two currents also feature recognizable differences in salinity, which enables to separate them. While the Atlantic water per definition features salinities above 35‰, the Arctic water typically has values below. Thus, the strong drop in salinity especially within the 500 m layer is indicating a border zone where low salinity Arctic water mixes in. The same seems to occur at the 200 m layer, which shows a slight increasing trend of 0.04% (Table 26). Here an inflow of high salinity Atlantic water could be the reason for the rise in salinity.

Additionally there are several marked minima visible, the largest around 1978 (Graph 31). This represents the “Great Salinity Anomaly”, which was a major pulse of fresh water reaching the Nordic Sea by the end of 1970 (Drange et al., 2005). This additional inflow of fresh water caused the salinity values to drop significantly, thus decreasing the amount of high salinity Atlantic water. Around 1978 the salinity also reaches its absolute minimum within the entire measuring period. This phenomenon of very low salinity values occurred more often, noticeable through several troughs (Graph 31). Thus there was another low around 1993, also potentially belonging to the “Great Salinity Anomalies” emerging in the Nordic Sea.

Beside that the largest fluctuations occur at 0 m depth (Graph 32). At Ytre Solund a slight increase in precipitation is visible, pointing out more precipitation at Station Mike, too (Table 2). Hence, the surface fluctuations in winter can be related to variations in precipitation. Beside that the 10 m and 25 m layers are quite similar, only slightly lower than the 0 m surface layer, representing similar fluctuations.

The summer salinity values of Station Mike show a similar trend like the winter values (Graph 31 and Graph 33). Thus there is a slight decline visible in all layers, except for the 200 m layer. Furthermore the drop is again strongest in the 300 m to 500 m layers, also confirmed by the trend lines (Graph 33). Thus these depths point out the border zone of water masses with different salinities. The same seems to occur at 200 m depth, which shows a rise of around 0.05%. Thus there seems to be inflow of Arctic water at 500 m depth, while the 200 m layer indicates increased Atlantic water.

Especially in the upper layers the graph shows huge fluctuations beyond the average range, which seem to be even larger than during the winter period (Graph 33). They can be related to higher precipitation, less evaporation or glacier melting in summer time and thus to the water input into the Nordic Sea within that period. As there was also a rise in temperature

and precipitation during that period, this potential reason is confirmed (Table 3 and Table 6). However, some of the troughs can also be associated with the “Great Salinity Anomalies” at the Nordic Sea, including the ones around 1978 and 1988.

However, these extreme episodes of very low salinities seem to be missing in the third period, which only shows smaller fluctuations, especially in the uppermost layers of 0 m to 25 m (Graph 33). According to the climate graphs, the strongest rise in precipitation took place from the first to the second period, while it was only small from the second to the third (Graph 3). Thus the larger fluctuations seem to also represent stronger variations in precipitation during the first two periods.

4.4.4.2 Temperature:

The winter temperatures at the Nordic Sea show a slight rise in temperature within the measured period (Table 36). This increase is most pronounced in the 0 m layer of the upper water masses and then again in the 200 m to 400 m layers. Reason for the increase being strongest in the 0 m layer could be the direct and strongest influence of air temperature variations, evaporation and precipitation on the uppermost surface water layer. Thus, by comparing it with the air temperature similar trends are visible, indicating a connection (Table 5). Hence the rise in temperature in the upper water masses can be explained with a simultaneous rise in global air temperature.

Beside that the strong increase in temperature in the 200 m to 500 m layers seems to represent the inflow of another water mass (Graph 36). Thus the rise in temperature seems to point towards an increased inflow of warm Atlantic water, what is mixed in during the winter period. As the largest fluctuations also seem to occur in the 300 m layer, this also points towards a mixing of different water masses, causing large variations. A similar explanation seems to fit for the drop in temperature in the 500 m layer, which might represents the border of inflowing cold Atlantic water.

In 1961 the winter surface water masses depict a huge peak, visible in the 0 m to 25 m layers (Graph 37). At the same time also a peak in air temperature is visible (Graph 5), potentially being responsible for the increase in sea surface temperature. The 0 m layer additionally shows the largest fluctuations at all, which is caused by the strongest influence from outside factors on the uppermost water layer.

Beside that there is a cold period visible from 1983 until 1997, including two especially big troughs in 1993 and 1996 (Graph 36). These show a decline in temperature from 7.1°C to about 5.9°C, marking a period with very cold winter temperatures. According to Eldevik et al. (2014) this cold period occurred as a response to the decreased northern hemisphere summer insolation. This caused a change in temperature and in inflow of Atlantic water, finally leading to this cold period (Graph 36).

What is also noticeable is a general change in temperature conditions in winter, at the 0 m to 25 m layers (Graph 37). Thus before 1982 the 10 m and 25 m layers often show higher temperatures than the 0 m layer. This characteristic is only the case once after 1982, when the 25 m layer is crossing the 0 m layer during the period 2003 to 2005. Main reason for that might be an increased warming of the uppermost 0 m layer due to increased solar insolation.

Except for the 500 m layer, there is a rising trend visible in all layers in the summer temperature at Station Mike (Table 30). Like in the winter period this increase is largest in the 0 m and 200 m to 400 m layers. Thus it confirms the previous theory about its potential origin. While the strong rise in the 0 m layer can be related to it being influenced most by temperature fluctuations in the atmosphere, the deeper layers seem to be the mixing places of different water masses, in this case of warm Atlantic water causing a rise in temperature. Regarding the drop in the 500 m layer, this seems to point out the inflow of cold Arctic water. Overall the summer values show a similar trend to the winter data, however being different from the Sognesjøen. Reason for that can be the increased land effect at the Sognesjøen, as well as the darkening of the coastal water in summer.

Overall the rise in temperature seems to be strongest between the second and third period (Graph 38). This trend can also be seen in the air temperatures due to a strong rise around 1990 (Graph 6). Thus the general rise in air temperature seems to have contributed to this increase in water temperature. Beside that overall trend, there is a large temperature peak visible in the 0 m layer in 2004, pointing out the highest temperature measured at all (Graph 39). However, there does not seem to be the same peak in air temperature, again indicating an additional influence factor (Graph 6).

4.4.5 Conclusion

Overall, by examining the different seasons, it seems possible to determine the direction of the hydrographical changes in the different water bodies. By comparing the signals visible in the fjords with the signs in the Nordic Sea it is thereby shown, that the Nordic Sea does not seem to be the main reason for the larger variations occurring in the fjords. Thus, Station Mike mainly depicts the global situation, however not exactly similar to the local one. Furthermore the sometimes visible drop in the fjords winter salinities, as well as the rise in summer salinities seems to strongly indicate an influence through the water power plants. Especially with getting deeper inside the Sognefjord, in the Sogndalsfjord and Barsnesfjord the signals seem to be strongest. This indicates the main signals to come from inside the fjord. However, sometimes more than one factor seems to be able for causing the changes, thus it is difficult to assess the relative impact from the various factors.

4.5 Discussion Objective 5

Can the origin of these changes in the fjord hydrography be ascertained and be classified to effects caused by climate, water power plants or both?

4.5.1 Discussion

4.5.1.1 Temperature:

Tables 31 and 32 depict the changes in summer and winter temperatures in °C from period one to period three. The focus is thereby lying on the surface depths of 0 m to 25 m. The red colored values in the column of the Outer Barsnesfjord are emphasizing that these data only represent the change from period one to period two, due to a lack of measurements. The green values in the columns of the inner parts of the Sognefjord depict the indirect calculated value, represented by exchanged basin basin water. As the bottom water of the Sogndalsfjord is changed in summer time, it represents the summer water of 20 m/25 m depth of the Sognefjord. With the sill at 10 m depth the basin water of the Barsnesfjord is renewed in winter time, thus depicting the 10 m winter water of the Sognefjord. Thus it depicts the 10 m and 25 m depth at the Sognefjord, respectively.

Winter Season: Temperature Change [°C]					
Period 1 - Period 3					
Depth	Station Mike	Sognesjøen	Inner parts of Sognefjord - Basin water	Sogndalsfjord	Outer Barsnesfjord
0m/1m	0,73	0.32		-0.68	-0.13
10m	0,50	0.68	1.80	-0.12	1.68
20m/25m	0,35	n.d.		0.83	1.21

Table 31: Winter temperature change between period 1 and 3 at all measuring stations for the depths from 0 m to 25 m. The values in the column of the Outer Barsnesfjord (red) display the fact, that the values only show the difference between period 1 and 2, due to lack of data. The 10 m value for the inner part of the Sognefjord (green) is given through the basin water of the Barsnesfjord.

Summer Season: Temperature Change [°C]					
Period 1 - Period 3					
Depth	Station Mike	Sognesjøen	Inner parts of Sognefjord - Basin water	Sogndalsfjord	Outer Barsnesfjord
0m/1m	0,72	1.12		n.d.	0.45
10m	0,51	0.87		n.d.	2.66
20m/25m	0,34	n.d.	2.04	n.d.	1.77

Table 32: Summer temperature change between period 1 and 3 at all measuring stations for the depths from 0 m to 25 m. The 25 m value for the inner part of the Sognefjord (green) is given through the basin water of the Barsnesfjord.

Beside that the Tables 33 and 34 show the change in air temperature between the first, pre-impact and third, full-impact period for the winter and the summer season. Flesland thereby mainly represents the climate of the Nordic Sea and the Sognesjøen, while Fjærland depicts the overall temperature in the Sogndalsfjord and Barsnesfjord region.

Winter Season: Change Climate Period 1 - Period 3		
[°C]	Flesland	Fjærland
	1.11	1.67

Table 33: Change in summer air temperature in °C, apparent between period 1 and 3 for the weather stations at Flesland and Fjærland.

Summer Season: Change Climate Period 1 - Period 3		
[°C]	Flesland	Fjærland
	0.40	0.30

Table 34: Change in summer air temperature in °C, apparent between period 1 and 3 for the weather stations at Flesland and Fjærland.

As can be seen in Table 31, there is a declining temperature trend visible in the winter season at 0 m /1 m depth, going from Station Mike inwards the fjord. Hence, the largest drop in temperature is visible in the Sogndalsfjord, accounting for -0.68°C . The slight rise at 0 m/1 m depth at Station Mike and the Sognesjøen can be related to the simultaneous rise in air temperature at Flesland, of around 1.11°C (Table 33). However, the decline in temperature at the Sogndalsfjord in 0 m/1 m and 10 m counteracts with the simultaneously rising temperature at Fjærland. Thus, there must be an additional cooling factor, causing the drop. As the average temperatures of the winter water at the Sogndalsfjord level around 5°C in the 0 m layer (Table 17), inflowing 4°C cold fresh water from water power plant damming would have a cooling effect. Thus the decline at the Sogndalsfjord and further inside at the Outer Barsnesfjord seems to strongly be connected with an increased inflow of cold, dammed fresh water.

Against that the temperatures at 10 m and 20 m/25 m depth show an increasing trend, with going deeper into the fjord (Table 31). Even though in general the warming of the water masses can be explained by the coincident warming of the climate, there additionally seems to be an internal fjord effect, magnifying this increase with going deeper inside the fjord. This explanation is also supported, regarding the change in summer temperature (Table 6). Thus it is apparent that the changes in water temperature outside the fjord seem to become more pronounced and stronger with going inwards. There is a declining trend visible at 0 m/1 m depth from Station Mike towards the Outer Barsnesfjord. Against that the 10 m and 20 m/25 m layers depict a rise in temperature, being strongest at the innermost end of the fjord. Overall summer and winter period thereby show the same trend, with increasing temperatures at 10 m to 20 m/25 m depth, while there is a decline visible at 0 m. In both cases the tendency increases with getting deeper into the fjord, respectively.

In general this fjord magnifying phenomenon could be caused by several reasons. One possible cause could be the difference in heat penetration in the different fjord regions. At the innermost part, in the Barsnesfjord, the Årøy-River is bringing in a lot of cold fresh water. This water has a lower salinity and thus lower density than salt water, hence floating in the uppermost layer. Additionally the fresh water inflow contains large amounts of particles, causing a high turbidity at this innermost point of the fjord. Due to this high turbidity, incoming solar radiation cannot penetrate deep into the water masses and an increased reflection takes place. Thus there is only a small warming effect, however mainly compensated by the high turbidity. Against that the turbidity declines further out of the

fjord, leading to a stronger effect of the incoming solar radiation, which finally also penetrates deeper into the water masses. Additionally there is less reflection, altogether causing a stronger warming of the upper water layers. Overall this causes the water temperatures to rise, outside the fjord. Beside that the coastal water at the Sognesjøen has become darker due to increased inflow of precipitation, as already shown by Aksnes et al. (2009). This finally causes relatively more heat absorption at shallower depths, thus increasing the temperature in these upper layers. The increased heat is then transported inwards with the compensation current, thus again leading to a warming effect within the fjord. Regarding the trends, visible in Table 31 and 32, this difference in solar heat penetration could at least partly explain the warming being stronger deeper inside the fjord in the 10 m to 25 m layers.

The second, most likely explanation is the Land-Ocean-Effect, occurring due to different heat capacities of land and water. As water has a higher heat capacity than land, it takes much longer to heat it up. This is also the reason, why the ocean climate is showing fewer extremes, as the water masses balance these out. Due to this effect, the Nordic Sea in general warms slower than the fjords, as these are surrounded by land masses. In case of the Sognefjord, the land masses of the Sogn of Fjordane region heat up faster than the water in the fjord, emitting parts of this heat into the water. This already causes the fjords to be warmer than the large Nordic Sea and thus the region of Station Mike. Additionally, the fjords are getting smaller with going deeper inland. This causes the warming effect due to the surrounding land masses to become stronger, as it is more land influencing now only smaller surface water masses. The same phenomenon could also cause a cooling. Thus less solar radiation could cause the land masses to cool down faster than the water masses, finally causing the emittance of colder radiation, also influencing the water masses. Overall, this Land-Ocean-Effect seems to also be able to cause the magnified temperature increase or drop at the Sogndalsfjord and Barsnesfjord, compared to Sognesjøen and Station Mike (Table 31 and Table 32).

Nevertheless, while the warming trend in the 10 m and 20 m/25 m layers of the winter water seems to be correlated with the solar heat penetration and the Land-Ocean-Effect, the reversed trend at 0 m/1 m depth, depicting the temperatures to become colder deeper inside the fjord strongly points toward increased inflow of colder fresh water through the damming of the water power plants.

Additionally there is a difference visible, regarding the direct measurement of the 10 m winter water of the Sognefjord and the indirect calculated value through the basin water of the Barsnesfjord. Thus the direct measurements show a value of 0.68°C, while the indirect calculation with the basin water depicts a temperature of 1.80°C (Table 31). However, the most probable reason for this could be found in the different times of measurement. Hence the direct value represents data showing the water inflow from January, February and March. Against that the indirect value depicts the inflow from December, January and February, thus causing warmer averages. Considering the indirect changes in summer temperature, a difference in the 20 m/25 m layer of the Sognesjøen is visible (Table 32). Thus, while there are no direct measurements of this layer available, the indirect calculations show a temperature of 2.04°C (Table 32).

4.5.1.2 Salinity:

The Tables 35 and 36 show the changes in summer and winter salinities in ‰ from the first, the pre-impact period and the third, the full-impact period. Thereby the focus again is on the uppermost 0 m to 25 m layers. The red colored values in the column of the Outer Barsnesfjord are due to the fact, that these data only represent the change from period one to period two. The green value in the columns of the inner parts of the Sognefjord are showing the indirect calculated salinity change in ‰ in the 10 m to 25 m layers, visible through basin water exchange.

Winter Season: Salinity Change [‰]					
Period 1 - Period 3					
Depth	Station Mike	Sognesjøen	Inner part of Sognefjord - Basin water	Sogndalsfjord	Outer Barsnesfjord
0m/1m	-0,02	-0.77		-5.27	-6.72
10m	-0,02	-0.58	-0.66	-1.16	-3.87
20m/25m	-0,02	n.d.		0.11	-3.02

Table 35: Winter salinity changes from period 1 to 3 in ‰ for all measuring stations at the depths from 0 m/1 m to 20 m/25 m. The red figures in the column of the Barsnesfjord display the fact that they only show the difference between period 1 and 2, due to lack of data. The 10 m value for the inner part of the Sognefjord (green) is given through the basin water of the Barsnesfjord.

Summer Season: Salinity Change [‰]					
Period 1 - Period 3					
Depth	Station Mike	Sognesjøen	Inner part of Sognefjord - Basin water	Sogndalsfjord	Outer Barsnesfjord
0m/1m	-0,02	0.15		n.d.	-1.47
10m	-0,03	-0.32		n.d.	-1.12
20m/25m	-0,02	n.d.	0.07	n.d.	-0.72

Table 36: Summer salinity changes from period 1 to 3 in ‰ for all measuring stations at the depths from 0 m/1 m to 20 m/25 m. The 25 m value for the inner part of the Sognefjord (green) is given through the basin water of the Barsnesfjord.

Beside that the Tables 37 and 38 depict the change in precipitation from the first to the third period in mm/year at the four climate stations. Hafslø thereby represents the region of the Sogndalsfjord and Barsnesfjord, while Ytre Solund depicts the Sognesjøen region.

Winter Season: Change Precipitation Period 1 - Period 3				
[mm/year]	Fana Stend, Bergen	Ytre Solund	Lavik	Hafslø
	156.41	83.42	159.63	83.86

Table 37: Change in winter precipitation in mm/year, apparent between period 1 and 3 for the climate stations at Fana Stend, Ytre Solund, Lavik and Hafslø.

Summer Season: Change Precipitation Period 1 - Period 3				
[mm/year]	Fana Stend, Bergen	Ytre Solund	Lavik	Hafslø
	56.14	10.87	45.87	25.25

Table 38: Change in summer precipitation in mm/year, apparent between period 1 and 3 for the climate stations at Fana Stend, Ytre Solund, Lavik and Hafslø.

As can be seen in the Tables 35 and 36, like the temperature the salinity changes from period one to three also show a decreasing trend, magnifying from Station Mike inwards. Thus the salinity of these surface layers also seems to be influenced by amplifying factors, which cause a stronger drop with getting deeper into the fjord. In general the declining salinity trend in this upper water layers can be related to the simultaneous rise in precipitation (Table 37 and 38). Regarding the winter season, there is an almost equal rise in precipitation at Ytre Solund and Hafslø of around 83 mm/year, which represent the respective regions (Table 37). However, there is a significantly larger drop in salinity at the Sogndalsfjord and Barsnesfjord, compared to the Sognesjøen. While the salinity only drops 0.77‰ at the Sognesjøen, there is a decline of 5.27‰ and 6.72‰ visible in the inner parts of the fjord (Table 35). Even though the value of the Barsnesfjord only represents the

change between period one and two, already the drop at the Sogndalsfjord is significantly larger. Overall, this clearly points out the presence of further influences. As a drop in winter salinity also can occur due to increased fresh water inflow through the water power plants, this strongly indicates an effect of the hydroelectric power plants.

Against that, the summer precipitation shows slightly stronger differences, thus fitting with the stronger decline in salinity at the inner end of the fjord (Table 38). Additionally, as mentioned before, in summer time the water power plants release less fresh water, also supporting the thesis of significant influences through hydroelectric power production. Furthermore it is apparent that there is an increase in summer salinity at 0 m/1 m depth at the Sognesjøen, thus showing an exception from the else declining trend. This rise accounts for only 0.15‰ (Table 36). Due to the ocean currents, the Sognesjøen is influenced by all the water power plants located not only in the Sogn of Fjordane region, but also along the Norwegian west coast south of the Sognefjord. As in summer less water is released from the dammed rivers, this could cause a rise in surface salinity, especially visible at the strongly influenced Sognesjøen. Additionally the increase in precipitation in this region is only small, accounting for 10.87 mm/year (Table 38) and thus not compensating for the reduced release of fresh water. As the Sogndalsfjord and Outer Barsnesfjord are mainly influenced by the plants in the direct surrounding, the larger increase in precipitation visible at Hafslo might make up for the loss of fresh water there.

Additionally the salinities increase at each station with increasing depth, except for Station Mike. However, this is due to the low salinity fresh water, also featuring a lower density and thus floating in the uppermost layers. Against that the more saline water masses are in the deeper layers, thus causing the values to increase. This is especially visible in the fjords, as the Nordic Sea is of much larger size and thus showing small changes less obviously.

By comparing the direct winter values with the indirect calculated differences it is obvious, that there is a slight difference regarding the 10 m water layer of the Sognefjord. While the direct value accounts for -0.58‰, the indirect change represented through the basin water of the Barsnesfjord shows -0.66‰ (Table 35). Like in case of the water temperature, the reason for that can again be the direct and more permanent effect from the outside factors on the 10 m layer than on the basin water. As the values additionally again depict different periods, this seems to explain the differences in salinity.

Regarding the summer salinity changes, a similar situation like in case of the temperature values is apparent (Table 36). Thus now a value for the 20 m/25 m layer of the Sognesjøen

is visible, however, slightly larger than expected. Hence a value of 0.07‰ is shown, not depicting the declining salinity trend. However, again the smaller influence on the basin water can be the reason for this situation, thus causing a fewer drop in salinity than it would have done on the direct 20 m/25 m water layer.

4.5.2 Conclusion

Especially regarding the overall change in surface salinity, it seems possible to determine the direction and thus sources of the changes within the fjords. The general salinity trend is showing a larger decline in winter and a smaller rise in summer, being strongest in the inner parts of the Sognefjord and thus in the Sogndalsfjord and Barsnesfjord. As could be seen there is a drop in salinity at all stations in winter, however becoming stronger with getting deeper into the fjord. Beside that the average amount of precipitation also increases, both, at Ytre Solund as well as at Hafslø, however in relative values being strongest at Hafslø. Against that there is a significantly larger drop in salinity further inside the fjord, at the Sogndalsfjord and Outer Barsnesfjord. Thus, while the Sognesjøen seems to be mainly influenced by the rise in precipitation or accumulated effects from the fjords upstream, by getting deeper inside the fjord the rise in precipitation seems too small to explain the salinity changes deeper inside the fjord. This strongly points towards an influence due to hydroelectric power production, causing higher water inflow in winter and thus reduction in surface salinities.

The explanation for the water power plants being able to cause these changes can also be seen in Figure 15. In a natural flowing regime there is noticeably less water inflow in winter, due to snow accumulation and less precipitation. Overall this leads to higher salinity values, especially in the surface layers of the fjords. Beside that there is a large water inflow in summer, due to snow melt and large precipitation. Thus the surface salinity values usually decrease during the warm period of the year. However, by building of water power plants using dams, there is a change in the periods of water inflow into the fjord. According to the demand of energy, more water is released into the fjords in winter time, as people need more electricity for heating. Against that in summer time less water is released, as less heating energy is required and more water is stored in dams. Hence, the winter surface salinities drop due to increased water inflow, while the summer salinity values would increase if not counteracted by increased precipitation and more melting of glaciers.

According to this, it is very likely that especially the visible drop in winter salinity is connected to the running of the water power plants.

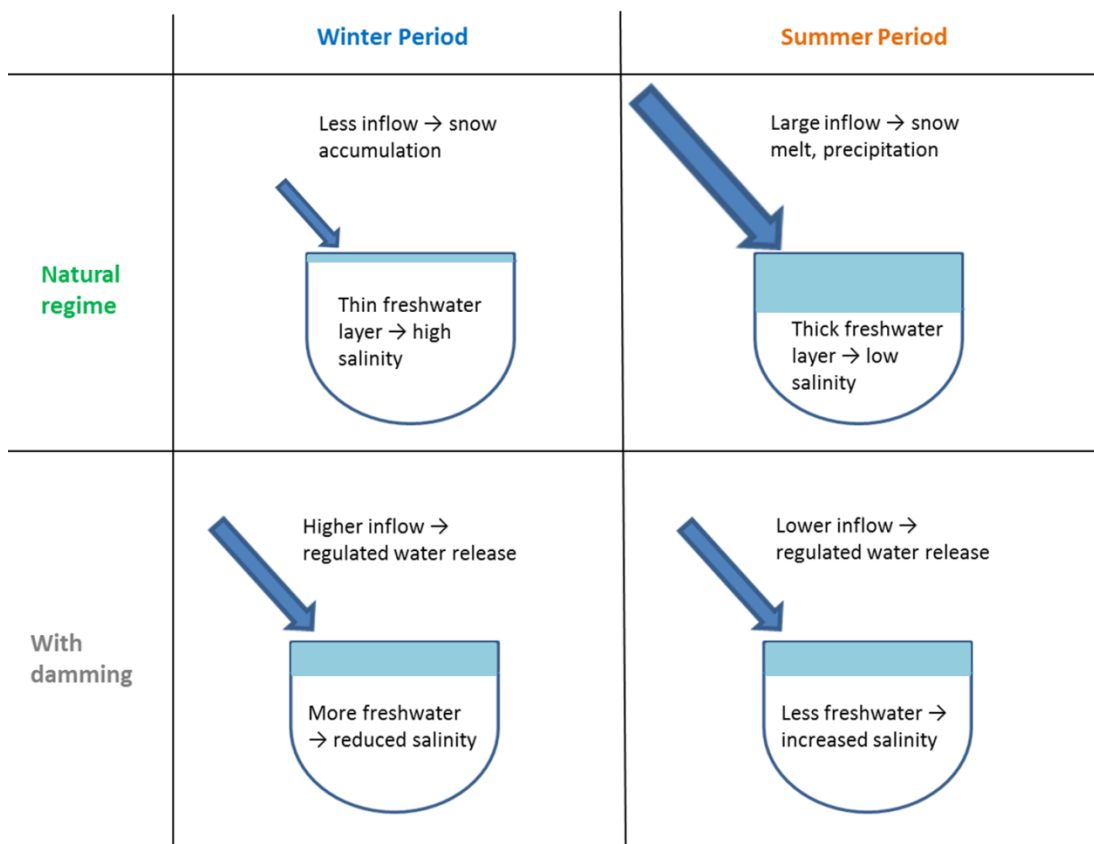


Figure 15: Effects of hydroelectric power production with damming on the seasonal water inflow to the fjords and thus the salinity concentrations of the upper water layers. The light blue areas show the fresh water layers.

This hypothesis is additionally supported by the fact that the most pronounced hydrographical changes in the fjord water have been found in the upper surface water masses. Moreover the changes are stronger in the Inner parts of the fjord. This also correlates with the water power plant signals from the fjords south of the Sognefjord, being transported and thus accumulated into the Sognefjord. Overall the changes in winter and summer salinities seem to be strongly influenced by hydroelectric energy production.

Against that the water temperature is more likely to be influenced by climate changes. Due to the fact that in most of the data there was a similar trend visible in both, water and air temperature, this indicates a close correlation of these factors. However, very remarkable is the magnifying effect of the temperature changes with getting deeper into the fjord. Regarding the temperature data and Tables 31 and 32 there is an increase in water temperature visible that seems to be mainly related to a simultaneous rise in air

temperature and partly also to the changed inflow of fresh water with different temperatures through the water power plants.

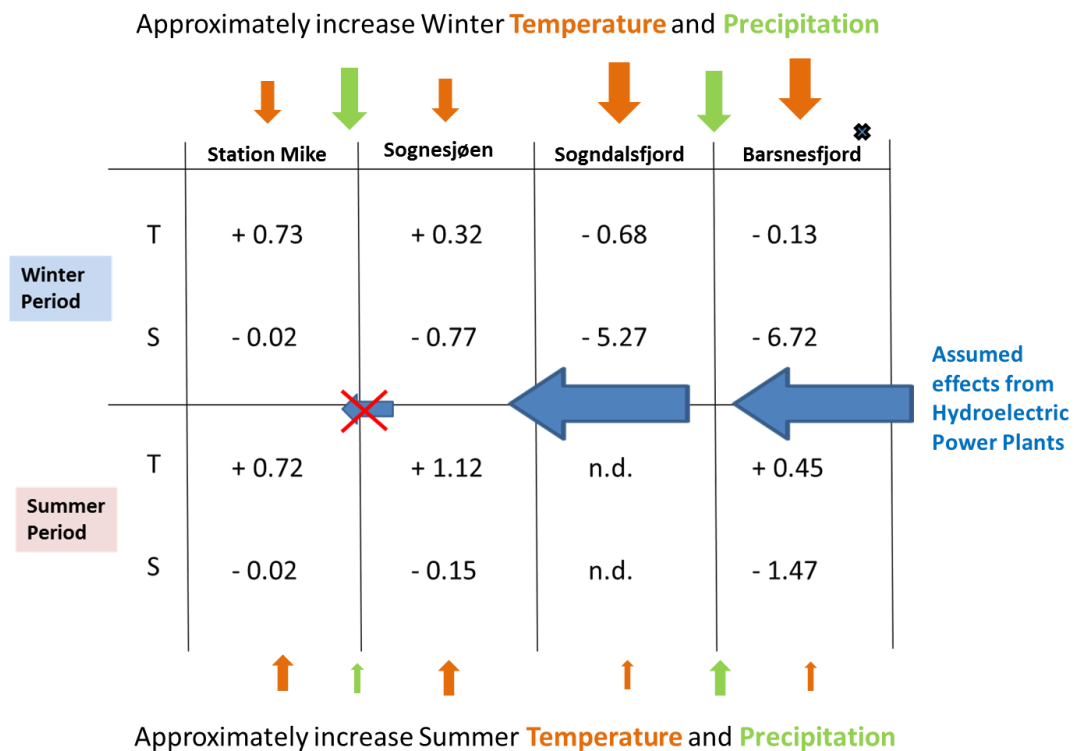


Figure 16: Change in salinity (S) and temperature (T) at 0 m/1 m depth from period one to three in the different water bodies. Additionally the different arrows depict the various climate influences and their relative strength on the single regions. The cross at the Barsnesfjord marks the fact, that the temperature and salinity values only show the difference between period one and two.

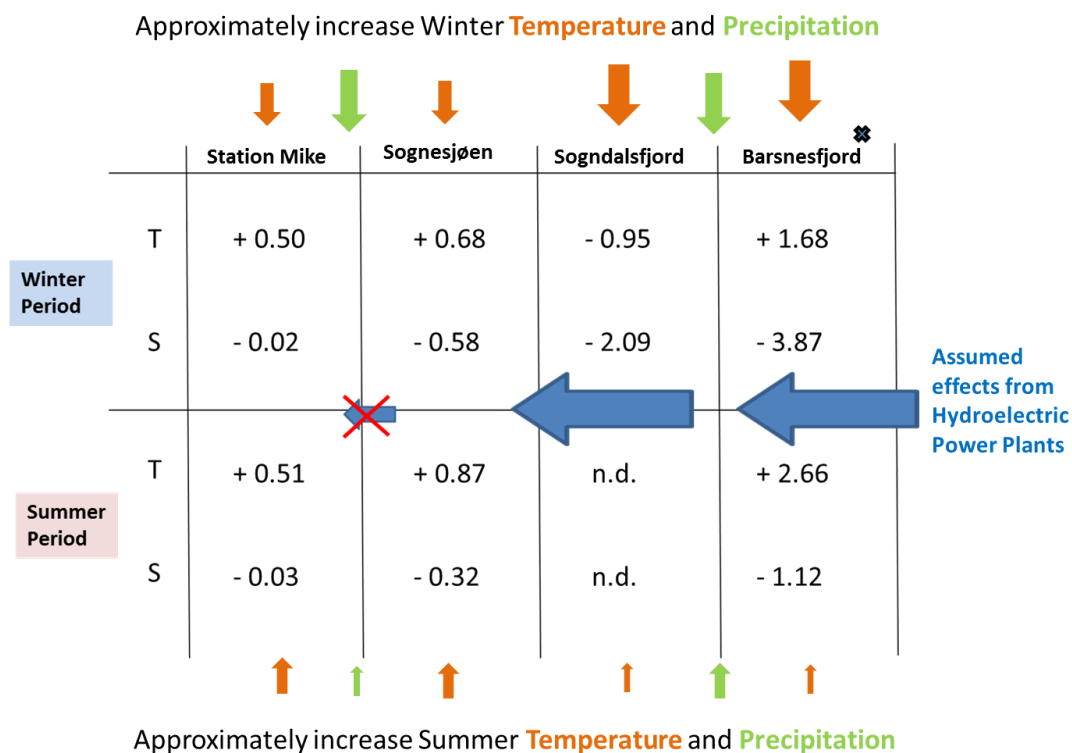


Figure 17: Change in salinity (S) and temperature (T) at 10 m depth from period one to three in the different water bodies. Additionally the different arrows depict the various climate influences and their relative strength on the single regions. The cross at the Barsnesfjord marks the fact, that the temperature and salinity values only show the difference between period one and two.

As can finally be seen in Figure 16 and Figure 17, the main reason for changes in salinity is coming from inside the fjord, thus pointing towards the building of the water power plants. Hence the changes are especially pronounced in the Inner part of the Sognefjord, in the tributaries Sogndalsfjord and Barsnesfjord. However, the water power plants do not have any effects on the Nordic Sea values. Additionally, parts of the changes in salinity are also caused by simultaneous changes in air temperature and precipitation. Overall the main effects are coming from inside the fjord, while the Nordic Sea only has negligible effects on the salinity and temperature fluctuations.

Regarding the temperature changes only, there seem to be two main influences, the overall increase in air temperature due to global warming as well as the influence of inflowing fresh water. Additionally some interesting internal fjord processes seem to exist, amplifying the warming of the water masses with getting deeper inside the fjord. The most likely causes of this seem to be the Land-Ocean-Effect as well as the difference in heat penetration due to particles and darkening of the coastal water.

4.5.3 Possible biological consequences of hydrographic changes

4.5.3.1 Salinity

Regarding the changes in salinity, there are several consequences possible in respect of the fjord biology. However, the biological aspects have not been examined in the frame of this bachelor thesis, thus making a clear statement difficult. Nevertheless the biological consequences could provide interesting and important information about the future development of the fjords and thus should be studied as a separate proxy.

4.5.3.2 Temperature

The heating of the fjord water masses can also have influences on the fjord biology. Many of the plants and organisms living in a fjord depend on the water depths and there prevailing temperatures. Changes in the general water temperatures at the single depths can thus have significant consequences, as they can change the bearable temperatures of the plants and organisms at these depths. Thus the warming trend in the upper 0 m to 20 m layers also affects plants and organisms living at these depths. One example is the Sugar Kelp (*Saccharina latissima*), which is proposed to disappear in the Hardangerfjord due to rising temperatures. The plant previously was growing at the border zone of its bearable temperatures (Dale, pers. com.). However these temperatures seem to have changed, potentially causing the plants to get less. The extreme warming within the Hardangerfjord can maybe also be related to fjord internal amplification of a general warming trend. Thus, it seems like similar effects of fjord internal amplifications of warming trends might already happened in other fjord environments, making it a general fjord property. According to this possibility and its potential biological consequences, a further research of this algae also in the Sognefjord would maybe give more information.

Beside that also the heating of the basin water could have remarkable consequences. The warmer temperatures of the basin water could lead to a higher O₂-consumption, finally causing anoxia in the stagnant bottom water. This is the case in the Sogndalsfjord and the Barsnesfjord, as shown by Kaufmann (2014). Overall this shows wide-ranging effects of hydrographical changes on the fjord biology, which should be further investigated in specific researches.

5. Conclusion

The main aim of this bachelor thesis was to investigate potential changes in the water hydrography of the Sognefjord, especially in salinity and temperature due to building of the water power plants or changes in local and/or global climate. Therefore this potential connection to the building of the water power plants around the 1960s and the overall climate change was examined, to ascertain the final reason for the changes in hydrography of the Sognefjord.

- According to the hydrographical data, there are changes in both, salinity and temperature values of the surface water masses of the fjords. Thus at 0 m depth the winter salinity values decline around -20.68% in the Sogndalsfjord and -46.39% at the Barsnesfjord, however only from period one to two (Tables 8 and 14). At the Sognesjøen the salinity declines only -2.36% and at Station Mike -0.06% (Tables 20 and 26). The summer salinity values drop at 72.19% at the Barsnesfjord and -0.07% at Station Mike but increase at 0.51% at the Sognesjøen (Tables 9, 27 and 21). The winter temperature declines at -12.31% at the Sogndalsfjord and -3.33% from period one to two at the Barsnesfjord, while it rises at 9.63% at Station Mike and 5.39% at the Sognesjøen (Tables 17, 11, 29 and 23). Against that the summer temperature in general rises, accounting for 3.34% at the Outer Barsnesfjord, 10.18% at the Sognesjøen and 9.37% at Station Mike (Tables 12, 24 and 30). However, regarding the relative temperature values in %, there has to be a precaution when interpreting them, especially with low, absolute values. For the absolute values see the tables, respectively.

- During the investigated time period a significant change in air temperature is verifiable, as well as a general increase in precipitation. This is especially visible regarding the different periods. Thus the winter temperature rises 98.10% at Flesland and drops -63.76% at Fjærland (Table 5), while the summer temperature increases 3.49% at Flesland and 2.45% at Fjærland (Table 6). Overall the temperature rise is largest in winter time at Fjærland, which also represents the largest range of fluctuations, pointing out more winter precipitation to come down as rain in the low lands. The winter precipitation rises around 30% at Fana Stend, Lavik and Hafslø, while it only increases around 19% at Ytre Solund (Table 2). In summer the precipitation rises around 15% at Fana Stend, Lavik and Hafslø and

around 4% at Ytre Solund (Table 3). In general the relative increase in precipitation is largest in the inner parts of the fjord.

- In general the interaction of the different influencing factors leads to different effects in summer and winter time. During winter period a co-working of the single factors takes place, as the rise in precipitation and the increased inflow of fresh water due to hydroelectric power plants both cause a reduction in surface salinity. Against that, in summer time a counteracting of the different factors takes place, as there is increased precipitation and glacier melting, however, balanced out by the reduced release of fresh water through the water power plants.
- The winter temperature at 0 m/1 m depth at the Sogndalsfjord drops around -0.68°C from period one to period three, despite a simultaneous rise in air temperature (Table 31). Thus it indicates an increased inflow of cold dammed fresh water due to the water power plants. The same is valid for the Outer Barsnesfjords 0 m/1 m layer.
- According to the drop in temperature during winter time, despite the coincident increase in air temperature, it seems likely that these variations show a relation to the water power plants. This is also supported by the stronger decline in water temperature visible further inside the fjord and thus closer to the hydroelectric power plants. Thus the temperature at 0 m/1 m depth decreases -0.68°C at the Sogndalsfjord (Table 31), while the air temperature rises 1.67°C at Fjærland (Table 33).
- The changes in temperature in all layers become amplified with increasing distance from the Nordic Sea, thus showing some kind of internal fjord effects, magnifying the increasing temperature trends with getting deeper into the fjord (Table 31 and 32).
- The amplification of the changing temperatures with getting deeper into the fjord is probably mainly caused by a Land-Ocean-Effect, as well as by the difference in heat penetration in the different regions due to particles and darkening of the coastal water.

- While there is an almost equal rise in absolute precipitation of around 83 mm/year at Ytre Solund and Hafslo (Table 39), there is a significantly larger drop in winter salinity at the Sogndalsfjord and the Barsnesfjord, accounting for around 5.27‰ and 6.72‰, compared to the Sognesjøen which only shows a drop of 0.77‰ (Table 37). Even though the relative increase in precipitation is larger at Hafslo, this clearly points out the increased inflow of fresh water due to hydroelectric energy production.
- There is a significantly stronger decline in summer salinity at 25 m depth at the Outer Baresnesfjord, accounting for -0.72‰ compared to the Sognesjøen, only depicting -0.02‰ due to indirect basin water exchange (Table 38). This phenomenon can be connected with the simultaneous increase in precipitation seen at Hafslo, accounting for 25.25 mm/year (Table 39).
- Especially the increased water release in winter time due to hydroelectric energy production has verifiable influences on the fjords salinity values of the surface water layers, causing a drop of 5.27‰ at 0 m at the Sogndalsfjord (Table 14). Also in summer times slight changes in salinity are visible and likely to be related to the water power plants. However, the changes are counteracted by increased precipitation and melting of glaciers due to higher air temperatures.
- Overall the bachelor thesis depicts the importance of long-time data series, to enable the evaluation of various environmental effects.
- The hydrographical changes in the fjords also propose significant consequences regarding the fjord biology. Thus the increase in water temperature affects plants and organisms living in the fjords. Additionally it can cause anoxic conditions in the deeper parts of the fjords. However, as this paper did not directly examine the biological consequences, a clear statement is difficult. Thus a further study of the biological consequences in separate researches is suggested.

6. References

- Aksnes, D.L., Dupont, N., Staby, A., Fiksen, Ø., Kaartvedt, S., Aure, J., 2009: Coastal water darkening and implications for mesopelagic regime shifts in Norwegian fjords. In: Marine Ecology Progress Series Vol. 387, pp. 39-49
- Anonymous, 2000: Oskar Commission for the Protection of the Marine Environment of the North-East Atlantic. Quality Status Report 2000. OSPAR Commission, London
- Anonymous, 2004: The West Norwegian Fjords – Norwegian Nomination 2004 UNESCO World Heritage List. Norwegian Ministry of the Environment, Oslo
- Anonymous, 2012: Regional plan med tema knytt til vasskraftutbygging, Sogn og Fjordane Fylkeskommune, Online access at:
[http://www.sfj.no/cmsff/cmsmm.nsf/lupGraphics/Vedteken11.12.2012%20Regional%20plan%20med%20tema%20knytt%20til%20vasskraftutbygging.pdf/\\$file/Vedteken11.12.2012%20Regional%20plan%20med%20tema%20knytt%20til%20vasskraftutbygging.pdf](http://www.sfj.no/cmsff/cmsmm.nsf/lupGraphics/Vedteken11.12.2012%20Regional%20plan%20med%20tema%20knytt%20til%20vasskraftutbygging.pdf/$file/Vedteken11.12.2012%20Regional%20plan%20med%20tema%20knytt%20til%20vasskraftutbygging.pdf),
 20.05.2015
- Anonymous, 2014: Regionalplan for vassforvaltning for Sogn og Fjordane vassregion 2016-2021. Sogn og Fjordane Fylkeskommune, Leikanger
- Aarseth, I., Nesje, A., Fredin, O., 2008: Unesco fjords – From Nærøyfjorden to Geirangerfjord. In: 33 IGC, The Nordic Countries excursion No 31
- Crescentini, M., Bennati, M., Tartagni, M., 2012: Design of integrated and autonomous conductivity-temperature-depth (CTD) sensors. In: AEU – International Journal of Electronics and Communications, Vol. 66, pp. 630-635
- Dale, T., 2015: Professor at the Sogn og Fjordane University College, personal communication
- Dale, T., Hovgaard, P., 1993: En undersøkelse av resipientforholdene i Sogndalsfjorden, Barsnesfjorden og Kaupangerbukten i perioden 1991-1993. A study on the recipients Sogndalsfjorden, Barsnesfjorden and Kaupangerbukten in the period 1991-1993. Sogn og Fjordane Distriktshøgskule, Sogndal
- Drange, H., Dokken, T., Furevik, T., Gerdes, R., Berger, W., Nesje, A., Orvik, K.A., Skagseth, Ø., Skjelvan, I., Østerhus, S., 2005: The Nordic Seas: An Overview. In: The Nordic Seas: An Integrated Perspective. AGU Monograph 158, pp. 199 – 220, Washington DC

E-Klima, 2015: *eKlima – Norwegian Meteorological Institute*. Online access at: http://sharki.oslo.dnmi.no/portal/page?_pageid=73,39035,73_39049&_dad=portal&_schema=PORTAL&6009_BATCHORDER_3197941, 24.04.2015

Eldevik, T., Risebrobakken, B., Bjune, A.E., Andersson, C., Birks, H.J.B., Dokken, T.M., Drange, H., Glessmer, M.S., Li, C., Nilsen, J.E.Ø., Ottera, O.H, Richter, K., Skagseth, Ø., 2014: A brief history of climate – the northern seas from the Last Glacial Maximum to global warming. In: *Quaternary Science Reviews* 106, pp. 225-246, Geophysical Institute, Bergen

EuroSites (2015a): *European Ocean Observatory Network*. Online access at: <http://www.eurosites.info/stationm.php>, 16.04.2015

EuroSites (2015b): *European Ocean Observatory Network*. Online access at: <http://www.eurosites.info/stationm/data.php>, 16.04.2015

Furevik, T., Mauritzen, C., Ingvaldsen, R, 2006: The Flow of Atlantic Water to the Nordic Seas and Arctic Ocean. In: *Arctic Alpine Ecosystems and People in a Changing Environment*. Springer, Bergen

Gonzalez, D., Kilinc, A., Weidmann, N., 2011: Renewable Energy Development – Hydropower in Norway. Seminar papers in international finance and economics, University of Applied Sciences Nuremberg

Haakstad, M., Kögeler, J.W., Dahle, S., 1994: Studies of sea surface temperatures in selected northern Norwegian fjords using Landsat TM data. *Polar Research* 13, pp. 95-103

Hermansen, H. O., 1974: *Sognefjordens Hydrografi og vannutveksling*. University of Bergen, 1974, Cand. real. thesis

Hurdle, B.G., 1986: *The Nordic Seas*. Springer-Verlag, New York, Berlin, Heidelberg, Tokyo

IMR (2015a): Institute of Marine Research. Online access at: <http://www.imr.no/en>, 20.04.2015

IMR (2015b): Institute of Marine Research. Online access at: <http://www.imr.no/forskning/forskningsdata/stasjoner/view?station=Sognesjoen>, 20.04.2015

Kaufmann, S., 2014: A 100 year hydrographical record of the Barsnesfjord, Western Norway and its environmental application. University of Applied Science, Bingen, Bachelor thesis

Lawson, K., Larson, N.G., 2001: CTD. In: Encyclopedia of Ocean Sciences, Vol. 1, pp. 579-588, Sea-Bird Electronics Inc., Bellevue, Washington USA

Løddøen, T.K., 1998: Interpreting Mesolithic axe deposits from a region in western Norway. In: Archaeologica Baltica 2. The Archaeology of Lithuania and Western Norway: Status and Perspectives. Vilnius: Lithuanian Institute of History, pp. 195-204

Manzetti, S., Stenersen, J.H.V., 2010: A critical view of the environmental condition of the Sognefjord. In: Marine Pollution Bulletin 60, pp. 2167-2174

Mikalsen, G., Sejrup, H.P., 2000: Oxygen Isotope Composition of Fjord and River Water in the Sognefjorden Drainage Area, Western Norway. Implications for Paleoclimate Studies. In: Estuarine, Coastal and Shelf Science 50, pp. 441-448

Mill, H.R., 1900: The Pettersson-Nansen Insulating Water-Bottle. In: The Geographical Journal Vol. 16, pp. 469-471

Nesje, A., Whillans, I.M., 1994: Erosion of Sognefjord, Norway. In Geomorphology 9, pp. 33-45

NOAA (2015): *National Oceanic And Atmospheric Administration*. Online access at: http://www.aoml.noaa.gov/phod/amo_faq.php, 29.05.2015

NVE (2015): *Norwegian Water Resources and Energy Directorate*. Online access at: <http://www.nve.no/en/>, 16.04.2015

Opdal, A.F., Asknes, D.L., Rosland, R., Fiksen, Ø., 2013. Sognefjorden – en oppsummering av litteratur og kunnskapsstatus om fjord-økologi og vannkraftutbygging. In: Uni Computing Technical Report Nr. 32, Bergen

Paetzel, M., Dale, T., 2010: Climate proxies for recent fjord sediments in the inner Sognefjord region, Western Norway. In: Geological Society, London, Special Publications 2010; pp. 271-288

Paetzel, M., Schrader, H., 1991: Heavy metal (Zn, Cu, Pb) accumulation in the Barsnesfjord: Western Norway. In: Norsk Geologisk Tidsskrift, Vol. 71, pp. 65-73, Oslo

Skjoldal, H.R., Sætre, R., Færnø, A., Misund, O.A., Røttingen, I., 2004: The Norwegian Sea Ecosystem. Tapir Academic Press, Trondheim

- Skofteland, E., 1970: Hydrografiske undersøkelser i indre del av Sognefjorden. Vassdragsdirektoratet, Rapport 3/70
- Stigebrandt A., 1981: A Mechanism Governing the Estuarine Circulation in Deep, Strongly Stratified Fjords. *Estuarine, Coastal and Shelf Science* 13, pp. 197-211
- Stigebrandt A., 2001: Fjordenv – A water quality model for fjords and other inshore waters. Earth Sciences Centre, Göteborg University, C40, 2001
- Syvitski, J.P.M, Burrell, D.C., Skei, J.M., 1987. Fjords: Processes and Products. Springer-Verlag, New York, Berlin, Heidelberg, London, Paris, Tokyo
- Sætre, R., 2007. The Norwegian Coastal Current – Oceanography and Climate. Tapir Academic Press, Trondheim
- Urdal, K., Sægrov, H., 2008: Fiskeundersøkingar i Årøyelva i 2006 og 2007. Rådgivende Biologer AS 1067, Bergen
- Venneman, M., 2014: Effects of a new bridge on an intertidal mudflat in the Outer Barsnesfjord, Western Norway. University of Applied Sciences, Larenstein, Bachelor thesis
- Walczowski, W., 2014: Atlantic Water in the Nordic Seas. Properties, Variability, Climatic Importance. Springer International Publishing, Switzerland

7. Figure References

- Figure 1: Formation process of a fjord (09.05.2015). Online access at:
http://upload.wikimedia.org/wikipedia/commons/f/fb/Fjord_genesis.png
- Figure 2: Main water structure within a fjord (09.05.2015). Online access at:
<http://www.imr.no/images/bildearkiv/2013/06/figur-9.jpg/en?size=medium>
- Figure 3: Water circulation within a fjord, Theresa Reß
- Figure 4: The Barsnesfjord, Theresa Reß
- Figure 5: The Sogndalsfjord, Theresa Reß
- Figure 6: The Sognesjøen, Theresa Reß
- Figure 7: The Nordic Seas current system (23.05.2015): Online access at:
https://encrypted-tbn3.gstatic.com/images?q=tbn:ANd9GcTIRz2BA5drvidxnoDM31OIUe_6YLilpX9dYL7KtSs0BNPyodaoOw
- Figure 8: Water Power Stations in the region of the inner Sognefjord: Solbakken, R., Henriksen, K., Reitan, K.I., Arff, J., Ellingsen, I.H., Hindar, K., Fiske, P., Robertsen, G., Finstad, B., Aas, Ø., Johnsen, B.O., 2012: Innsamling og sammenstilling av relevant kunnskap om Sognefjorden. Rapport Sintef Fiskeri og Havbruk, p. 46, Trondheim
- Figure 9: Water drainage to the Aurlandsfjord: Opdal, A.F., Aksnes, D.L., Rosland, R., Fiksen, Ø., 2013: Sognefjorden – en oppsummering av litteratur og kunnskapsstatus om fjord-økologi og vannkraftutbygging. Uni Computing Technical Report Nr. 32, Fig. 4.6, p. 21, Bergen
- Figure 10: Pre-defined periods for the building of the large water power plants
- Figure 11: Map showing the climate stations, Theresa Reß
- Figure 12: Map showing the stations of the hydrographic sampling, Theresa Reß
- Figure 13: CTD sensor (22.05.2015). Online access at:
http://www.schmidtocean.org/files/24bottlerosette_polarstern.jpg
- Figure 14: Nansen water bottle (22.05.2015). Online access at:
http://oceanworld.tamu.edu/students/satellites/images/nansen_bottle_1.jpg
- Figure 15: Effects of hydroelectric power plants with dams, Theresa Reß
- Figure 16: Conclusion with water from 0 m/1 m depth, Theresa Reß
- Figure 17: Conclusion with water from 10 m depth, Theresa Reß

8. Appendix (on CD-Rom)

8.1 Appendix I – Rawdata Climate

8.2 Appendix II – Rawdata Barsnesfjord

8.3 Appendix III – Rawdata Sogndalsfjord

8.4 Appendix IV – Rawdata Sognesjøen

8.5 Appendix V – Rawdata Station Mike

8.6 Appendix VI – Seasonal Graphs and Tables of all data

8.7 Appendix VII – Bachelor thesis